1990

Kinetics and mechanisms of the reactions of alkyl radicals with oxygen and with complexes of Co(III), Ru(III), and Ni(II)

Douglas G. Kelley
Iowa State University

Order Number 9110514

Kinetics and mechanisms of the reactions of alkyl radicals with oxygen and with complexes of Co(III), Ru(III), and Ni(II)

Kelley, Douglas G., Ph.D.

Iowa State University, 1990

U·M·I
300 N. Zeeb Rd.
Ann Arbor, MI 48106

Kinetics and mechanisms of the reactions of alkyl radicals with oxygen and with complexes of Co(III), Ru(III), and Ni(II)

by

Douglas G. Kelley

A Dissertation Submitted to the
Graduate Faculty in Partial Fulfillment of the
Requirements for the Degree of
DOCTOR OF PHILOSOPHY

Department: Chemistry
Major: Inorganic Chemistry

Approved:

Signature was redacted for privacy.

In Charge of Major Work

Signature was redacted for privacy.

For the Major Department

Signature was redacted for privacy.

For the Graduate College

Iowa State University
Ames, Iowa

1990

TABLE OF CONTENTS

GENERAL INTRODUCTION

Part I describes the kinetics and mechanisms of the reactions of ethyl radical with $Co(NH_3)_5X^{2+}$, $Ru(NH_3)_5X^{2+}$, and $Co(dmgH)_2(X)(Y)$ (dmgH = dimethylglyoxime; X = Br, Cl, N_3, SCN; Y = H_2O, CH_3CN) complexes, studied by laser flash photolysis (using $ABTS^{\bullet-}$ (2,2′-azino-bis(3-ethylbenzthiazoline-6-sulfonic acid)) as kinetic probe). The products of these reactions were largely the ethyl halide and ethyl thiocyanate, substantiating an inner-sphere mechanism. Minor yields of C_2H_4 were also found, suggesting a small contribution from the outer-sphere oxidation of $^{\bullet}C_2H_5$.

Part II describes the kinetics of colligation reactions of β-$Ni(cyclam)^{2+}$ (cyclam = 1,4,8,11-tetraazacyclotetradecane) with alkyl radicals and the subsequent unimolecular homolysis of $RNi(cyclam)H_2O^{2+}$ complexes, studied using laser flash photolysis. The colligation and homolysis rate constants were strongly influenced by steric and electronic factors. Kinetic and thermodynamic data obtained from these reactions were compared with those for other σ-bonded organometallic complexes.

Part III describes the kinetics of the unimolecular homolysis of a series of $RNi(cyclam)H_2O^{2+}$, monitoring the formation of the oxygen insertion product $RO_2Ni(cyclam)H_2O^{2+}$. The rate constants

for the reactions of alkyl radicals with oxygen were obtained and compared to those measured in the gas phase.

PART I. KINETICS AND MECHANISMS OF THE REACTIONS BETWEEN ETHYL RADICALS AND COMPLEXES OF COBALT(III) AND RUTHENIUM(III)

INTRODUCTION

The mechanisms of reduction of pentaammine halo cobalt(III) and ruthenium(III) complexes have been extensively studied, with the nature of the electron donor varying from metal ions and metal polypyridyl complexes[1] to α-hydroxyalkyl radicals.[2] The occurrence of reactions of such free radicals as $I^{\bullet}$, $HO^{\bullet}$, $SO_4^{\bullet-}$, and $^{\bullet}CH_3$ with pentaamminehalocobalt(III) complexes was first reported by Haim and Taube,[3] who found nearly quantitative formation of $Co(H_2O)_6^{2+}$. The studies with methyl radicals were of exploratory nature; no kinetic data were sought, and the organic products were not determined. They postulated that the reaction of methyl radicals might occur by the equation:

$$Co(NH_3)_5X^{2+} + {}^{\bullet}CH_3 + 5\ H^+ \longrightarrow Co^{2+} + CH_3X + 5\ NH_4^+ \qquad (1)$$

Our goal in this work has been to conduct kinetic measurements by means of laser flash photolysis experiments, to determine the products formed, and to examine the mechanism of this reaction. We have done this for the ethyl radical, which gives less volatile products than methyl. The source of $^{\bullet}C_2H_5$ is the photohomolysis of ethylcobalt complexes, $C_2H_5Co(dmgH)_2OH_2$ (mostly) and $C_2H_5Co(cyclam)H_2O^{2+}$ (occasionally).[4,5] The laser

flash provides the method by which the radicals are produced in a short time (<1 μs) and at concentration levels high enough to be kinetically useful.

Because the Co(III) and Ru(III) complexes to be examined in this study possess relatively small molar absorptivities in the visible region, a competing chromophore is required as a probe to follow the kinetics. This probe must react rapidly with alkyl radicals, must have a large molar absorptivity in the low-energy visible spectral region, and must not undergo thermal reactions with either the ethylcobalt precursor or the transition metal substrate complex.

Our search[6] for a kinetic probe led us to $ABTS^{2-}$, which is readily oxidized to $ABTS^{\bullet-}$. The radical anion is quite persistent, with a lifetime of many weeks in aerated aqueous solutions, and is brightly colored.[7]

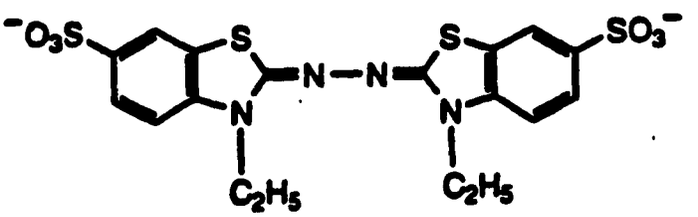

$ABTS^{2-}$

Wolfenden and Willson were the first to employ $ABTS^{\bullet-}$ as a kinetic probe, following the reactions of alcohols, organic acids, and amino acids with free radicals generated by pulse

radiolysis.[8] More recent studies have further demonstrated the spectroscopic utility of $ABTS^{\bullet-}$ as a scavenger of reactive intermediates,[9] as an indicator for the determination of enzymatic activity,[10] and as a kinetic probe in competion reactions.[11] We also used hexachloroiridate(IV) ion as a probe in one instance to verify the $ABTS^{\bullet-}$ method. Rate constants thus obtained were compared with relative rates measured in competition studies by product ratios.

EXPERIMENTAL

Reagents

The cobalt(III)[12] and ruthenium(III)[13] complexes were prepared by literature procedures, as were the metal polypyridyl complexes.[14] The ethyl cobalt radical precursors, $C_2H_5Co(dmgH)_2L$ (L + H_2O[15] or pyridine[16]) and $[C_2H_5Co(cyclam)H_2O](ClO_4)_2$[17] were also prepared by published procedures. Commercial sources provided $(NH_4)_2$ABTS (Sigma), methyl viologen dichloride (Aldrich), and $(NH_4)_2[IrCl_6]$ (Aldrich). Reagent stock solutions were prepared as needed and kept in the dark, with solutions of $Co(dmgH)_2(H_2O)Cl$, $Co(dmg_2H_3)Cl_2$, $Co(dmgH)_2(H_2O)Br$, $Co(dmg_2H_3)Br_2$, $Co(NH_3)_5N_3^{2+}$, and $Co(NH_3)_5SCN^{2+}$ kept at 0°C to inhibit hydrolysis. All solutions were prepared from distilled water which was purified by passage through a Milli-Q Millipore reagent water system.

For our purposes the most efficient way to prepare $ABTS^{\bullet-}$ was to mix solutions of $ABTS^{2-}$ and Ce(IV) in nearly equal volume and concentration,[18] but with a slight deficiency of Ce(IV) so that further oxidation to give the neutral ABTS species was avoided, along with any possible reaction chemistry of cerium(IV).

Figure I-1 shows the UV-visible spectrum of $ABTS^{\bullet-}$ created by the slow oxidation of $ABTS^{2-}$ using H_2O_2. Solutions of $(H_2O)_5CrC_2H_5^{2+}$ were prepared from the reaction of Cr^{2+} with tert-amyl hydroperoxide.[19] These solutions were ion exchanged on Sephadex SP-25 in an ice-jacketed column and used immediately after the organochromium emerged from the column.

Kinetics

Control experiments were done to explore the photohomolysis of $C_2H_5Co(dmgH)_2H_2O$. The loss in concentration of this complex during a typical laser flash was 6.5 ± 1.5 μM, determined by the absorbance decrease at 440 nm (ε_{440} = 1350 L mol^{-1} cm^{-1}). This measurement was done at $[H^+]$ = 1.0 M (μ = 1.0 M), where the cobalt(II) complex $Co(dmgH)_2(H_2O)_2$ very rapidly demetallates. The formation of the cobalt(II) product was then examined at pH 7 (μ = 1.0 M), where it is stable (ε_{440} = 3500 L mol^{-1} cm^{-1}). The increase in $[Co(dmgH)_2(H_2O)_2]$ was 5.1 ± 0.9 μM, which matches the loss in ethylcobalt(III) complex within experimental error.

Laser flash photolysis was employed to study the kinetics of these reactions. The system used has been described by Connolly[20] and is based on another system in the literature.[21] The dyes used were Coumarin 460 and LD 490, which emit light in the spectroscopic region where $C_2H_5Co(dmgH)_2H_2O$ has an absorbance

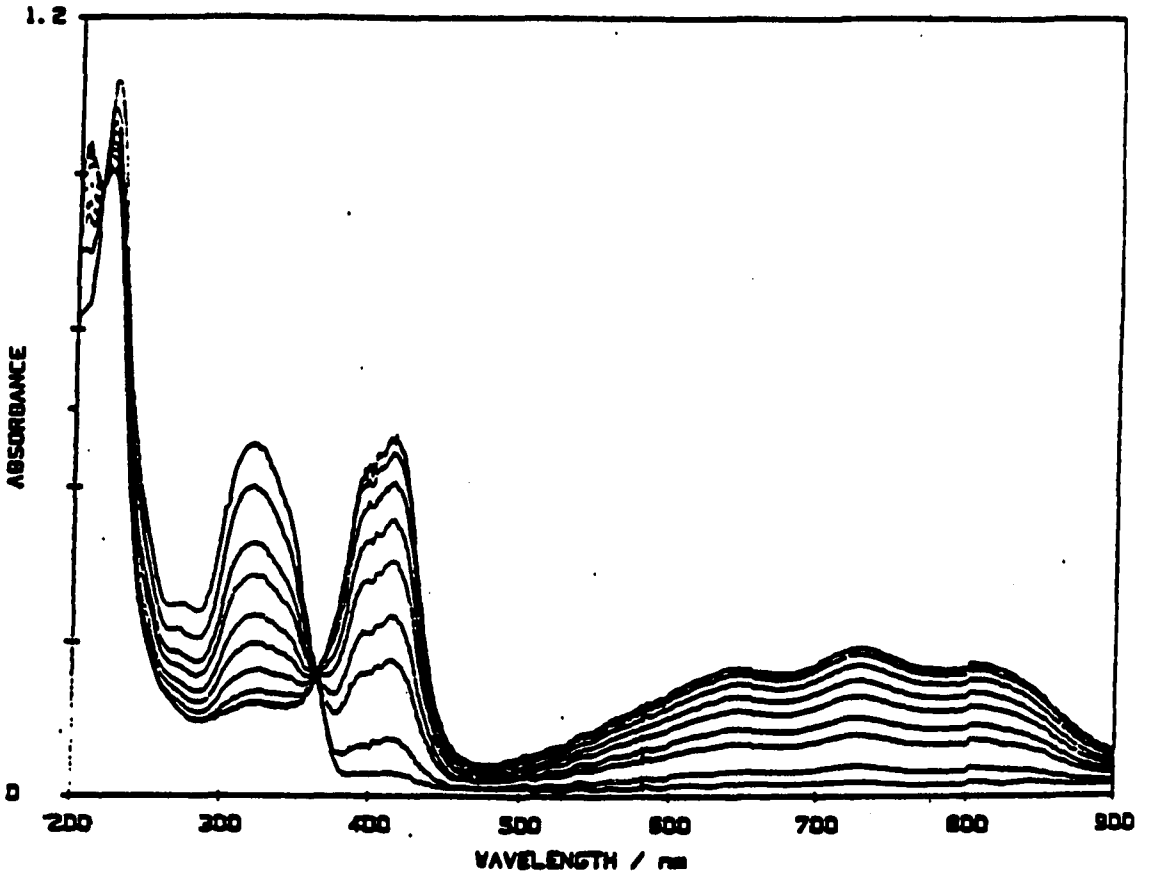

Figure I-1. UV-visible spectral changes during the reaction of $ABTS^{2-}$ with H_2O_2 to give $ABTS^{\bullet-}$ in 0.01 M $HClO_4$ solution. Scans were taken at 3 minute intervals. The reagent concentrations were $[ABTS^{2-}]$ = 50 μM and $[H_2O_2]$ = 150 μM

maximum (450 - 500 nm). It should be noted that $ABTS^{\bullet-}$ possesses a relatively transparent absorption window in this region, permitting the laser photolysis of the alkylcobalt species. The reactions were monitored under argon by following the increase of transmittance at an absorption maximum of the particular chromophore: $ABTS^{\bullet-}$ (ε_{650} = 1.0 x 10^4 L mol^{-1} cm^{-1})[18] and $IrCl_6^{2-}$ (ε_{487} = 4.09 x 10^3 L mol^{-1} cm^{-1}).[22] In a typical experiment, a deaerated sample solution was prepared in a 1-cm quartz cell and flashed by a 0.6 μs laser pulse from a Phase-R DL-1100 pulsed dye laser. A monitoring beam, provided by a 50 W quartz-halogen lamp, passed through the cell at right angles to the laser beam. The light transmitted through the cell passed through an Instruments SA grating monochromator, was detected by a Hamamatsu R928 photomultiplier tube, and the resulting signal was collected and stored on a Nicolet model 2090-3A digitizing oscilloscope. The reactions were monitored by following the changes in voltage (transmittance) over time at an absorption maximum of the particular kinetic probe reagent. The Nicolet oscilloscope was interfaced with an Apple II Plus microcomputer, which converted voltage vs. time data to absorbance vs. time data.

Data Analysis

Laser flash photolysis of solutions containing $C_2H_5Co(dmgH)_2H_2O$ generated ethyl radicals that disappeared by two pathways. One is the radical self-reactions, eq 2, which proceed at a known rate (k_d = 1.2 x 10^9 L mol^{-1} s^{-1})[23] and yields ethane, ethylene and butane in a relative ratio 1:1:2.3, consistent with that previously reported for ethyl radicals in aqueous solution.[24] The other is the reaction with the excess reagent $ABTS^{\bullet-}$ (eq 3) with rate constant, k_A. Digitized absorbance vs. time data generated by these reactions were analyzed by a nonlinear least-squares program and were fit well by first-order kinetics: $D_t = D_\infty + (D_o - D_\infty)\exp(-k_\psi t)$, where D = absorbance.

$$2\ {}^{\bullet}C_2H_5 \longrightarrow C_2H_4 + C_2H_6,\ C_4H_{10} \qquad k_d \qquad (2)$$

$${}^{\bullet}C_2H_5 + ABTS^{\bullet-} \longrightarrow [ABTS\text{-}C_2H_5]^{2-} + H^+ \qquad k_A \qquad (3)$$

$$-d[{}^{\bullet}C_2H_5]/dt = 2k_d[{}^{\bullet}C_2H_5]^2 + k_A[{}^{\bullet}C_2H_5][ABTS^{\bullet-}] \qquad (4a)$$

The simplicity of this treatment is really an approximation, since the self-reactions do make a very small second-order contribution to the reaction rate. For these experiments the

value of $[^{\bullet}C_2H_5]$ was approximated as the average value of the initial and final values, reducing eq 4a to a pseudo-first-order kinetic expression, eq 4b.

$$k_{\psi} = 2k_d[^{\bullet}C_2H_5]_{ave} + k_A[ABTS^{\bullet-}]_{ave} \qquad (4b)$$

The validity of this approximation is explained in the following paragraphs.

The $[^{\bullet}C_2H_5]_i$ can be obtained from the loss of absorbance of $ABTS^{\bullet-}$ in each experiment, after allowance for the percent of reaction going by the $ABTS^{\bullet-}$ pathway (eq 5). By designing experiments with $[ABTS^{\bullet-}]_i > 10[^{\bullet}C_2H_5]_i$, the dramatic changes

$$[^{\bullet}C_2H_5]_{ave} = \frac{k_{\psi}[ABTS^{\bullet-}]_{lost}/2}{k_A[ABTS^{\bullet-}]_{ave}} \qquad (5)$$

in the magnitude of the term $2k_d[^{\bullet}C_2H_5]_{ave}$ are small (< 10%) compared to the $ABTS^{\bullet-}$ term. Therefore, this method is valid despite the fact that $^{\bullet}C_2H_5$ decays completely during the experiment. Plots of k_{ψ} vs. $[ABTS^{\bullet-}]_{ave}$ are linear with a small intercept representing the self-reactions. Pseudo-first-order rate constants corrected for the self-reactions, k_{corr}, were obtained using an iterative process employing eq 6 until a reproducible value for k_A was obtained. The plot of k_{corr} vs.

$$k_{corr} = k_\psi - 2k_d \frac{k_\psi[ABTS^{\bullet-}]_{lost}/2}{k_A[ABTS^{\bullet-}]_{ave}} = k_A[ABTS^{\bullet-}]_{ave} \qquad (6)$$

$[ABTS^{\bullet-}]_{ave}$, shown in **Figure I-2** for the reaction with ethyl radical, was linear and passes through the origin. The validity of this method was verified by using a numerical integration program, KINSIM,[25] and the specified rate constants to generate values of $[ABTS^{\bullet-}]_{ave}$ as a function of time. First-order analyses of these simulated data agreed with the treatment implied by eq 4b.

Reactions were performed analogously in the presence of the metal halide substrate, with the additional reaction (eq 7) contributing a third term to the rate law (eq 8).[26]

$$^{\bullet}C_2H_5 + L_nCo^{III}X \longrightarrow C_2H_5X + L_nCo^{II} \qquad k_{Co} \qquad (7)$$

$$k_\psi = 2k_d[^{\bullet}C_2H_5]_{ave} + k_A[ABTS^{\bullet-}]_{ave} + k_{Co}[L_nCo^{III}X] \qquad (8)$$

In these experiments, the excess concentrations of $ABTS^{\bullet-}$ and $L_nCo^{III}X$ were both varied. Flashing a reaction solution four times generated four values of k_ψ with $[L_nCo^{III}X]$ effectively remaining constant. The terms for the radical self-reactions and the $ABTS^{\bullet-}$ reaction were subtracted from the pseudo-first-order

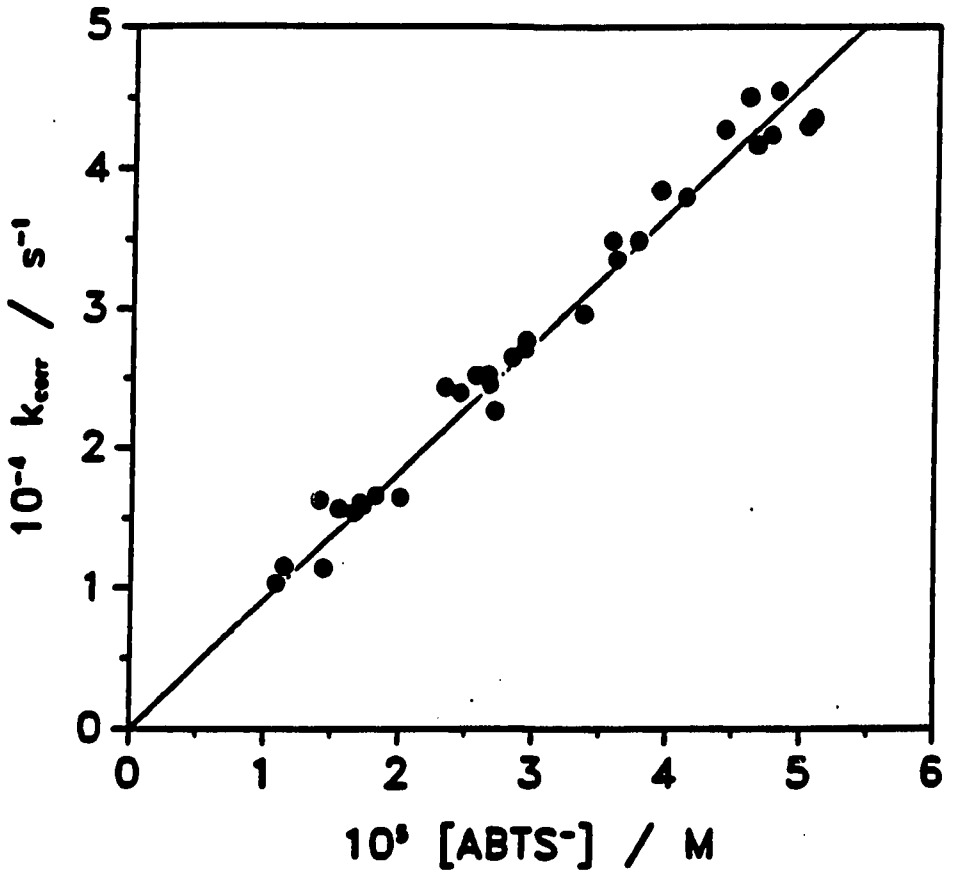

Figure I-2. The plot of k_{corr} versus $[ABTS^{\bullet-}]_{ave}$ for the reaction of $^{\bullet}C_2H_5$ with $ABTS^{\bullet-}$

rate constants at each $ABTS^{\bullet-}$ concentration to give values of k_{corr}, eq 10. The data were plotted using the average value of k_{corr} vs. $[L^nCo^{III}X]$, eq 9.

$$k_{corr} = k_\psi - 2k_d[{}^\bullet C_2H_5]_{ave} - k_A[ABTS^{\bullet-}]_{ave} = k_{Co}[L_nCo^{III}X] \quad (9)$$

$$k_{corr} = k_\psi - 2k_d \frac{k_\psi[ABTS^{\bullet-}]_{lost}/2}{k_A[ABTS^{\bullet-}]_{ave}} - k_A[ABTS^{\bullet-}]_{ave} \quad (10)$$

Bimolecular rate constants were obtained by using each corrected rate constant, k_{corr}, and corresponding $L_nCo^{III}X$ concentration in a linear least-squares analysis.

A further correction was necessary in the data analysis for $Co(dmg_2H_3)Cl_2$ and $Co(dmgH)_2(H_2O)Cl$, in that these complexes have significant absorption at 650 nm, with ε = 20 and 15 L mol^{-1} cm^{-1}, respectively. Allowance for this absorbance contribution was made in the calculation of the initial $ABTS^{\bullet-}$ concentration (eq 11). The same was true when $[IrCl_6^{2-}]$ was

$$[ABTS^{\bullet-}]_i = \frac{Abs_{total} - \{[CoCl]_i \times \varepsilon(CoCl)_{650}\}}{\varepsilon(ABTS^{\bullet-})_{650}} \quad (11)$$

followed at 487 nm; allowance was made for both $C_2H_5Co(dmgH)_2OH_2$ (ε_{487} = 5.0 x 10^2 L mol^{-1} cm^{-1}) and $Co(NH_3)_5Br^{2+}$ (ε_{487} = 32

L mol^{-1} cm^{-1}).

Gas Chromatography

Reaction products were determined using a Hewlett-Packard model 5790A series gas chromatograph with a 3390A series integrator. Ethyl halides were determined on Carbopak and OV-101 columns, and ethylene on a VZ10 column.

Relative rate constants were determined for pairs of metal complexes by a competition method in which $^{\bullet}C_2H_5$ was photochemically generated in solutions containing $Co(NH_3)_5Cl^{2+}$ and $Co(NH_3)_5Br^{2+}$ complexes, or the ruthenium(III) analogues. Solutions containing $Co(dmgH)_2(X)(Cl)$ ($X = H_2O$, Cl) and $Co(NH_3)_5Br^{2+}$ were also analyzed. The ratio C_2H_5Cl/C_2H_5Br was determined gas chromatographically, and the relative rate constants were calculated as in eq 12. These

$$\frac{k_{Cl}}{k_{Br}} = \frac{[C_2H_5Cl]_\infty}{[C_2H_5Br]_\infty} \times \frac{[Co(NH_3)_5Br^{2+}]_{ave}}{[Co(NH_3)_5Cl^{2+}]_{ave}} \qquad (12)$$

studies were performed by placing an anaerobic 1-cm quartz cuvette, filled to capacity with the desired combination of reagents, before a Pyrex-filtered sunlamp for three minutes. Photolysis was continued until $C_2H_5Co(dmgH)_2H_2O$ was completely destroyed. This method was employed for solutions at pH 2, to

lessen decomposition of the GC column at high acid concentrations.

RESULTS

Reactions of Ethyl Radical with $L_nCo^{III}X$ Complexes

All the reactions with ethyl radical were studied in deaerated 0.50 M H_2SO_4 under pseudo-first-order conditions with $ABTS^{\bullet-}$ and $L_nCo^{III}X$ in excess. Typical reagent concentrations were about 20 μM $C_2H_5Co(dmgH)_2H_2O$ and 19-37 μM $ABTS^{\bullet-}$. The $L_nCo^{III}X$ concentrations were varied in a range where a measurable effect on the pseudo-first-order rate constants, k_ψ, was found. For example, the concentration of $Co(NH_3)_5Br^{2+}$ ranged from (0.50 - 5.0) x 10^{-3} M. No thermal reaction between the various $L_nCo^{III}X$ species and $ABTS^{\bullet-}$ was observed, nor did $ABTS^{\bullet-}$ react with ethylcobaloxime. The competition reactions (eqs 2, 3, and 7) were monitored at 650 nm and observed to obey the pseudo-first-order rate law (eq 8).

$$2\ {}^{\bullet}C_2H_5 \longrightarrow C_2H_4 + C_2H_6 + C_4H_{10} \qquad k_d \qquad (2)$$

$${}^{\bullet}C_2H_5 + ABTS^{\bullet-} \longrightarrow [ABTS\text{-}C_2H_5]^{2-} + H^+ \qquad k_A \qquad (3)$$

$${}^{\bullet}C_2H_5 + L_nCo^{III}X \longrightarrow C_2H_5X + L_nCo^{II} \qquad k_{Co} \qquad (7)$$

$$k_\psi = 2k_d[{}^{\bullet}C_2H_5]_{ave} + k_A[ABTS^{\bullet-}]_{ave} + k_{Co}[L_nCo^{III}X] \qquad (8)$$

Typical results for six complexes are presented, $Co(NH_3)_5Br^{2+}$, $Co(NH_3)_5SCN^{2+}$, and $Co(NH_3)_5N_3^{2+}$ in **Figure I-3** and $ClCo(dmgH)_2H_2O$, $Co(dmg_2H_3)Cl_2$, and $BrCo(dmgH)_2CH_3CN$ in **Figure I-4**, where the linear dependence of k_{corr} upon cobalt concentration is shown (eq 9). The slope of each line gives the rate constant for the

$$k_{corr} = k_\psi - 2kd[{}^\bullet C_2H_5]_{ave} - k_A[ABTS^{\bullet-}]_{ave} = k_{Co}[L_nCo^{III}X] \quad (9)$$

reaction of ${}^\bullet C_2H_5$ with the Co(III) substrate, k_{Co}, and these are listed in **Table I-1**. The rate constant measured for the reaction of ${}^\bullet C_2H_5$ with trans-$Co(en)_2Cl_2^+$ was obtained from a single experiment near the concentration limit of the Co(III) complex. In view of the subtractions involved in calculating k_{corr}, the precision of the individual k_{Co}-values was estimated to be about 20%. The values of k_ψ and k_{corr} are listed in **Tables A-1 to A-8**. All of these rate constants are pH independent in the range 0-7.

Separate determinations of k_{Co} for the reaction of ${}^\bullet C_2H_5$ with $Co(NH_3)_5Br^{2+}$ were made with $ABTS^{\bullet-}$ and $IrCl_6^{2-}$ as chromophores. The agreement of the two values of k_{Co}, 2.6×10^6 and 3.0×10^6 L mol^{-1} s^{-1}, is within experimental error. The plot of k_{corr} vs. $[Co(NH_3)_5Br^{2+}]$ displayed in **Figure I-3** contains data points from both the $ABTS^{\bullet-}$ and $IrCl_6^{2-}$ competition methods.

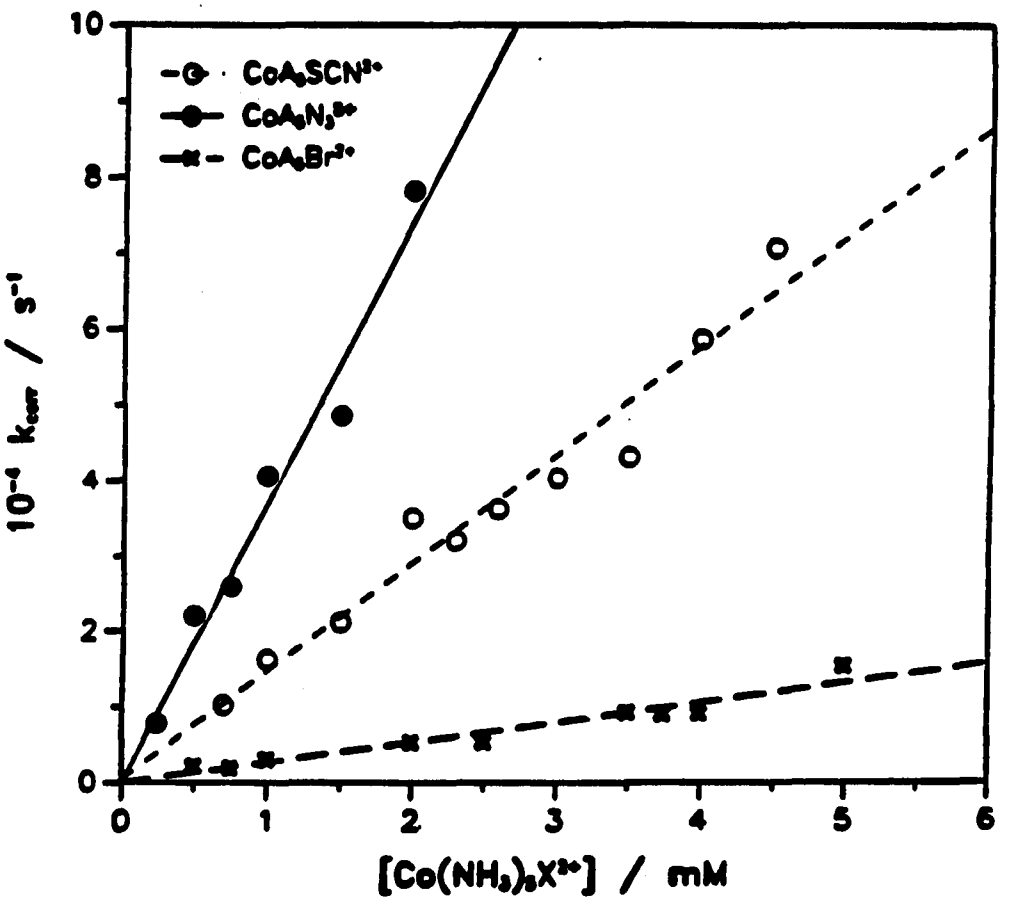

Figure I-3. The plot of the corrected rate constants versus $[L_nCo^{III}X]$ for the reaction of ethyl radical with cobalt(III) complexes. Kinetic data were obtained in 0.50 M H_2SO_4 at 23°C. Data are shown for the complexes $Co(NH_3)_5Br^{2+}$ (using both the $ABTS^{\bullet-}$ and $IrCl_6^{2-}$ methods), $Co(NH_3)_5SCN^{2+}$, $Co(NH_3)_5N_3^{2+}$

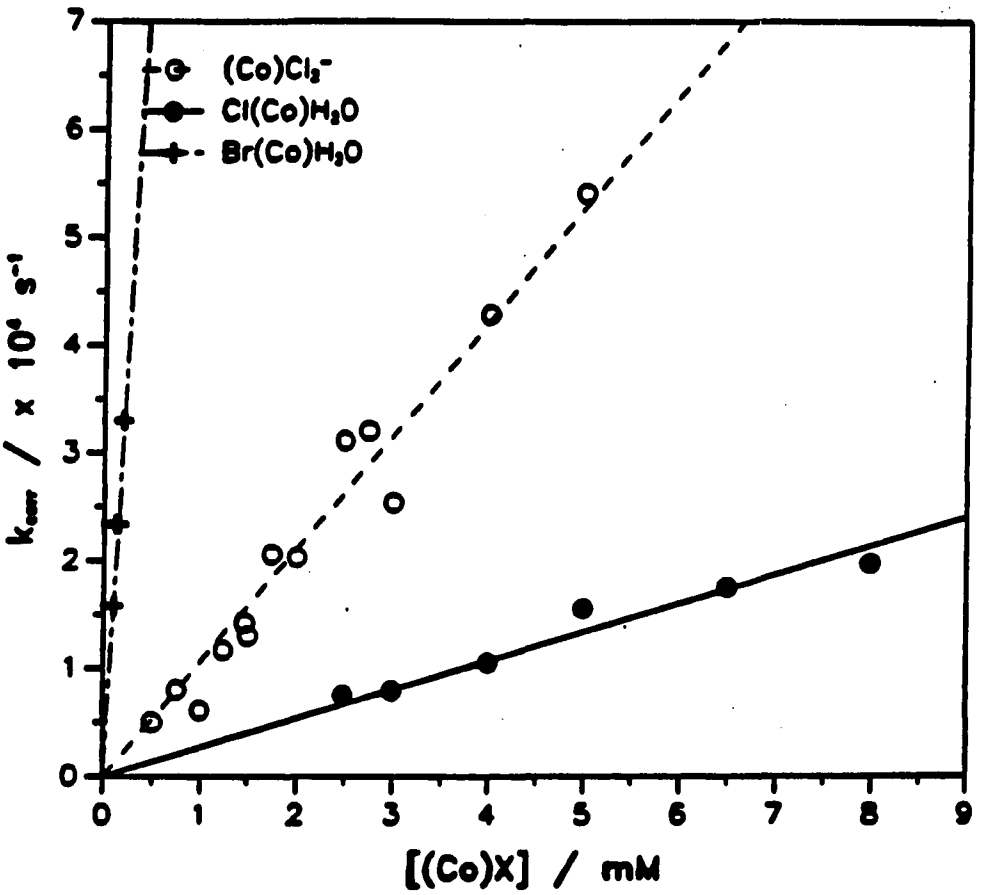

Figure I-4. The plot of the corrected rate constants versus $[L_nCo^{III}X]$ for the reaction of ethyl radical with cobalt(III) complexes. Kinetic data were obtained in 0.50 M H_2SO_4 at 23°C. Data are shown for the complexes $ClCo(dmgH)_2H_2O$, $Co(dmg_2H_3)Cl_2$, and $BrCo(dmgH)_2CH_3CN$

Table I-1. Summary of rate constants[a] for reduction of cobalt(III) complexes by ethyl radical

Co(III) complexes	$k_{Co}/10^6$ L mol^{-1} s^{-1}	
	Laser Flash Photolysis [b]	Product Ratios [c]
$Co(NH_3)_5Cl^{2+}$	< 0.3	0.018
$Co(NH_3)_5Br^{2+}$	2.6(3.0)[d]	
$Co(NH_3)_5N_3^{2+}$	37	
$Co(NH_3)_5SCN^{2+}$	14	
$Co(NH_3)_5NCS^{2+}$	< 0.2	
$Co(NH_3)_5H_2O^{2+}$	< 0.2	
$Co(NH_3)_5F^{2+}$	< 0.2	
$Co(NH_3)_5CN^{2+}$	< 0.4	
trans-$Co(en)_2Cl_2^+$	~0.6	
cis-$Co(en)_2Cl_2^+$	< 0.2	
cis-$Co(en)_2(H_2O)Cl^{2+}$	< 0.3	
$ClCo(dmgH)_2H_2O$	2.3	3
$Co(dmg_2H_3)Cl_2$	10.5	6
$BrCo(dmgH)_2CH_3CN$	160	
$Co(dmg_2H_3)Br_2$	530	

[a]At 23 ± 2 °C, with an estimated precision of ± 20%. [b]With $ABTS^{\bullet-}$ as chromophore in 0.50 M H_2SO_4. [c]Relative to k = 2.6 x 10^6 L mol^{-1} s^{-1} for $Co(NH_3)_5Br^{2+}$ in 0.01 M $HClO_4$. [d]With $IrCl_6^{2-}$ as chromophore.

The method fails for many of the chloro-containing cobalt complexes, whose values of k_{Co} are low. Roughly speaking, we are unable to determine a rate constant smaller than about 5×10^5 L mol^{-1} s^{-1}, although the actual limit depends on the solubility of the given Co(III) complex. Upper limits on the rate constants for a number of slowly reacting compounds are also given in **Table I-1**.

The product ratio method was applied to the complexes $Co(NH_3)_5Cl^{2+}$, $Co(dmgH)_2(H_2O)Cl$, and $Co(dmg_2H_3)Cl_2$ relative to $Co(NH_3)_5Br^{2+}$. The ethyl halides were determined by analysis of the solution phase of the reaction solutions. The ratio of $[C_2H_5Cl]/[C_2H_5Br]$ was then plotted against the ratio $[L_nCo^{III}Cl]/[Co(NH_3)_5Br^{2+}]$ according to eq 10. These data are listed in **Tables A-9 to A-11**. For example, the competition between $Co(NH_3)_5Cl^{2+}$ and $Co(NH_3)_5Br^{2+}$ afforded a ratio $k_{Cl}/k_{Br} = 6.4 \times 10^{-3}$. This in turn gave $k_{Cl} = 1.8 \times 10^4$ L mol^{-1} s^{-1}, a value much smaller than the laser technique is capable of measuring. The rate constants for $Co(NH_3)_5Cl^{2+}$ and the two chlorocobaloxime complexes are shown opposite those obtained flash photolytically in **Table I-1**.

Reactions of Ethyl Radical with $Ru(NH_3)_5X^{2+}$

Kinetic studies were limited to two complexes, $Ru(NH_3)_5Br^{2+}$ and $Ru(NH_3)_5Cl^{2+}$. Laser flash photolysis studies were performed using $Ru(NH_3)_5Br^{2+}$ with $IrCl_6^{2-}$ as chromophore. The pseudo-first-order rate constants obtained at low $Ru(NH_3)_5Br^{2+}$ concentration, listed in **Table A-12**, gave a linear correlation with a slope of $k_{RuBr} = 1.6 \times 10^7$ L mol^{-1} s^{-1}. At higher concentrations k_ψ decreased with increasing $[Ru(NH_3)_5Br^{2+}]$ until precipitation occurred. Attempts to use $ABTS^{\bullet-}$ as chromophore were completely unsuccessful, with k_ψ inexplicably decreasing with increasing $[Ru(NH_3)_5Br^{2+}]$ from the outset.

A second approach to obtain k_{RuBr} was taken in which the thermal reaction of $(H_2O)_5CrC_2H_5^{2+}$ with $Fe(bpy)_3^{3+}$ was used to provide the source of ethyl radicals, eq 13. The excess reagents, $Fe(bpy)_3^{3+}$ (eq 14) and $Ru(NH_3)_5Br^{2+}$ (eq 15), then compete for the radical.

$$(H_2O)_5CrC_2H_5^{2+} + Fe(bpy)_3^{3+} \longrightarrow {}^{\bullet}C_2H_5 + Cr_{aq}^{2+} + Fe(bpy)_3^{2+} \quad (13)$$

$${}^{\bullet}C_2H_5 + Fe(bpy)_3^{3+} \longrightarrow Fe(bpy)_3^{2+} + C_2H_4 + H^+ \quad (14)$$

$${}^{\bullet}C_2H_5 + Ru(NH_3)_5Br^{2+} + H_2O \longrightarrow C_2H_5Br + Ru(NH_3)_5H_2O^{2+} \quad (15)$$

Reaction solutions were prepared with concentrations 0.13 mM $(H_2O)_5CrC_2H_5^{2+}$, 0.40 mM $Fe(bpy)_3^{3+}$, 5.0 mM $Ru(NH_3)_5Br^{2+}$, and 0.10 M $HClO_4$. The reaction was run in a septum-sealed 1-cm spectrophotometer cell filled to capacity to minimize the vapor space above the solution. In each of three identical trials the concentration of ethyl bromide produced was 3.0×10^{-5} M (determined by gas-chromatographic calibration with standard solutions of C_2H_5Br). This corresponds to 23% of the total ethyl radicals reacting with $Ru(NH_3)_5Br^{2+}$ as in eq 15. Since all other pathways were negligible, 77% of the ethyl radicals reacted with $Fe(bpy)_3^{3+}$. With $k_{14} = 9.2 \times 10^8$ L mol^{-1} s^{-1} (vide infra), this yields a rate constant of $k_{RuBr} = 2.2 \times 10^7$ L mol^{-1} s^{-1}.

The final approach taken to gain a further estimate for k_{RuBr} involved another product ratio method. First, the competition of $Ru(NH_3)_5Cl^{2+}$ and $Co(NH_3)_5Br^{2+}$ was employed. From the ratio of ethyl chloride to ethyl bromide and the known rate constant for $Co(NH_3)_5Br^{2+}$, a value of $k_{RuCl} = 6 \times 10^6$ L mol^{-1} s^{-1} was determined (using eq 10). Then, a second competition between $Ru(NH_3)_5Cl^{2+}$ and $Ru(NH_3)_5Br^{2+}$ gave product ratios such that $k_{RuCl}/k_{RuBr} = 0.094$, from which $k_{RuBr} = 7 \times 10^7$ L mol^{-1} s^{-1}. These data are listed in **Table A-13 and A-14**.

Product Analysis

Gas chromatographic measurements were made for several of the cobalt and ruthenium complexes to determine the identity and quantity of the product(s) formed. These experiments were performed by slowly photolyzing ethylcobaloxime in the presence of excess metal halide complex so that all other reaction pathways of $^{\bullet}C_2H_5$ were prevented. In each case the ethyl halide was detected in at least 90% yield. Specifically, the percent of the original concentration of $C_2H_5Co(dmgH)_2H_2O$ found as ethyl halide was: $Co(NH_3)_5Br^{2+}$, > 95%; $Co(NH_3)_5Cl^{2+}$, > 90%; $Ru(NH_3)_5Br^{2+}$, > 93%; $Ru(NH_3)_5Cl^{2+}$, > 90%; $Co(dmg_2H_3)Cl_2$, > 90%; $Co(dmgH)_2(H_2O)Cl$, > 90%. Control experiments showed that the presence of high concentrations of free halide in the photolyzed solutions was immaterial.

Experiments were also carried out to determine the product(s) of the reaction between $^{\bullet}C_2H_5$ and $Co(NH_3)_5SCN^{2+}$. Both C_2H_5SCN and C_2H_5NCS were used as GC standards. The only organic product detected in the solution phase was C_2H_5SCN; no C_2H_5NCS was detected. Ethylene was detected in the vapor above the photolyzed solution. Photolysis of $C_2H_5Co(dmgH)_2H_2O$ in concentrated solutions of $Co(NH_3)_5NCS^{2+}$ gave no detectable formation of C_2H_5SCN or C_2H_5NCS; only ethyl radical self-reaction products were observed.

In the case of each metal halide, a small amount of C_2H_4 was detected amounting by difference to an estimated 5 - 10%. Ethylene was not a result of self-reactions because ethane and butane were not present.

Reactions of Ethyl Radical with Chromophores

In the course of this study, rate constants were measured for the reactions of ethyl radical with certain chromophores and chromogens we used or attempted to use. The values of k_ψ are listed in **Tables A-15 to A-19** for each chromophore studied. Rate constants for the substrates $ABTS^{\bullet-}$, $MV^{\bullet+}$, $IrCl_6^{2-}$, $Fe(bpy)_3^{3+}$, $Fe(phen)_3^{3+}$, and $Cr(bpy)_3^{3+}$ are given in **Table I-2**. The determination of the $MV^{\bullet+}$ rate constant required careful purification of ethylcobaloxime to avoid the rapid oxidation by $Co(dmgH)_2(H_2O)^+$ impurities. The experiments with $ABTS^{\bullet-}$ were without complication and the rate constants for a series of alkyl radicals were readily obtained; these are listed in **Table I-3**. The values of k_ψ are listed in **Tables A-20 to A-34** for each alkyl radical studied.

In two separate determinations, the $IrCl_6^{2-}$ rate constant was obtained by adding deaerated $C_2H_5Co(dmgH)_2H_2O$ to the reaction solution just prior to the flash to avoid the slow thermal

Table I-2. Rate constants[a] for the reactions of ethyl radical with various chromophoric substrates

Compound	$k/10^9$ L mol^{-1} s^{-1}	Reference
$ABTS^{\bullet-}$	0.92	This work
$MV^{\bullet+}$	1.2	This work
	1.0	4[b]
$IrCl_6^{2-}$	2.8	This work
	2.7	This work[c]
	3.1	22[d]
$Fe(phen)_3^{3+}$	1.5	This work
	1.0	32[e]
$Fe(bpy)_3^{3+}$	0.92	This work[f]
$Cr(bpy)_3^{3+}$	0.018	This work

[a]In aqueous solution at 23 ± 2 °C with $C_2H_5Co(dmgH)_2H_2O$ as the source of $^{\bullet}C_2H_5$. [b]With $C_2H_5Co(cyclam)H_2O^{2+}$ as radical precursor. [c]With $ABTS^{\bullet-}$ as kinetic probe. [d]By pulse radiolysis. [e]By pulse radiolysis. [f]With $C_2H_5Co(cyclam)H_2O^{2+}$ as radical precursor, to avoid thermal reactions.

Table I-3. Rate constants[a] for the reactions of alkyl radical with $ABTS^{\bullet-}$

alkyl radical	$k_A/10^9$ L mol^{-1} s^{-1}
CH_3	1.0 ± 0.1
C_2H_5	0.92 ± 0.08
C_3H_7	1.0 ± 0.1
$1\text{-}C_4H_9$	1.1 ± 0.1
$1\text{-}C_5H_{11}$	0.96 ± 0.09
$1\text{-}C_6H_{13}$	0.88 ± 0.08
$1\text{-}C_7H_{15}$	0.98 ± 0.09
$1\text{-}C_8H_{17}$	1.1 ± 0.1
iso-butyl	0.95 ± 0.09
$C_6H_5CH_2$	1.0 ± 0.1
$2\text{-}C_3H_7$	1.2 ± 0.1
$cyclo\text{-}C_5H_9$	1.0 ± 0.1
CH_3OCH_2	1.5 ± 0.2
$ClCH_2$	1.0 ± 0.1
$BrCH_2$	1.7 ± 0.2

[a]Using 0.50 M H_2SO_4 or 1.0 M $HClO_4$ at 23 ± 0.5 °C.

reaction of $IrCl_6^{2-}$ with ethylcobaloxime.[27] A rate constant of $k_{Ir} = 2.8 \times 10^9$ L mol^{-1} s^{-1} was determined directly for the reaction of $IrCl_6^{2-}$ with $^{\bullet}C_2H_5$ by monitoring the loss of absorbance at 487 nm. In addition, an indirect determination of k_{Ir} was obtained by competition with $ABTS^{\bullet-}$. These kinetics were monitored at the $ABTS^{\bullet-}$ wavelength, 650 nm (**Table A-35**), and yielded $k_{Ir} = 2.7 \times 10^9$ L mol^{-1} s^{-1}.

Because the thermal reactions of $Fe(bpy)_3^{3+}$ and $Fe(phen)_3^{3+}$ with ethylcobaloxime were so fast, the more inert $C_2H_5Co(cyclam)H_2O^{2+}$ radical precursor was used. Finally, determination of the $Cr(bpy)_3^{3+}$ rate constant required the presence of iodide to quench the excited state, $^{*}Cr(bpy)_3^{3+}$, formed in the flash.[28]

Varied products were formed in these reactions. For example, the reaction of $^{\bullet}C_2H_5$ with $ABTS^{\bullet-}$ yielded about 30% ethylene and 70% nonvolatile product(s), presumed to be a species in which substitution of C_2H_5 at an aromatic ring carbon has taken place, eq 3. A large amount of C_2H_4 was formed in the reactions of $^{\bullet}C_2H_5$ with $Fe(bpy)_3^{3+}$ and $Fe(phen)_3^{3+}$ (eq 14), indicating that ring substitution products are either minor or absent. On the other hand, with $Cr(bpy)_3^{3+}$ no ethane, ethylene, or butane was formed. A strong and readily detected chromium(II)-bipyridyl absorption at 560 nm was observed. Ethyl chloride was the major product of the

reaction between $^{\bullet}C_2H_5$ and $IrCl_6^{2-}$, although traces of ethylene were also detected.[22]

DISCUSSION

Reactions of Ethyl Radical with Co(III) and Ru(III) Complexes

Ethyl radicals, generated along with $Co(dmgH)_2(H_2O)_2$ in the flash photolysis of $C_2H_5Co(dmgH)_2H_2O$ (eq 16), have been shown to react with $Co(NH_3)_5X^{2+}$, $Co(dmgH)(X)(Y)$, and $Ru(NH_3)_5X^{2+}$ complexes (X = Br, Cl; Y = H_2O, CH_3CN) through the use of kinetic probe reagents. Under acidic conditions $Co(dmgH)_2(H_2O)_2$ decomposes to give Co_{aq}^{2+} and dimethylglyoxime, eq 17.[29]

$$C_2H_5Co(dmgH)_2H_2O + H_2O + h\nu \longrightarrow {}^{\bullet}C_2H_5 + Co(dmgH)_2(H_2O)_2 \quad (16)$$

$$Co(dmgH)_2(H_2O)_2 + 2\ H^+ \longrightarrow Co_{aq}^{2+} + 2\ dmgH_2 \quad (17)$$

The formation of C_2H_5X from the reactions of ${}^{\bullet}C_2H_5$ with these metal halides directly substantiates an inner-sphere mechanism for these reactions. Therefore, the early supposition by Haim and Taube[1] has been proven correct. The rate constants for these reactions, k_{Co}, are listed in **Table I-1** and range from 10^4 to 10^8 L mol^{-1} s^{-1}. The agreement in the k_{Co}-values for the reaction of ${}^{\bullet}C_2H_5$ with $Co(NH_3)_5Br^{2+}$ obtained from the $ABTS^{\bullet-}$ and $IrCl_6^{2-}$ kinetic probe methods assists in confirming the correctness of the procedures adopted.

The rate constants follow the so-called "normal" reactivity order, with (F) < Cl < Br, for both the pentaammine halo series and the dimethylglyoxime derivatives. The higher reactivity of the dimethylglyoxime complexes as compared to the pentaammines can be accounted for by the stablizing effect of the macrocyclic ligand toward Co(II) formation in the transition state.

A kinetic trans-effect was displayed by the dichlorocobalt complexes, trans-$Co(en)_2Cl_2^+$ and cis-$Co(en)_2Cl_2^+$, as evidenced by the measurable reactivity of $^{\bullet}C_2H_5$ with the trans-substituted species.

The detection of C_2H_5SCN from the reaction of $Co(NH_3)_5SCN^{2+}$ with $^{\bullet}C_2H_5$ also establishes an inner-sphere mechanism. Furthermore, quantitative formation of the sulfur-bound product indicates that the reaction proceeds entirely by an adjacent attack mechanism. We suggest that the relatively small size permits the more ready approach of $^{\bullet}C_2H_5$ to the sulfur atom in the primary coordination sphere of cobalt. The enhanced polarizability of sulfur over that of nitrogen may also explain the "electron-mediating ability" of sulfur in this reaction.[30]

While $Co(NH_3)_5SCN^{2+}$ was shown to react rapidly with $^{\bullet}C_2H_5$ with a rate constant of $k = 1.4 \times 10^7$ L mol^{-1} s^{-1}, the reaction with $Co(NH_3)_5NCS^{2+}$ was too slow to measure using this method ($k < 2 \times 10^5$ L mol^{-1} s^{-1}). The reactivity ratio is probably even

higher than the upper limit suggests. For example, Fe^{2+}, V^{2+}, Cr^{2+}, and $Co(CN)_5^{3-}$ have k_{SCN}/k_{NCS} ratios of >4 x 10^4, 10^2, 10^4, and 10^{2-3}, respectively.[31]

The reactivity of $Co(NH_3)_5N_3^{2+}$ ($k = 3.7 \times 10^7$ L mol^{-1} s^{-1}) is somewhat higher than that of $Co(NH_3)_5SCN^{2+}$, whereas the opposite is true for metal reductants.[1] Although the product of the azide reaction was not determined, this inverted reactivity trend can be rationalized by considering the affinity of a carbon-centered radical for the N=N bonds of the coordinated azide ion. The ability of metal cations to coordinate olefinic species is low, resulting in lower rates of reaction for $Co(NH_3)_5N_3^{2+}$. Of the metal ions studied only Cr^{2+}, which has a high affinity for nitrogen, has a rate of reaction with $Co(NH_3)_5N_3^{2+}$ which is comparable to that with $Co(NH_3)_5SCN^{2+}$.[31] On the other hand, $^{\bullet}C_2H_5$ has a greater affinity for double bonds and thus reacts more readily with $Co(NH_3)_5N_3^{2+}$.

Comparison was made between the laser flash photolysis and the product ratio method. Our initial intent to monitor the reactions of $Co(NH_3)_5Br^{2+}$ and $Co(NH_3)_5Cl^{2+}$ with $^{\bullet}C_2H_5$ using both methods was prevented by the low reactivity of $Co(NH_3)_5Cl^{2+}$. Instead the comparison was performed using the sufficiently reactive chloro- and dichlorocobaloxime complexes, having rate

constants 2.3×10^6 and 1.05×10^7 L mol^{-1} s^{-1}, respectively. The rate constants from the product ratio method were only in fair agreement with the flash photolytically determined values, **Table I-1**, although the agreement was sufficiently close to suggest that both procedures are correct in concept and execution.

The complexes $Ru(NH_3)_5X^{2+}$ (X = Br, Cl) are more reactive than their cobalt counterparts by factors of 300 (Cl) and 10 (Br). The greater reactivity of ruthenium was also observed in their reductions by α-hydroxyalkyl radicals.[2]

Reactions of Ethyl Radical with Chromophores

Rate constants for the reactions of $^{\bullet}C_2H_5$ with chromophoric reagents are shown in **Table I-2**. The ability to reproduce known rate constants for the reaction of $^{\bullet}C_2H_5$ with $MV^{\bullet+}$,[4] $k_{MV} = 1.2 \times 10^9$ L mol^{-1} s^{-1}, $IrCl_6^{2-}$,[22] $k_{Ir} = 2.8 \times 10^9$ L mol^{-1} s^{-1}, and $Fe(phen)_3^{3+}$,[32] $k_{Fe} = 1.5 \times 10^9$ L mol^{-1} s^{-1}, in the pH range 0-7 has revealed that laser flash photolysis of $C_2H_5Co(dmgH)_2H_2O$ is a useful and clean method for generating reagent concentrations of $^{\bullet}C_2H_5$.

The primary chromophore in this study, $ABTS^{\bullet-}$, was shown to react with $^{\bullet}C_2H_5$ (eq 3) with a rate constant $k_A = 9.2 \times 10^8$ L mol^{-1} s^{-1}, **Table I-3**.

The agreement of the reported rate constant, $k_{Ir} = 3.1 \times 10^9$ L mol^{-1} s^{-1}, with the directly determined value of k_{Ir} and the value determined indirectly using $ABTS^{\bullet-}$ adds further credibility to the $ABTS^{\bullet-}$ kinetic probe method.

The reactions of $^{\bullet}C_2H_5$ with $Fe(bpy)_3^{3+}$ and $Fe(phen)_3^{3+}$ (E° = 1.0 V) have second-order rate constants on the order of 10^9 L mol^{-1} s^{-1} and produce the outer-sphere product, C_2H_4 (eq 14).[32] On the other hand, $Cr(bpy)_3^{3+}$ (E° = -0.26 V) reacts more slowly, having a rate constant of 1.8×10^7 L mol^{-1} s^{-1}, and yields nonvolatile product(s) (presumably $Cr(bpy)_2(bpy\text{-}C_2H_5)^{2+}$, eq 18). The great difference in reduction potentials for these compounds

$$Cr(bpy)_3^{3+} + {}^{\bullet}C_2H_5 \longrightarrow Cr(bpy)_2(bpy\text{-}C_2H_5)^{2+} + H^+ \qquad (18)$$

could result in significantly different mechanisms for reaction with $^{\bullet}C_2H_5$. The large driving force present in the reactions, coupled with the lability of $Fe(bpy)_3^{3+}$ and $Fe(phen)_3^{3+}$, suggests that electron transfer between the ethyl radical and Fe(III) could occur within the interstices of the bipyridine ligands.[32] It is likely that the reaction of $^{\bullet}C_2H_5$ with the substitutionally inert $Cr(bpy)_3^{3+}$ goes by a more sluggish ring addition mechanism.

Summary

The kinetics of the reactions of $^{\bullet}C_2H_5$ with $Co(NH_3)_5X^{2+}$, $Ru(NH_3)_5X^{2+}$, and $Co(dmgH)_2(X)(Y)$ (X = Br, Cl, N_3, SCN; Y = H_2O, CH_3CN) complexes were studied using laser flash photolysis of ethylcobalt complexes. The kinetics were obtained by the kinetic probe method using $ABTS^{\bullet-}$ and $IrCl_6^{2-}$. Some relative rate constants were also determined by a competition method based on ethyl halide product ratios. The products of these reactions are largely (> 90%) the ethyl halide and ethyl thiocyanate, substantiating an inner-sphere mechanism. Minor but regular yields of C_2H_4 are also found (< 10%), suggesting a small contribution from the outer-sphere oxidation of $^{\bullet}C_2H_5$.

BIBLIOGRAPHY

1. Haim, A. Prog. Inorg. Chem. 1983, 30, 326.

2. Meyerstein, D.; Cohen, H. J. C. S. Dalton 1977, 1056

3. Haim, A.; Taube, H. J. Am. Chem. Soc. 1963, 85, 495.

4. Bakac, A.; Espenson, J. H. Inorg. Chem. 1989, 28, 3901.

5. Bakac, A.; Espenson, J. H. Inorg. Chem. 1989, 28, 4319.

6. The methyl viologen radical cation, $MV^{\bullet+}$, used successfully as a kinetic probe in reactions involving reducing substrates,[4,5] could not be employed in the present system because of its incompatability with the Co(III) and Ru(III) complexes.

7. Hunig, S. Justis Leibigs Ann. de Chemie 1964, 676, 32.

8. Wolfenden, B. S.; Willson, R. L. J. C. S. Perkin Trans II 1982, 805.

9. (a) Rush, J. D.; Koppenol, W. H. J. Am. Chem. Soc. 1988, 110, 4957; (b) Lindsay Smith, J. R.; Balasubramanian, P. N.; Bruice, T. C. J. Am. Chem. Soc. 1988, 110, 7411.

10. Majkic-Singh, N.; Bogavac, L.; Kalimanovska, V.; Jelic, Z.; Spasic, S. Clinica Chimica Acta 1987, 162, 29.

11. Erban-Russ, M.; Michel, C.; Bors, W.; Saran, M. J. Phys. Chem. 1987, 91, 2362.

12. (a) Diehl, H. Inorg. Syn. 1939, 1, 187. (b) Lalor, G. C.; Moelwyn-Hughes, E. A. J. Chem. Soc. 1963, 1560. (c) Carlin, R. L.; Edwards, J. O. J. Inorg. Nucl. Chem. 1958, 6, 217. (d) Buckingham, D. A.; Creaser, I. I.; Sargeson, A. M. Inorg. Chem. 1970, 9, 655. (e) Basolo, F.; Murmann, R. K. Inorg. Syn. 1953, 4, 172. (f) Siebart, H. Z. Anorg. Allgem. Chem. 1974, 327, 63. (g) Costa, G.; Tauhzer, G.; Puxeddu, A. Inorg. Chim. Acta 1969, 3, 45; (h) McHatton, R. C. Ph. D. Dissertation, Iowa State University, Ames Iowa, 1982. (i) Bailar, J. C. Inorg. Syn. 1946, 2, 222. (j) Vaughn, J. W.; Lindholm, R. D. Inorg. Syn. 1967, 9, 163.

13. Taube, H. Inorg. Syn. 1986, 24, 258.

14. (a) Baker, B. R.; Mehta, B. D. Inorg. Chem. 1965, 4, 808. (b) Kochi, J. K.; Wong, C. L. J. Am. Chem. Soc. 1979, 101, 5593.

15. Yamazaki, N.; Hohokabe, Y. Bull. Chem. Soc. Japan 1971, 44, 63.

16. Schrauzer, G. N. Inorg. Syn. 1968, 11, 65.

17. Bakac, A.; Espenson, J. H. Inorg. Chem. 1987, 26, 4353.

18. Maruthamuthu, P.; Venkatasubramanian, L.; Dharalingham, P. Bull. Chem. Soc. Japan 1987, 60, 1113.

19. (a) Schmidt, W.; Swinehart, J. H.; Taube, H. J. Am. Chem. Soc. 1971, 93, 1117; (b) Leslie, J. P., II; Espenson, J. H. J. Am. Chem. Soc. 1976, 98, 4839.

20. Connolly, P. Ph.D. Dissertation, Iowa State University, Ames, Iowa, 1985.

21. (a) Melton, J. D.; Espenson, J. H.; Bakac, A. Inorg. Chem. 1986, 25, 4104; (b) Hoselton, M. A.; Lin, C.-T.; Schwartz, H. A.; Sutin, N. J. Am. Chem. Soc. 1978, 100, 2383. The energy of the laser pulse is 250 mJ.

22. Steenken, S.; Neta, P. J. Am. Chem. Soc. 1982, 104, 1244.

23. Hickel, B. J. Phys. Chem. 1975, 79, 1054.

24. Bakac, A.; Espenson, J. H. J. Phys. Chem. 1986, 90, 325.

25. Barshop, B. A.; Wrenn, R. F.; Frieden, C. Anal. Biochem. 1983, 130, 130.

26. Eq 7 is an approximate representation, in that C_2H_4 was also formed in minor amount (vide infra).

27. Halpern, J. Angew. Chem. Int. Ed. Engl. 1985, 24, 274 and references cited therein.

28. Serpone, N.; Jamieson, M. A.; Henry, M. S.; Hoffmann, M. Z.; Bolletta, F.; Maestri, M. J. Am. Chem. Soc. 1979, 101, 2907.

29. Gjerde, H. B.; Espenson, J. H. Organometallics 1982, 1, 435.

30. (a) Shea, C.; Haim, A. J. Am. Chem. Soc. 1971, 93, 3055.
(b) Haim, A.; Sutin, N. J. Am. Chem. Soc. 1966, 88, 434.
(c) Haim, A.; Sutin, N. J. Am. Chem. Soc. 1965, 87, 4210.

31. (a) Fay, D. P.; Sutin, N. Inorg. Chem. 1970, 9, 1291;
(b) Haim, A. J. Am. Chem. Soc. 1963, 85, 1016;
(c) Espenson, J. H. Inorg, Chem. 1965, 4, 121;
(d) Candlin, J. P.; Halpern, J.; Trimm, D. L. J. Am. Chem. Soc. 1964, 86, 1019; (e) Shea, C.; Haim, A. Inorg. Chem. 1973, 12, 3013. These rate constants have been summarized in Ref. 1.

32. Grodkowski, J.; Neta, P.; Schlesener, C. J.; Kochi, J. K. J. Phys. Chem. 1985, 89, 4373.

APPENDIX

Table A-1. Kinetic data of the reaction of ethyl radical with $Co(NH_3)_5Br^{2+}$

Conditions: $[C_2H_5Co(dmgH)_2H_2O]$ = 30 μM

λ = 650 nm

T = 23 ± 2 °C, in 0.50 M H_2SO_4

$[P]_{ave}/\mu M$	$[P]_L$[a]/μM	$[Co(NH_3)_5Br^{2+}]$/mM	$10^{-4}k_\psi/s^{-1}$	$10^{-4}k_{corr}/s^{-1}$
34.0	1.7	5.00	4.91	1.62
33.7	1.1	5.00	4.61	1.45
32.6	2.4	4.00	4.16	0.903
32.0	2.3	4.00	4.07	0.880
32.7	2.3	4.00	4.24	0.991
30.9	2.0	4.00	3.90	0.853
35.1	1.5	3.75	4.23	0.899
34.2	2.0	3.50	4.22	0.898
34.6	2.0	3.50	4.30	0.944
34.1	2.2	2.50	3.93	0.607
33.8	2.3	2.50	3.77	0.459
32.3	1.4	2.00	3.69	0.641
31.5	1.6	2.00	3.67	0.665
30.9	1.9	2.00	3.41	0.417
30.4	1.4	2.00	3.26	0.378
31.4	2.8	1.00	3.41	0.275
30.0	2.8	1.00	3.32	0.307
28.7	2.4	1.00	3.14	0.294
28.8	2.5	1.00	3.19	0.322
39.9	3.1	0.75	4.04	0.131
39.0	2.3	0.75	3.95	0.219
37.1	2.0	0.75	3.87	0.343
37.7	2.0	0.75	3.64	0.060
27.8	2.5	0.50	2.97	0.203
27.3	2.6	0.50	2.96	0.224

[a] $[P]_L$ refers to the concentration of $ABTS^{\bullet-}$ consumed or 'lost' in the reaction.

Table A-2. Kinetic data of the reaction of ethyl radical with $Co(NH_3)_5Br^{2+}$

Conditions: $[C_2H_5Co(dmgH)_2H_2O]$ = 30 μM
λ = 487 nm
T = 23 ± 2 °C, in 0.50 M H_2SO_4

$[P]_{ave}/\mu M$	$[P]_L$[a]/μM	$[Co(NH_3)_5Br^{2+}]/mM$	$10^{-4}k_\psi/s^{-1}$	$10^{-4}k_{corr}/s^{-1}$
12.7	3.9	2.00	5.20	1.26
16.4	2.8	2.70	5.23	0.45
13.9	4.1	2.70	5.12	0.81
9.9	2.3	2.70	3.67	0.68
14.4	3.2	3.40	5.00	1.10
12.7	3.3	3.40	5.25	1.77
16.5	2.6	4.30	5.60	1.14
13.9	2.5	4.30	5.25	1.46
12.3	3.1	4.30	6.13	2.73
13.9	2.7	5.00	6.13	1.98
9.5	2.4	5.00	5.05	2.08
16.1	2.6	5.80	6.55	1.83
12.6	3.2	5.80	6.42	2.50
11.8	2.4	5.80	5.45	1.88
10.7	2.3	5.80	5.57	2.30
15.2	2.4	6.50	5.86	1.39
11.1	2.4	6.50	5.33	1.92
10.2	2.5	6.50	5.15	1.95
14.3	2.6	7.50	7.19	2.90

[a] $[P]_L$ refers to the concentration of $IrCl_6^{2-}$ consumed or 'lost' in the reaction.

Table A-3. Kinetic data of the reaction of ethyl radical with $Co(dmg_2H_3)Cl_2$
Conditions: $[C_2H_5Co(dmgH)_2H_2O]$ = 30 μM
λ = 650 nm
T = 23 ± 2 °C, in 0.50 M H_2SO_4

$[P]_{ave}$/μM	$[P]_L$[a]/μM	$[Co(dmg_2H_3)Cl_2]$/mM	$10^{-4}k_\psi/s^{-1}$	$10^{-4}k_{corr}/s^{-1}$
32.8	1.8	0.50	3.61	0.47
31.4	1.4	0.50	3.50	0.53
34.5	1.5	0.75	4.00	0.73
34.4	1.4	0.75	4.11	0.87
31.6	1.6	1.00	3.63	0.59
31.6	1.8	1.00	3.68	0.62
31.4	1.4	1.00	3.62	0.63
33.0	1.8	1.25	4.20	0.99
32.6	1.5	1.25	4.49	1.36
32.5	2.0	1.47	4.67	1.45
32.6	1.6	1.47	4.16	1.00
30.5	1.7	1.47	4.78	1.79
30.2	1.6	1.47	4.38	1.44
35.5	1.4	1.50	4.70	1.32
34.5	1.0	1.50	4.49	1.27
34.6	1.0	1.50	4.53	1.30
34.9	1.2	1.75	5.58	2.30
34.5	1.1	1.75	5.10	1.85
34.3	0.9	1.75	5.23	2.03
31.2	2.2	2.00	5.40	2.21
29.7	1.7	2.00	5.02	2.06
28.4	1.5	2.00	4.56	1.75
28.2	1.4	2.00	4.85	2.08
34.8	1.3	2.25	6.66	3.33
34.9	1.4	2.25	6.33	2.97
35.4	0.8	2.50	6.28	2.98
35.4	0.8	2.50	6.56	3.27
35.5	0.7	2.50	6.75	3.46
36.8	1.8	2.50	6.38	2.77
35.6	1.9	2.75	6.54	2.99
35.3	1.7	2.75	6.90	3.42
35.1	1.6	2.75	6.58	3.14
34.6	1.6	2.75	6.70	3.30
31.2	1.8	3.00	5.75	2.59
30.6	1.6	3.00	5.57	2.49
29.8	1.6	3.00	5.66	2.65
29.4	1.5	3.00	5.38	2.42
36.2	1.9	3.50	6.16	2.55
35.7	1.9	3.50	6.10	2.53
35.5	1.6	3.50	6.08	2.57
35.0	1.2	3.50	6.39	3.01
35.0	1.3	3.50	6.00	2.60
38.3	1.8	4.00	7.89	4.08
37.7	1.5	4.00	8.12	4.44
37.3	1.4	4.00	7.94	4.31
34.5	1.2	5.00	8.52	5.13
31.5	1.1	5.00	8.74	5.62
31.3	1.0	5.00	8.52	5.44

[a] $[P]_L$ refers to the concentration of $ABTS^{\bullet-}$ consumed or 'lost' in the reaction.

Table A-4. Kinetic data of the reaction of ethyl radical with $ClCo(dmgH)_2H_2O$

Conditions: $[C_2H_5Co(dmgH)_2H_2O]$ = 30 μM

λ = 650 nm

T = 23 ± 2 °C, in 0.50 M H_2SO_4

$[P]_{ave}/\mu M$	$[P]_L$[a]/μM	$[ClCo(dmgH)_2H_2O]/mM$	$10^{-4}k_\psi/s^{-1}$	$10^{-4}k_{corr}/s^{-1}$
30.2	2.3	1.50	3.53	0.557
29.1	2.3	1.50	3.57	0.693
31.5	3.0	2.50	3.83	0.619
29.8	3.1	2.50	3.92	0.837
27.4	2.5	2.50	3.68	0.894
26.8	2.1	2.50	3.32	0.647
30.5	2.1	3.00	3.67	0.668
29.0	1.8	3.00	3.54	0.712
28.8	1.4	3.00	3.61	0.857
27.7	2.2	3.00	3.61	0.833
26.5	1.8	3.00	3.50	0.887
30.5	2.4	4.00	3.88	0.809
27.5	2.4	4.00	3.79	0.972
26.5	1.9	4.00	3.54	0.891
26.8	2.3	4.00	3.95	1.21
26.0	1.8	4.00	3.74	1.15
28.2	1.9	5.00	4.38	1.57
27.7	1.7	5.00	4.27	1.53
28.4	2.4	6.50	4.62	1.66
27.2	1.8	6.50	4.50	1.76
25.6	2.0	6.50	4.28	1.63
26.2	1.3	6.50	4.50	1.94
26.1	3.5	8.00	4.92	1.84
24.8	1.7	8.00	4.56	2.01
23.7	2.3	8.00	4.44	1.84
22.6	2.1	8.00	4.67	2.20

[a] $[P]_L$ refers to the concentration of $ABTS^{\bullet-}$ consumed or 'lost' in the reaction.

Table A-5. Kinetic data of the reaction of ethyl radical with $Co(dmg_2H_3)Br_2$

Conditions: $[C_2H_5Co(dmgH)_2H_2O]$ = 30 μM

λ = 650 nm

T = 23 ± 2 °C, in 0.50 M H_2SO_4

$[P]_{ave}/\mu M$	$[P]_L$[a]/μM	$[Co(dmg_2H_3)Br_2]/\mu M$	$10^{-4}k_\psi/s^{-1}$	$10^{-4}k_{corr}/s^{-1}$
25.2	1.5	20.0	3.73	1.31
24.9	1.5	20.0	3.46	1.07
23.7	1.4	20.0	3.40	1.12
25.1	0.8	35.0	4.30	1.94
25.0	1.1	35.0	4.18	1.77
24.4	1.1	35.0	4.37	2.01
31.0	0.9	38.0	4.26	1.37
30.6	1.0	38.0	4.83	1.96
30.4	0.8	50.0	6.33	3.48
30.0	1.0	50.0	5.61	2.76
25.3	1.1	50.0	5.20	2.72
24.9	0.9	50.0	6.51	4.11
24.2	1.0	50.0	6.15	3.79
24.7	1.1	60.0	6.09	3.63
23.6	1.0	60.0	5.67	3.33
24.1	0.6	75.0	7.08	4.77
24.1	0.9	90.0	6.71	4.27

[a] $[P]_L$ refers to the concentration of $ABTS^{\bullet-}$ consumed or 'lost' in the reaction.

Table A-6. Kinetic data of the reaction of ethyl radical with $BrCo(dmgH)_2CH_3CN$

Conditions: $[C_2H_5Co(dmgH)_2H_2O]$ = 30 μM

λ = 650 nm

T = 23 ± 2 °C, in 0.50 M H_2SO_4

$[P]_{ave}/\mu M$	$[P]_L$[a]/μM	$[BrCo(dmgH)_2L]/\mu M$	$10^{-4}k_\psi/s^{-1}$	$10^{-4}k_{corr}/s^{-1}$
22.1	0.6	100	3.96	1.88
21.8	0.9	100	3.98	1.87
21.2	1.0	100	3.07	0.99
20.7	1.0	125	4.59	2.53
19.8	1.1	125	4.51	2.50
19.7	0.8	125	3.92	1.99
19.8	0.8	150	4.54	2.58
19.3	0.8	150	4.01	2.20
22.0	0.8	200	5.61	3.43
21.3	0.7	200	5.25	3.16

[a] $[P]_L$ refers to the concentration of $ABTS^{\bullet-}$ consumed or 'lost' in the reaction; L = CH_3CN.

Table A-7. Kinetic data of the reaction of ethyl radical with $Co(NH_3)_5N_3^{2+}$

Conditions: $[C_2H_5Co(dmgH)_2H_2O]$ = 30 μM

λ = 650 nm

T = 23 ± 2 °C, in 0.50 M H_2SO_4

$[P]_{ave}/\mu M$	$[P]_L$[a]/μM	$[Co(NH_3)_5N_3^{2+}]/mM$	$10^{-4}k_\psi/s^{-1}$	$10^{-4}k_{corr}/s^{-1}$
27.8	2.9	0.25	3.53	0.604
26.5	2.8	0.25	3.58	0.779
25.5	2.3	0.25	3.59	0.960
29.2	2.6	0.50	4.90	1.81
28.3	2.7	0.50	5.29	2.25
27.4	2.3	0.50	5.18	2.29
27.0	2.4	0.50	5.34	2.46
33.8	1.5	0.75	5.86	2.55
33.8	1.1	0.75	6.27	3.04
34.1	1.3	0.75	5.52	2.22
33.3	1.1	0.75	5.74	2.55
29.8	2.5	1.00	7.95	4.64
29.2	2.5	1.00	8.29	5.02
28.8	2.3	1.00	8.13	4.95
33.3	2.2	1.00	6.58	3.08
33.4	1.7	1.00	7.16	3.78
32.2	1.8	1.00	6.82	3.51
32.9	1.7	1.00	6.76	3.42
33.4	1.6	1.50	8.24	4.78
33.2	1.8	1.50	7.78	4.27
28.0	1.6	1.50	8.74	5.70
28.2	1.8	1.50	7.81	4.68
30.1	3.0	2.00	12.7	8.72
30.4	2.8	2.00	11.8	7.91
30.7	2.8	2.00	11.2	7.32
30.7	3.0	2.00	11.2	7.18

[a] $[P]_L$ refers to the concentration of $ABTS^{\bullet-}$ consumed or 'lost' in the reaction.

Table A-8. Kinetic data of the reaction of ethyl radical with $Co(NH_3)_5SCN^{2+}$

Conditions: $[C_2H_5Co(dmgH)_2H_2O]$ = 30 μM
λ = 650 nm
T = 23 ± 2 °C, in 0.50 M H_2SO_4

$[P]_{ave}/\mu M$	$[P]_L$[a]/μM	$[Co(NH_3)_5SCN^{2+}]/mM$	$10^{-4}k_{\psi}/s^{-1}$	$10^{-4}k_{corr}/s^{-1}$
30.7	2.2	0.70	4.04	1.07
29.6	2.0	0.70	3.89	1.04
28.7	1.8	0.70	3.80	1.06
28.6	1.7	0.70	3.63	0.92
33.5	1.4	1.00	4.60	1.50
33.3	1.1	1.00	4.81	1.78
33.9	1.6	1.00	4.76	1.59
28.9	1.2	1.50	4.83	2.11
28.8	1.7	1.50	4.65	1.84
28.3	1.5	1.50	4.70	1.97
27.7	1.3	1.50	5.14	2.50
34.8	1.3	2.00	6.37	3.11
33.8	1.0	2.00	6.63	3.52
34.1	0.9	2.00	6.99	3.88
22.2	0.9	2.30	5.16	3.00
22.0	0.7	2.30	5.37	3.28
22.4	0.8	2.30	5.47	3.32
32.3	1.3	2.59	6.50	3.41
31.8	1.1	2.59	6.98	3.98
32.1	0.9	2.59	6.70	3.72
32.0	0.9	2.59	6.32	3.35
23.2	1.0	3.00	6.10	3.78
23.0	0.7	3.00	6.13	3.93
22.8	0.8	3.00	6.58	4.37
24.3	1.1	3.50	6.78	4.30
23.9	1.0	3.50	6.64	4.25
23.4	1.0	3.50	6.73	4.36
23.0	0.9	4.00	8.42	6.08
22.8	0.9	4.00	7.75	5.43
23.1	0.8	4.00	8.24	5.94
23.5	0.7	4.00	8.25	5.96
23.7	0.8	4.50	9.76	7.38
23.5	0.8	4.50	9.10	6.74

[a] $[P]_L$ refers to the concentration of $ABTS^{\bullet-}$ consumed or 'lost' in the reaction.

Table A-9. Competition between $Co(NH_3)_5Br^{2+}$ and $Co(NH_3)_5Cl^{2+}$ for ethyl radical
Conditions: $[C_2H_5Co(dmgH)_2H_2O]$ = 0.20 mM in 0.01 M H_2SO_4

$[Co(NH_3)_5Cl^{2+}]/[Co(NH_3)_5Br^{2+}]$[a]	$[C_2H_5Cl]_\infty/[C_2H_5Br]_\infty$[b]
94	0.55
59	0.44
35	0.23
14	0.13
8	0.086

[a] $[Co(NH_3)_5Cl^{2+}]_i$ and $[Co(NH_3)_5Br^{2+}]_i \geq 1.0$ mM. [b] Ratio obtained from GC peak areas after photolysis of $C_2H_5Co(dmgH)_2H_2O$ was completed (about 3 minutes).

Table A-10. Competition between $Co(NH_3)_5Br^{2+}$ and $Co(dmg_2H_3)Cl_2$ for ethyl radical
Conditions: $[C_2H_5Co(dmgH)_2H_2O]$ = 0.20 mM in 0.01 M H_2SO_4

$[Co(dmg_2H_3)Cl_2]/[Co(NH_3)_5Br^{2+}]$[a]	$[C_2H_5Cl]_\infty/[C_2H_5Br]_\infty$[b]
0.200	0.50
0.231	0.46
0.272	0.64
0.330	0.71
0.333	0.68
0.500	1.09
0.599	1.20

[a] $[Co(dmg_2H_3)Cl_2]_i$ and $[Co(NH_3)_5Br^{2+}]_i \geq 1.0$ mM. [b] Ratio obtained from GC peak areas after photolysis of $C_2H_5Co(dmgH)_2H_2O$ was completed (about 3 minutes).

Table A-11. Competition between $Co(NH_3)_5Br^{2+}$ and $ClCo(dmgH)_2H_2O$ for ethyl radical

Conditions: $[C_2H_5Co(dmgH)_2H_2O]$ = 0.20 mM in 0.01 M H_2SO_4

$[ClCo(dmgH)_2H_2O]/[Co(NH_3)_5Br^{2+}]$[a]	$[C_2H_5Cl]_\infty/[C_2H_5Br]_\infty$[b]
0.27	0.37
0.43	0.56
0.64	0.79
1.00	1.10
1.40	1.57

[a] $[ClCo(dmgH)_2H_2O]_i$ and $[Co(NH_3)_5Br^{2+}]_i \geq 1.0$ mM. [b] Ratio obtained from GC peak areas after photolysis of $C_2H_5Co(dmgH)_2H_2O$ was completed (about 3 minutes).

Table A-12. Kinetic data of the reaction of ethyl radical with $Ru(NH_3)_5Br^{2+}$

Conditions: $[C_2H_5Co(dmgH)_2H_2O]$ = 30 μM

λ = 487 nm

T = 23 ± 2 °C, in 0.50 M H_2SO_4

$[IrCl_6^{2-}]_{ave}$/μM	$[IrCl_6^{2-}]_L$[a]/μM	$[Ru(NH_3)_5Br^{2+}]$/mM	$10^{-4}k_\psi/s^{-1}$
17.3	2.4	0.260	5.45
17.7	2.9	0.380	5.69
17.3	3.0	0.475	5.91
17.4	2.5	0.570	6.31
21.9	2.2	0.700	6.38
18.3	2.4	0.730	5.75
20.7	2.6	0.940	7.33
21.9	2.7	1.23	6.81
21.4	3.0	1.46	6.80
15.8	1.9	1.67	4.92
22.4	2.3	1.75	5.63
24.0	2.0	1.96[b]	5.36
19.2	1.5	2.42[b]	5.80
19.6	1.6	3.10[b]	4.37
18.1	2.3	3.90[b]	4.30

[a] $[IrCl_6^{2-}]_L$ refers to the concentration of $IrCl_6^{2-}$ consumed or 'lost' in the reaction. [b] The solution became cloudy ~1 minute after mixing the reagents.

Table A-13. Competition between $Co(NH_3)_5Br^{2+}$ and $Ru(NH_3)_5Cl^{2+}$ for ethyl radical
Conditions: $[C_2H_5Co(dmgH)_2H_2O]$ = 0.20 mM in 0.01 M H_2SO_4

$[Ru(NH_3)_5Cl^{2+}]/[Co(NH_3)_5Br^{2+}]$[a]	$[C_2H_5Cl]_\infty/[C_2H_5Br]_\infty$[b]
0.17	0.39
0.19	0.47
0.22	0.50
0.29	0.66
0.37	0.79
0.47	1.01

[a] $[Ru(NH_3)_5Cl^{2+}]_i$ and $[Co(NH_3)_5Br^{2+}]_i \geq 1.0$ mM. [b] Ratio obtained from GC peak areas after photolysis of $C_2H_5Co(dmgH)_2H_2O$ was completed (about 3 minutes).

Table A-14. Competition between $Ru(NH_3)_5Br^{2+}$ and $Ru(NH_3)_5Cl^{2+}$ for ethyl radical
Conditions: $[C_2H_5Co(dmgH)_2H_2O]$ = 0.20 mM in 0.01 M H_2SO_4

$[Ru(NH_3)_5Cl^{2+}]/[Ru(NH_3)_5Br^{2+}]$[a]	$[C_2H_5Cl]_\infty/[C_2H_5Br]_\infty$[b]
2.1	0.151
2.8	0.281
3.4	0.284
4.0	0.411
4.6	0.473
5.2	0.471
5.8	0.539

[a] $[Ru(NH_3)_5Cl^{2+}]_i$ and $[Ru(NH_3)_5Br^{2+}]_i \geq 1.0$ mM. [b] Ratio obtained from GC peak areas after photolysis of $C_2H_5Co(dmgH)_2H_2O$ was completed (about 3 minutes).

Table A-15. Kinetic data of the reaction of ethyl radical with $MV^{\bullet+}$

Conditions: $[C_2H_5Co(dmgH)_2H_2O] = 30\ \mu M$
$\lambda = 600$ nm
$T = 23 \pm 2\ ^{\circ}C$, in 0.010 M $HClO_4$

$[MV^{\bullet+}]_{ave}/\mu M$	$[MV^{\bullet+}]_L$[a]$/\mu M$	$10^{-4}k_{\psi}/s^{-1}$
13	2.7	2.36
13	1.5	2.46
16	1.6	2.51
17	2.5	2.27
19	2.3	2.54
20	3.0	3.09
22	4.5	3.27
24	3.4	3.28
26	1.9	3.73
31	2.8	3.66
34	4.0	3.77
45	2.5	6.28
51	2.4	5.63
53	3.3	6.83
53	4.0	6.40
55	3.7	6.91
61	5.0	7.47
73	5.1	9.60
76	5.5	9.46

[a] $[MV^{\bullet+}]_L$ refers to the concentration of $MV^{\bullet+}$ consumed or 'lost' in the reaction.

Table A-16. Kinetic data of the reaction of ethyl radical with $IrCl_6^{2-}$

Conditions: $[C_2H_5Co(dmgH)_2H_2O]$ = 30 μM
λ = 600 nm
T = 23 ± 2 °C, in 0.50 M H_2SO_4

$[IrCl_6^{2-}]_{ave}/\mu M$	$[IrCl_6^{2-}]_L$[a]/μM	$10^{-4}k_\psi/s^{-1}$
37.6	2.4	11.7
37.0	2.3	12.6
36.4	3.4	10.9
36.4	3.4	11.6
34.3	2.8	11.4
33.8	3.7	9.95
32.9	3.3	9.10
32.5	3.9	9.64
31.5	3.7	10.9
30.4	3.2	8.67
28.1	3.7	9.03
26.7	3.8	8.17
26.7	3.4	9.03
25.2	4.0	7.51
25.2	3.8	7.59
24.6	5.3	7.58
23.8	3.6	7.87
23.0	4.7	7.69
22.5	4.2	7.97
21.5	4.4	7.76
20.8	3.4	7.50
19.4	4.2	6.84
17.7	3.6	7.10
17.1	3.9	5.46
16.3	2.5	7.32
15.4	4.2	5.31
15.1	2.9	4.93
13.2	3.9	5.38
12.6	3.3	4.54

[a] $[IrCl_6^{2-}]_L$ refers to the concentration of $IrCl_6^{2-}$ consumed or 'lost' in the reaction.

Table A-17. Kinetic data of the reaction of ethyl radical with $Fe(phen)_3^{3+}$
Conditions: $[C_2H_5Co(dmgH)_2H_2O]$ = 30 μM
λ = 510 nm
T = 23 ± 2 °C, in 0.50 M H_2SO_4

$[Fe(phen)_3^{3+}]_{ave}$/μM	$[Fe(phen)_3^{2+}]_f$[a]/μM	$10^{-4}k_\psi/s^{-1}$
12	1.0	1.84
21	0.9	3.03
22	0.8	3.27
29	1.0	4.14
31	1.3	4.39
37	1.0	5.95
43	0.8	6.19

[a] $[Fe(phen)_3^{2+}]_f$ refers to the concentration of $Fe(phen)_3^{2+}$ formed in the reaction.

Table A-18. Kinetic data of the reaction of ethyl radical with $Fe(bpy)_3^{3+}$
Conditions: $[C_2H_5Co(dmgH)_2H_2O]$ = 30 μM
λ = 520 nm
T = 23 ± 2 °C, in 0.50 M H_2SO_4

$[Fe(bpy)_3^{2+}]_{ave}$/μM	$[Fe(bpy)_3^{2+}]_f$[a]/μM	$10^{-4}k_\psi/s^{-1}$
75.0	1.7	7.88
73.9	1.6	7.90
71.3	1.8	7.38
68.7	1.5	6.92
66.5	1.6	6.56
65.2	1.7	6.48
63.5	1.5	7.02
58.2	1.4	6.05
56.1	1.3	5.95
52.4	1.4	5.34
50.1	2.0	5.31
48.0	1.9	5.38
42.3	1.6	4.53
39.6	1.4	4.71
39.5	1.3	4.69
34.8	1.0	4.17
25.8	1.5	3.14
24.2	1.4	2.63
20.5	1.0	2.97
19.4	0.9	2.36

[a] $[Fe(bpy)_3^{2+}]_f$ refers to the concentration of $Fe(bpy)_3^{2+}$ formed in the reaction.

Table A-19. Kinetic data of the reaction of ethyl radical with $Cr(bpy)_3^{3+}$

Conditions: $[C_2H_5Co(dmgH)_2H_2O]$ = 50 μM
λ = 560 nm, T = 23 ± 2 °C
in 0.05 M NaI and 0.50 M H_2SO_4

$[Cr(bpy)_3^{3+}]_{ave}$/mM	$[Cr(bpy)_3^{2+}]_f$[a]/μM	$10^{-4}k_\psi/s^{-1}$
0.50	b	3.21
0.50	b	2.59
0.50	b	3.01
0.70	2.4	1.90
0.90	2.6	3.46
1.00	b	3.46
1.00	b	4.03
1.30	2.8	3.68
2.00	3.5	4.30
2.00	3.2	4.74
2.00	b	5.88
2.00	b	4.72
2.00	b	5.35
2.00	b	4.37
2.50	b	5.58
3.00	3.0	7.03
3.00	3.1	8.07
3.00	3.4	7.18
3.50	4.0	7.57
3.50	3.9	8.54
3.50	3.3	6.86
3.50	6.4	8.26
3.50	5.1	7.87
4.00	b	9.08
4.50	2.5	9.18
4.50	2.7	9.35
5.00	2.0	10.0

[a] $[Cr(bpy)_3^{2+}]_f$ refers to the concentration of $Cr(bpy)_3^{2+}$ formed in the reaction. [b] $[Cr(bpy)_3^{2+}]_f$ = 4-5 μM.

Table A-20. Kinetic data of the reaction of methyl radical with $ABTS^{\bullet-}$

Conditions: $[CH_3Co(dmgH)_2H_2O]$ = 50 μM

λ = 650 nm

T = 23 ± 2 °C, in 0.50 M H_2SO_4

$[ABTS^{\bullet-}]_{ave}/\mu M$	$[ABTS^{\bullet-}]_L$[a]/μM	$10^{-4}k_\psi/s^{-1}$	$10^{-4}k_{corr}/s^{-1}$
20.0	4.2	2.74	1.82
17.3	4.1	2.66	1.71
16.5	3.8	2.63	1.75
14.8	3.8	2.51	1.58
30.9	5.1	3.87	2.85
27.7	5.1	3.65	2.59
26.4	4.6	3.54	2.60
24.7	4.5	3.31	2.38
39.9	4.9	4.84	3.94
37.5	4.8	4.41	3.52
35.1	4.8	4.33	3.42
32.4	4.3	4.20	3.39
51.1	4.8	6.28	5.44
48.1	5.0	6.16	5.27
61.7	4.4	7.00	6.26
59.2	5.0	6.97	6.11
54.6	4.8	6.73	5.90

[a] $[ABTS^{\bullet-}]_L$ refers to the concentration of $ABTS^{\bullet-}$ consumed or 'lost' in the reaction.

Table A-21. Kinetic data of the reaction of ethyl radical with $ABTS^{\bullet-}$

Conditions: $[C_2H_5Co(dmgH)_2H_2O]$ = 30 μM
λ = 650 nm
T = 23 ± 2 °C, in 0.50 M H_2SO_4

$[ABTS^{\bullet-}]_{ave}/\mu M$	$[ABTS^{\bullet-}]_L$[a]/μM	$10^{-4}k_\psi/s^{-1}$	$10^{-4}k_{corr}/s^{-1}$
50.8	5.2	4.92	4.34
50.8	4.6	4.86	4.35
50.3	4.4	4.78	4.29
48.1	4.4	5.03	4.54
47.6	1.4	4.37	4.23
46.6	1.5	4.32	4.16
46.0	1.4	4.65	4.50
44.2	1.5	4.43	4.27
41.3	3.8	4.22	3.79
39.4	3.1	4.18	3.84
37.7	1.9	3.68	3.48
36.1	4.6	3.89	3.35
35.8	2.0	3.69	3.48
33.7	4.7	3.52	2.96
29.4	3.7	3.20	2.77
29.3	1.6	2.88	2.71
28.4	1.6	2.82	2.65
27.1	1.6	2.44	2.27
26.7	1.6	2.63	2.46
26.6	3.8	2.99	2.53
25.7	3.9	2.99	2.52
24.5	3.5	2.82	2.40
23.4	3.2	2.82	2.44
20.0	5.3	2.42	1.65
18.2	2.7	1.99	1.66
17.3	2.4	1.88	1.59
17.0	3.9	2.14	1.61
16.6	2.2	1.80	1.54
15.5	3.3	2.01	1.57
14.4	4.0	1.73	1.14
14.1	2.8	2.01	1.63
11.5	3.0	1.57	1.15
10.9	2.4	1.35	1.03
9.9	4.2	1.61	0.78

[a] $[ABTS^{\bullet-}]_L$ refers to the concentration of $ABTS^{\bullet-}$ consumed or 'lost' in the reaction.

Table A-22. Kinetic data of the reaction of 1-propyl radical with $ABTS^{\bullet-}$

Conditions: $[C_3H_7Co(dmgH)_2H_2O]$ = 50 μM
λ = 650 nm
T = 23 ± 2 °C, in 1.0 M $HClO_4$

$[ABTS^{\bullet-}]_{ave}/\mu M$	$[ABTS^{\bullet-}]_L$[a]/μM	$10^{-4}k_\psi/s^{-1}$	$10^{-4}k_{corr}/s^{-1}$
39.5	7.8	5.03	4.01
36.5	7.9	4.53	3.52
32.7	7.6	4.42	3.36
30.5	6.5	4.08	3.18
59.3	7.0	6.88	6.04
55.9	6.3	6.26	5.53
52.5	6.2	5.80	5.09
49.7	5.4	5.54	4.92
43.9	8.0	5.67	4.60
39.5	6.3	4.63	3.87
36.7	6.4	4.31	3.54
29.8	6.1	3.71	2.93
27.8	5.5	3.45	2.73
24.4	5.5	3.49	2.68
22.2	5.2	3.29	2.50
24.3	4.8	3.03	2.41
21.1	4.3	2.93	2.32
18.9	4.1	2.79	2.17
16.5	3.6	2.50	1.94

[a] $[ABTS^{\bullet-}]_L$ refers to the concentration of $ABTS^{\bullet-}$ consumed or 'lost' in the reaction.

Table A-23. Kinetic data of the reaction of 1-butyl radical with $ABTS^{\bullet-}$

Conditions: $[C_4H_9Co(dmgH)_2H_2O]$ = 50 μM
λ = 650 nm
T = 23 ± 2 °C, in 1.0 M $HClO_4$

$[ABTS^{\bullet-}]_{ave}/\mu M$	$[ABTS^{\bullet-}]_L$[a]/μM	$10^{-4}k_\psi/s^{-1}$	$10^{-4}k_{corr}/s^{-1}$
65.3	4.5	7.59	7.05
63.2	4.0	8.02	7.49
61.1	4.0	6.51	6.07
59.4	3.6	6.71	6.29
56.7	3.8	6.49	6.04
55.3	3.7	6.03	5.60
53.1	3.5	5.99	5.58
51.6	3.6	5.50	5.10
44.2	4.5	4.66	4.18
42.1	3.9	4.58	4.13
39.7	3.5	4.21	3.82
38.2	3.3	4.17	3.79
36.0	3.3	3.99	3.61
37.4	2.9	3.98	3.66
32.7	2.9	3.88	3.52
30.9	2.9	3.69	3.33
31.1	4.7	4.04	3.40
29.1	4.5	3.65	3.06
27.4	4.3	3.81	3.19
25.5	4.0	3.23	2.70
23.7	3.6	3.28	2.76
22.2	3.7	3.32	2.74
20.5	3.4	3.20	2.65
19.1	3.3	3.06	2.51
22.4	7.8	2.99	1.88
19.0	6.9	2.79	1.71
16.5	6.3	2.59	1.55

[a] $[ABTS^{\bullet-}]_L$ refers to the concentration of $ABTS^{\bullet-}$ consumed or 'lost' in the reaction.

Table A-24. Kinetic data of the reaction of 1-pentyl radical with $ABTS^{\bullet-}$

Conditions: $[C_5H_{11}Co(dmgH)_2H_2O]$ = 50 μM
λ = 650 nm
T = 23 ± 2 °C, in 1.0 M $HClO_4$

$[ABTS^{\bullet-}]_{ave}/\mu M$	$[ABTS^{\bullet-}]_L$[a]/μM	$10^{-4}k_\psi/s^{-1}$	$10^{-4}k_{corr}/s^{-1}$
48.8	5.9	5.22	4.59
45.5	5.6	5.18	4.54
41.7	5.6	4.63	4.01
35.3	4.4	3.68	3.22
31.6	4.2	3.33	2.89
29.1	4.0	3.03	2.62
27.3	4.0	3.22	2.74
24.9	3.0	2.75	2.42
22.8	3.2	2.77	2.38
20.2	2.4	2.26	1.99
19.5	2.4	2.15	1.89

[a] $[ABTS^{\bullet-}]_L$ refers to the concentration of $ABTS^{\bullet-}$ consumed or 'lost' in the reaction.

Table A-25. Kinetic data of the reaction of 1-hexyl radical with $ABTS^{\bullet-}$

Conditions: $[C_6H_{13}Co(dmgH)_2H_2O]$ = 80 μM
λ = 650 nm
T = 23 ± 2 °C, in 1.0 M $HClO_4$

$[ABTS^{\bullet-}]_{ave}/\mu M$	$[ABTS^{\bullet-}]_L$[a]/μM	$10^{-4}k_\psi/s^{-1}$	$10^{-4}k_{corr}/s^{-1}$
58.9	6.0	5.86	5.25
53.7	6.6	5.72	5.02
48.4	6.5	4.93	4.27
41.4	6.8	4.12	3.44
37.7	4.5	3.66	3.22
34.0	4.2	3.34	2.93
30.0	4.0	3.01	2.61
23.0	2.8	2.30	2.03
21.4	3.0	2.04	1.75
18.2	2.6	1.67	1.43

[a] $[ABTS^{\bullet-}]_L$ refers to the concentration of $ABTS^{\bullet-}$ consumed or 'lost' in the reaction.

Table A-26. Kinetic data of the reaction of 1-heptyl radical with $ABTS^{\bullet-}$

Conditions: $[C_7H_{15}Co(dmgH)_2H_2O]$ = 80 μM
λ = 650 nm
T = 23 ± 2 °C, in 1.0 M $HClO_4$

$[ABTS^{\bullet-}]_{ave}/\mu M$	$[ABTS^{\bullet-}]_L$[a]/μM	$10^{-4}k_\psi/s^{-1}$	$10^{-4}k_{corr}/s^{-1}$
61.5	12	7.30	5.88
52.0	9.0	5.61	4.65
49.7	9.0	5.91	4.83
44.9	6.6	4.96	4.22
39.5	6.0	4.82	4.09
35.4	5.6	4.00	3.37
31.1	5.0	3.96	3.32
28.5	5.0	3.63	3.01
24.9	3.6	2.71	2.32
21.5	3.2	2.98	2.54
18.6	3.0	2.65	2.22
16.8	2.8	2.15	1.79
14.2	2.2	1.53	1.29

[a] $[ABTS^{\bullet-}]_L$ refers to the concentration of $ABTS^{\bullet-}$ consumed or 'lost' in the reaction.

Table A-27. Kinetic data of the reaction of 1-octyl radical with $ABTS^{\bullet-}$

Conditions: $[C_8H_{17}Co(dmgH)_2H_2O]$ = 80 μM
λ = 650 nm
T = 23 ± 2 °C, in 1.0 M $HClO_4$

$[ABTS^{\bullet-}]_{ave}/\mu M$	$[ABTS^{\bullet-}]_L$[a]/μM	$10^{-4}k_\psi/s^{-1}$	$10^{-4}k_{corr}/s^{-1}$
54.9	6.0	6.46	5.82
51.7	5.6	5.80	5.23
48.1	5.0	5.78	5.23
44.7	4.4	5.15	4.69
41.1	4.2	4.85	4.40
39.5	3.8	4.98	4.54
33.6	3.4	3.96	3.60
31.7	2.8	3.81	3.50
28.8	2.4	3.91	3.61
27.1	2.4	3.51	3.23
25.3	2.2	3.02	2.78
23.3	1.8	2.54	2.36
22.5	1.6	2.78	2.60
21.2	1.4	2.74	2.58
20.2	1.4	2.62	2.45

[a] $[ABTS^{\bullet-}]_L$ refers to the concentration of $ABTS^{\bullet-}$ consumed or 'lost' in the reaction.

Table A-28. Kinetic data of the reaction of iso-butyl radical with $ABTS^{\bullet-}$

Conditions: $[C_4H_9Co(dmgH)_2H_2O]$ = 50 μM

λ = 650 nm

T = 23 ± 2 °C, in 1.0 M $HClO_4$

$[ABTS^{\bullet-}]_{ave}/\mu M$	$[ABTS^{\bullet-}]_L$[a]/μM	$10^{-4}k_\psi/s^{-1}$	$10^{-4}k_{corr}/s^{-1}$
42.7	7.8	4.27	3.49
38.4	6.8	4.33	3.56
35.0	6.0	3.80	3.15
31.3	5.4	3.47	2.87
28.3	5.0	3.30	2.72
23.4	3.4	2.41	2.06
67.8	7.8	7.61	6.73
62.3	7.5	6.81	5.99
57.9	6.4	6.33	5.63
53.8	5.3	5.37	4.84
50.3	5.3	5.75	5.14
47.1	4.8	4.67	4.19
26.1	6.6	3.41	2.55
22.1	5.2	2.91	2.23
19.6	4.6	2.43	1.86
16.6	3.9	2.15	1.65

[a] $[ABTS^{\bullet-}]_L$ refers to the concentration of $ABTS^{\bullet-}$ consumed or 'lost' in the reaction.

Table A-29. Kinetic data of the reaction of benzyl radical with $ABTS^{\bullet-}$

Conditions: $[C_6H_5CH_2Co(dmgH)_2H_2O] = 50\ \mu M$
$\lambda = 650$ nm
$T = 23 \pm 2\ ^{o}C$, in 1.0 M $HClO_4$

$[ABTS^{\bullet-}]_{ave}/\mu M$	$[ABTS^{\bullet-}]_L$[a]$/\mu M$	$10^{-4}k_{\psi}/s^{-1}$	$10^{-4}k_{corr}/s^{-1}$
32.3	1.2	3.89	3.75
31.7	1.3	3.15	3.02
30.1	1.5	3.03	2.88
29.1	1.2	3.24	3.11
23.6	0.9	2.38	2.29
22.9	1.0	2.60	2.49
22.3	1.0	2.40	2.29
45.8	1.0	5.40	5.28
36.3	1.2	3.55	3.43
35.2	1.0	3.89	3.78
55.2	1.9	6.37	6.15
53.8	1.8	6.38	6.17
52.7	2.0	6.08	5.85
51.5	1.9	5.11	4.92
44.9	1.6	4.97	4.79
43.5	1.8	4.90	4.70
42.1	1.7	5.28	5.07
40.7	1.8	4.63	4.43
68.9	1.2	6.60	6.49
68.0	1.4	7.29	7.14
67.0	1.3	6.93	6.80
66.4	1.1	6.93	6.82
59.4	2.7	6.33	6.04
59.8	2.7	6.62	6.32
56.5	2.3	5.76	5.53
56.2	2.2	6.18	5.94
53.6	2.5	5.83	5.56
27.3	2.2	2.82	2.59
25.7	2.5	2.58	2.33
24.0	2.7	2.95	2.62
22.8	2.7	2.75	2.43

[a] $[ABTS^{\bullet-}]_L$ refers to the concentration of $ABTS^{\bullet-}$ consumed or 'lost' in the reaction.

Table A-30. Kinetic data of the reaction of 2-propyl radical with $ABTS^{\bullet-}$

Conditions: $[C_3H_7Co(dmgH)_2H_2O] = 50\ \mu M$

$\lambda = 650$ nm

$T = 23 \pm 2\ ^{o}C$, in 1.0 M $HClO_4$

$[ABTS^{\bullet-}]_{ave}/\mu M$	$[ABTS^{\bullet-}]_L$[a]$/\mu M$	$10^{-4}k_{\psi}/s^{-1}$	$10^{-4}k_{corr}/s^{-1}$
29.3	3.5	3.91	3.48
26.1	2.9	3.51	3.16
23.5	2.5	3.29	2.97
21.2	2.3	3.18	2.87
38.5	3.7	5.20	4.75
35.6	3.2	4.80	4.41
33.2	2.8	4.52	4.17
31.2	2.3	4.56	4.25
53.6	3.4	6.92	6.52
50.0	3.0	6.75	6.38
45.5	2.1	5.54	5.31
20.1	3.5	3.19	2.68
17.6	2.7	2.92	2.51
15.1	2.3	2.58	2.22
13.8	2.0	2.50	2.17
69.5	2.7	9.47	9.14
66.4	2.5	7.64	7.38
64.4	2.5	8.56	8.26
62.7	2.0	8.00	7.77
54.4	2.1	7.43	7.17
52.8	1.9	6.30	6.09
51.4	1.7	6.53	6.32

[a] $[ABTS^{\bullet-}]_L$ refers to the concentration of $ABTS^{\bullet-}$ consumed or 'lost' in the reaction.

Table A-31. Kinetic data of the reaction of cyclopentyl radical with $ABTS^{\bullet-}$

Conditions: $[c\text{-}C_5H_9Co(dmgH)_2H_2O] = 50\ \mu M$

$\lambda = 650$ nm

$T = 23 \pm 2\ ^{\circ}C$, in 1.0 M $HClO_4$

$[ABTS^{\bullet-}]_{ave}/\mu M$	$[ABTS^{\bullet-}]_L$[a]$/\mu M$	$10^{-4}k_{\psi}/s^{-1}$	$10^{-4}k_{corr}/s^{-1}$
41.7	8.0	4.90	3.94
32.7	6.6	4.09	3.25
27.0	5.8	3.69	2.88
22.6	5.2	3.38	2.89
56.3	2.6	6.25	5.96
54.5	2.6	5.85	5.57
52.5	2.8	6.11	5.78
51.4	2.0	5.47	5.25
38.3	4.0	5.12	4.57
31.7	4.8	3.46	2.93
26.3	4.2	3.09	2.59
23.0	3.6	2.73	2.29
20.0	3.4	2.51	2.07

[a] $[ABTS^{\bullet-}]_L$ refers to the concentration of $ABTS^{\bullet-}$ consumed or 'lost' in the reaction.

Table A-32. Kinetic data of the reaction of chloromethyl radical with $ABTS^{\bullet-}$

Conditions: $[ClCH_2Co(dmgH)_2H_2O]$ = 80 μM
λ = 650 nm
T = 23 ± 2 °C, in 1.0 M $HClO_4$

$[ABTS^{\bullet-}]_{ave}/\mu M$	$[ABTS^{\bullet-}]_L$[a]/μM	$10^{-4}k_\psi/s^{-1}$	$10^{-4}k_{corr}/s^{-1}$
59.2	4.6	6.66	6.14
57.3	4.4	6.47	5.97
54.4	4.4	6.22	5.72
51.9	4.8	5.65	5.13
50.0	4.4	5.79	5.28
48.5	4.0	5.20	4.77
48.3	3.4	5.37	4.99
46.1	4.0	4.98	4.55
42.8	4.0	4.92	4.46
41.3	4.4	4.29	3.83
39.3	4.2	4.15	3.71
38.4	4.0	3.86	3.46
36.9	3.6	3.61	3.26
36.2	3.2	3.54	3.23
35.0	3.2	3.67	3.33
34.4	3.2	3.69	3.35
32.9	3.8	3.72	3.29
30.6	3.8	3.32	2.91
30.0	3.4	3.13	2.78
27.5	4.1	3.20	2.72
24.6	3.4	3.14	2.71
22.6	3.2	2.94	2.52
20.8	2.8	2.63	2.28
18.9	3.0	2.42	2.04
16.3	2.5	2.19	1.86
13.3	2.6	1.63	1.31
11.9	2.4	1.83	1.46

[a] $[ABTS^{\bullet-}]_L$ refers to the concentration of $ABTS^{\bullet-}$ consumed or 'lost' in the reaction.

Table A-33. Kinetic data of the reaction of bromomethyl radical with $ABTS^{\bullet-}$

Conditions: $[BrCH_2Co(dmgH)_2H_2O]$ = 80 μM
λ = 650 nm
T = 23 ± 2 °C, in 1.0 M $HClO_4$

$[ABTS^{\bullet-}]_{ave}/\mu M$	$[ABTS^{\bullet-}]_L$[a]$/\mu M$	$10^{-4}k_\psi/s^{-1}$	$10^{-4}k_{corr}/s^{-1}$
25.9	3.0	4.32	4.01
23.3	3.0	4.10	3.77
22.5	3.3	4.30	3.90
35.2	3.2	5.80	5.47
33.6	3.7	5.87	5.47
32.4	3.5	5.52	5.15
30.9	3.7	5.36	4.96
30.2	3.1	5.13	4.80
26.4	3.0	4.85	4.51
38.9	2.9	6.67	6.36
37.2	3.3	6.35	6.00
36.0	3.2	6.07	5.73
34.9	3.2	6.22	5.86
33.2	3.5	5.72	5.34
31.2	3.5	5.46	5.08
30.0	3.4	5.33	4.95
28.5	3.4	5.19	4.80
54.1	3.3	9.80	9.43
50.9	3.5	9.12	8.73
50.0	2.6	8.78	8.49
49.3	3.2	8.35	8.01
47.9	3.3	9.30	8.90
46.5	3.3	8.10	7.74
70.5	2.7	11.4	11.1
67.9	3.3	11.2	10.9
65.0	3.5	12.0	11.6
63.0	3.6	11.6	11.1
61.0	3.0	9.74	9.44
60.0	3.4	10.1	9.76
58.8	3.5	10.1	9.74
57.2	3.5	9.44	8.97

[a] $[ABTS^{\bullet-}]_L$ refers to the concentration of $ABTS^{\bullet-}$ consumed or 'lost' in the reaction.

Table A-34. Kinetic data of the reaction of methoxymethyl radical with $ABTS^{\bullet-}$

Conditions: $[CH_3OCH_2Co(cyclam)H_2O^{2+}]^a$ = 200 μM
λ = 650 nm
T = 23 ± 2 °C, in 1.0 M $HClO_4$

$[ABTS^{\bullet-}]_{ave}$/μM	$[ABTS^{\bullet-}]_L{}^b$/μM	$10^{-4}k_\psi/s^{-1}$	$10^{-4}k_{corr}/s^{-1}$
70.3	1.6	11.0	10.8
68.9	1.6	10.8	10.6
66.7	1.8	9.98	9.79
64.5	1.6	9.77	9.60
63.2	1.4	9.74	9.59
62.5	1.6	9.51	9.34
61.3	1.6	8.74	8.58
60.2	1.6	8.71	8.54
58.9	1.6	8.18	8.02
56.0	1.4	8.12	7.96
54.2	1.6	8.72	8.54
51.4	1.6	6.82	6.67
50.2	1.6	7.39	7.22
37.6	1.6	5.24	5.08
36.5	1.4	5.58	5.43
35.7	1.4	5.68	5.52
34.8	1.4	6.24	6.06
34.0	1.6	5.01	4.84
32.6	1.4	4.94	4.79
31.6	1.6	4.85	4.67
30.9	1.4	5.05	4.91
30.0	1.6	4.49	4.32
28.9	1.4	4.70	4.54
27.9	1.2	4.99	4.84
32.8	1.2	4.34	4.22
31.1	1.4	4.15	4.02
28.9	1.2	3.83	3.73
28.2	1.4	4.17	4.02
26.7	1.2	4.56	4.41
25.2	1.2	3.87	3.74
23.3	1.0	3.79	3.67
22.5	1.0	3.22	3.12
21.6	1.0	3.81	3.68

[a] Due to thermal reaction of $ABTS^{\bullet-}$ with $CH_3OCH_2Co(dmgH)_2H_2O$.
[b] $[ABTS^{\bullet-}]_L$ refers to the concentration of $ABTS^{\bullet-}$ consumed or 'lost' in the reaction.

Table A-35. Kinetic data of the reaction of ethyl radical with $IrCl_6^{2-}$

Conditions: $[C_2H_5Co(dmgH)_2H_2O]$ = 30 μM
λ = 650 nm
T = 23 ± 2 °C, in 0.50 M H_2SO_4

$[P]_{ave}/\mu M$	$[P]_L$[a]/μM	$[IrCl_6^{2-}]/\mu M$	$10^{-4}k_\psi/s^{-1}$	$10^{-4}k_{corr}/s^{-1}$
33.3	0.6	29	11.36	8.27
33.1	0.9	28	10.43	7.23
32.7	1.1	27	10.84	7.59
33.1	1.0	25	10.90	7.71
32.2	0.9	23	9.29	6.20
33.3	1.1	19	9.20	6.02
32.9	1.2	18	8.53	5.35
31.9	1.3	17	7.44	4.31
34.9	1.0	14	7.57	4.34
34.3	1.2	13	7.14	3.91
33.5	1.2	12	6.68	3.50
33.3	1.4	11	6.32	3.12

[a] $[P]_L$ refers to the concentration of $ABTS^{\bullet-}$ consumed or 'lost' in the reaction.

PART II. KINETICS AND MECHANISMS OF THE FORMATION AND HOMOLYSIS OF A SERIES OF ORGANO(CYCLAM)NICKEL(III) COMPLEXES

INTRODUCTION

Studies of σ-bonded organometallic complexes in aqueous solution have focused primarily on the relatively stable complexes of $RCrL^{n+}$ and $RCoL^{n+}$ (R = alkyl, substituted alkyl, arylalkyl, etc.; L = H_2O, macrocycle, etc.).[1] Attempts to understand the chemistry of other transition metal organometallic complexes have suffered due to their relatively short-lifetimes and lack of intense UV-visible spectroscopic bands. Yet, because various transition metals have been discovered in σ-bonded organometallic intermediates in many aqueous biochemical, industrial, and organic processes there has been renewed interest in the formation and reactivity of new organometallic complexes.

Until recently little was known about the chemistry of alkylnickel complexes in aqueous solution. This is surprising as organonickel catalysts have been developed since the mid-1950s,[2] and the first of four enzymes containing functionally significant nickel was discovered in 1975.[3] ESR studies using ^{61}Ni-labeled enzymes have detected paramagnetic resonances which have been attributed to low concentrations of Ni(III) in certain hydrogenases[4] and Ni(I) in methyl coenzyme-M reductase (enzymes thought to involve organonickel intermediates),[5] suggesting that one-electron redox chemistry of Ni(II) may be catalytically

important. Similarly, Raney nickel catalyzed desulfurizations are thought to proceed by one-electron (radical) pathways.[6]

D'Aniello and Barefield[7] were the first to report the formation of a σ-bonded macrocyclic alkylnickel(II) complex, $CH_3Ni(tmc)^+$ (tmc = tetramethyl-1,4,8,11-tetraazacyclotetradecane). It was determined that while $RNi(tmc)^+$ hydrolyzes in aqueous solution,[8] oxidation of $RNi(tmc)^+$ with alkyl halides leads to homolysis via the intermediate $RNi(tmc)^{2+}$.[9] More recently the kinetics of formation and decomposition of $CH_3Ni(cyclam)H_2O^{2+}$ (cyclam = 1,4,8,11-tetraazacyclotetradecane) were studied using pulse radiolysis[10] and shown to conform to the equilibrium in eq 1.

$$CH_3Ni(cyclam)H_2O^{2+} \underset{k_{col}}{\overset{k_{hom}}{\rightleftharpoons}} CH_3^{\bullet} + Ni(cyclam)^{2+} + H_2O \qquad (1)$$

Reactions of alkyl radicals other than methyl with β-Ni(cyclam)$^{2+}$ (also known as the Trans III or R,R,S,S-

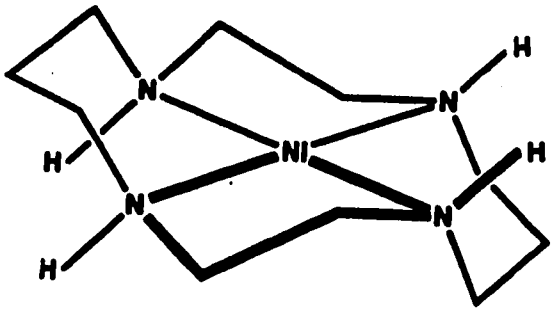

isomer)[11] were not performed due to the limitations of the pulse radiolysis technique:[12]

1) dialkyl sulfoxide radical precursors are neither commercially available nor readily prepared;
2) scavenging agents, necessary to remove highly energetic species generated in the pulse, are tranformed into less energetic radicals which may themselves react with the substrate of interest;
3) many hydrocarbons do not possess solubility and C-H bond reactivity required for hydrogen atom abstraction.

The purpose of the research described here is to i) devise a method to investigate the kinetics of colligation reactions of a series of alkyl radicals with β-Ni(cyclam)$^{2+}$, ii) investigate the kinetics of homolysis reactions for a series of RNi(cyclam)H_2O^{2+} complexes, iii) obtain thermodynamic data from the homolysis of C_2H_5Ni(cyclam)H_2O^{2+}, and iv) determine which form(s) of β-Ni(cyclam)$^{2+}$ is reactive by comparing kinetic and thermodynamic findings with those of RCo(III) and RCr(III) complexes.

To best fulfill this purpose the kinetics of colligation reactions of β-Ni(cyclam)$^{2+}$ with alkyl radicals and the subsequent unimolecular homolysis of RNi(cyclam)H_2O^{2+} complexes were studied using laser flash photolysis. Excitation at 460-490 nm induces

Co-C bond homolysis in the alkyl cobalt complexes, $RCo(dmgH)_2B$ (R = alkyl, substituted alkyl, arylalkyl; dmgH = dimethylgyloxime; B = H_2O, pyridine) and $RCo(cyclam)H_2O^{2+}$, to cleanly yield alkyl radicals, $R^{\bullet}$, in reagent concentrations and in a short time (< 1 μs).[12]

In the presence of β-$Ni(cyclam)^{2+}$ and a kinetic probe reagent, a single laser flash initiated a rapid chemical process which was followed by a second slower process. These were observed by monitoring the changing transmittance at an absorption maximum of a kinetic probe reagent with time. Both $MV^{\bullet+}$ (methyl viologen radical cation) and $ABTS^{\bullet-}$ (2,2′-azino-bis(3-ethylbenzthiazoline-6-sulfonic acid) radical anion) were employed as kinetic probe reagents in this study, but because $ABTS^{\bullet-}$ is much easier to handle and has rate constants for reactions with alkyl radicals that compare with those of $MV^{\bullet+}$, $ABTS^{\bullet-}$ was chosen as the primary chromophore.[13]

EXPERIMENTAL

Reagents

The alkylcobaloxime(pyridine),[14] alkylcobalt(cyclam) perchlorate,[15] and nickel(II)(cyclam) perchlorate complexes were prepared using literature procedures and characterized by UV-visible spectroscopy. The perchloric acid (Fisher), $(NH_4)_2ABTS$ (Sigma), molecular oxygen (99.5% pure, Air Products), and argon (99.99% pure, Air Products) were used as purchased. Reagent stock solutions were prepared as needed and stored in the dark. All solutions were prepared from distilled water which was purified by passage through a Milli-Q Millipore reagent water system.

Stock solutions of $ABTS^{\bullet-}$ were prepared by mixing aqueous acidic bromine with $ABTS^{2-}$ in nearly stoichiometric amounts.[16] The resulting green-blue solutions were thoroughly deaerated to remove excess Br_2. Methyl viologen perchlorate was prepared from the chloride salt and was recrystallized twice. Stock solutions of $MV^{\bullet+}$ were prepared by reducing deaerated acidic solutions (5.0 mM $HClO_4$) of MV^{2+} over Zn amalgam for about 40 seconds. The resulting deep blue solutions were decanted into a syringe (kept from air and light) and used immediately. Stock solutions of Ni(cyclam)$^{2+}$ were prepared by dissolving the perchlorate salt in

0.01 M $HClO_4$. The concentrations of these reagents were determined by UV-visible spectroscopic methods ($MV^{\bullet+}$, ε_{600} = 1.37 x 10^4 L mol^{-1} cm^{-1};[17] $Ni(cyclam)^{2+}$, ε_{448} = 45 L mol^{-1} cm^{-1};[11] $ABTS^{\bullet-}$, ε_{650} = 1.0 x 10^4 L mol^{-1} cm^{-1}).[16]

Kinetics

Laser flash photolysis was employed to study the kinetics of these reactions. The flashlamp-pumped dye laser system has been described by Connolly[18] and is based on another system in the literature.[19] The dye used was LD 490, which emits light in the spectral region where the alkylcobalt complexes have significant absorbances (490 nm). Both $MV^{\bullet+}$ and $ABTS^{\bullet-}$ possess relatively transparent absorption windows in this region, permitting the laser photolysis of the alkylcobalt species. Alkyl cobaloximes were the primary radical precursors used in this study, but $RCo(cyclam)H_2O^{2+}$ complexes were employed whenever available. In a typical experiment, a deaerated sample solution was prepared in a 1-cm quartz cell. The reaction solution was then flashed by a 0.6 μs laser pulse from a Phase-R DL-1100 pulsed dye laser, and the resulting signal was collected and stored on a Nicolet model 2090-3A digitizing oscilloscope. The reactions were monitored by following the changes in voltage (transmittance) over time at 650 nm. The oscilloscope was interfaced with an Apple II Plus

microcomputer, which converted voltage vs. time data to absorbance vs. time data.

Gas Chromatography

Reaction products were determined using a Hewlett-Packard model 5790A series gas chromatograph with a 3390A series integrator. Hydrocarbons were determined using a VZ-10 column.

Data Analysis

Solutions containing desired amounts of an alkylcobalt complex and $ABTS^{\bullet-}$ were flashed, generating alkyl radicals that disappeared by two pathways; undergoing self-reactions (eq 2) at a known rate constant, k_d, and reacting with the excess reagent $ABTS^{\bullet-}$ (eq 3) with known rate constant, k_A.[20] Digitized absorbance vs. time data generated by these reactions were analyzed by a nonlinear least-squares program and were fit well by first-order kinetics: $D_t = D_\infty + (D_o - D_\infty)\exp(-k_\psi t)$, where D = absorbance.

$$2\ R^{\bullet} \longrightarrow RH + R(-H),\ RR \qquad k_d \qquad (2)$$

$$R^{\bullet} + ABTS^{\bullet-} \longrightarrow \text{Products} \qquad k_A \qquad (3)$$

$$-d[R^{\bullet}]/dt = 2k_d[R^{\bullet}]^2 + k_A[R^{\bullet}][ABTS^{\bullet-}] \qquad (4a)$$

The simplicity of this treatment is really an approximation, since the self-reactions do make a very small second-order contribution to the reaction rate. For these experiments the value of $[R^{\bullet}]$ was approximated as the average value of the initial and final values, reducing eq 4a to a pseudo-first-order kinetic expression, eq 4b.

$$k_{\psi} = 2k_d[R^{\bullet}]_{ave} + k_A[ABTS^{\bullet-}]_{ave} \qquad (4b)$$

The $[R^{\bullet}]_{ave}$ can be obtained from the loss of absorbance of $ABTS^{\bullet-}$ in each experiment, after allowance for the percent of reaction going by the $ABTS^{\bullet-}$pathway (eq 5). Pseudo-first-

$$[R^{\bullet}]_{ave} = \frac{k_{\psi}[ABTS^{\bullet-}]_{lost}/2}{k_A[ABTS^{\bullet-}]_{ave}} \qquad (5)$$

order rate constants corrected for the self-reactions, k_{corr}, were obtained using an iterative process employing eq 6 until a reproducible value for k_A was obtained. The plots of k_{corr} vs.

$$k_{corr} = k_\psi - 2k_d \frac{k_\psi[ABTS^{\bullet-}]_{lost}/2}{k_A[ABTS^{\bullet-}]_{ave}} = k_A[ABTS^{\bullet-}]_{ave} \quad (6)$$

$[ABTS^{\bullet-}]_{ave}$ were linear and passed through the origin. The validity of this method was verified by using a numerical integration program, KINSIM,[21] and the specified rate constants to generate values of $[ABTS^{\bullet-}]_{ave}$ as a function of time. First-order analyses of these simulated data agreed with the treatment implied by eq 4b.

When β-Ni(cyclam)$^{2+}$ was present in the reaction solution, two separate pseudo-first-order reaction phases were observed. Analysis of the data from the fast decay of the chromophore (either $ABTS^{\bullet-}$ or $MV^{\bullet+}$) was performed using eq 7, where the two additional terms refer to the equilibrium reaction, eq 8.

$$k_\psi = 2k_d[R^\bullet]_{ave} + k_A[ABTS^{\bullet-}]_{ave} + k_{col}[Ni(cyclam)^{2+}] + k_{hom} \quad (7)$$

$$R^\bullet + Ni(cyclam)^{2+} + H_2O \underset{k_{hom}}{\overset{k_{col}}{}} RNi(cyclam)H_2O^{2+} \quad (8)$$

In these experiments, the excess concentrations of $ABTS^{\bullet-}$ and β-$Ni(cyclam)^{2+}$ were both varied. Flashing a reaction solution four times generated four values of k_ψ with $[Ni(cyclam^{2+}]$ effectively remaining constant. The data were plotted using the average value of k_{corr} (eq 9) vs. $[Ni(cyclam)^{2+}]$, having subtracted the k_d and k^A terms from k^Ψ at each $[ABTS^{\bullet-}]$ (eq 10).

$$k_{corr} = k_\psi - 2k_d[R^\bullet]_{ave} - k_A[ABTS^{\bullet-}]_{ave}$$
$$= k_{col}[Ni(cyclam)^{2+}] + k_{hom} \quad (9)$$

$$k_{corr} = k_\psi - 2k_d \frac{k_\psi[ABTS^{\bullet-}]_{lost}/2}{k_A[ABTS^{\bullet-}]_{ave}} - k_A[ABTS^{\bullet-}]_{ave} \quad (10)$$

Colligation rate constants were obtained by using each corrected rate constant, k_{corr}, and corresponding β-$Ni(cyclam)^{2+}$ concentration in a linear least-squares analysis.

Homolysis rate constants, k_{hom}, were obtained by monitoring the slower phase of the reaction. Again, both $[ABTS^{\bullet-}]$ and $[Ni(cyclam)^{2+}]$ were varied and the pseudo-first-order rate constants were analyzed according to eqs -8 and 3, giving the expression in eq 11.

$$RNi(cyclam)H_2O^{2+} \underset{k_{col}}{\overset{k_{hom}}{}} R^{\bullet} + Ni(cyclam)^{2+} + H_2O \qquad (-8)$$

$$R^{\bullet} + ABTS^{\bullet-} \xrightarrow{k_A} \text{Products} \qquad (3)$$

$$k_{\psi} = \frac{k_{hom}k_A[ABTS^{\bullet-}]_{ave}}{k_A[ABTS^{\bullet-}]_{ave} + k_{col}[Ni(cyclam)^{2+}]} \qquad (11)$$

The inverse of the pseudo-first-order rate constants, $1/k_{\psi}$, vs. $[Ni(cyclam)^{2+}]/[ABTS^{\bullet-}]_{ave}$ was plotted, and a nonlinear least-squares analysis gave homolysis rate constants, k_{hom}.

RESULTS

Kinetics of Colligation Reactions of β-Ni(cyclam)$^{2+}$ with Alkyl Radicals

All the reactions of β-Ni(cyclam)$^{2+}$ with alkyl radicals were studied in deaerated 0.10 M $HClO_4$ under pseudo-first-order conditions with β-Ni(cyclam)$^{2+}$ and $ABTS^{\bullet-}$ in excess. Similar results were obtained for reactions in which $MV^{\bullet+}$ was used in place of $ABTS^{\bullet-}$. The concentrations of the reagents were typically about 50 μM $RCo(dmgH)_2H_2O$ and 20-40 μM $ABTS^{\bullet-}$ (or $MV^{\bullet+}$). The β-Ni(cyclam)$^{2+}$ concentration was varied in a range where a measurable effect on the pseudo-first-order rate constants, k_ψ, was observed. A slow reaction was observed between $ABTS^{\bullet-}$ and $RCo(dmgH)_2H_2O$ where R = CH_3OCH_2, $ClCH_2$, $BrCH_2$, 2-C_3H_7, c-C_5H_9, and $C_6H_5CH_2$. Because of this, deaerated solutions of these alkylcobalt complexes were injected into the reaction cell just prior to photolysis. The competition reactions (eqs 2, 3, and 8) monitored at 650 nm were shown to obey a pseudo-first-order rate law (eq 7).

$$2\ R^{\bullet} \longrightarrow RH + R(-H),\ RR \qquad k_d \qquad (2)$$

$$R^{\bullet} + ABTS^{\bullet-} \longrightarrow \text{Products} \qquad k_A \qquad (3)$$

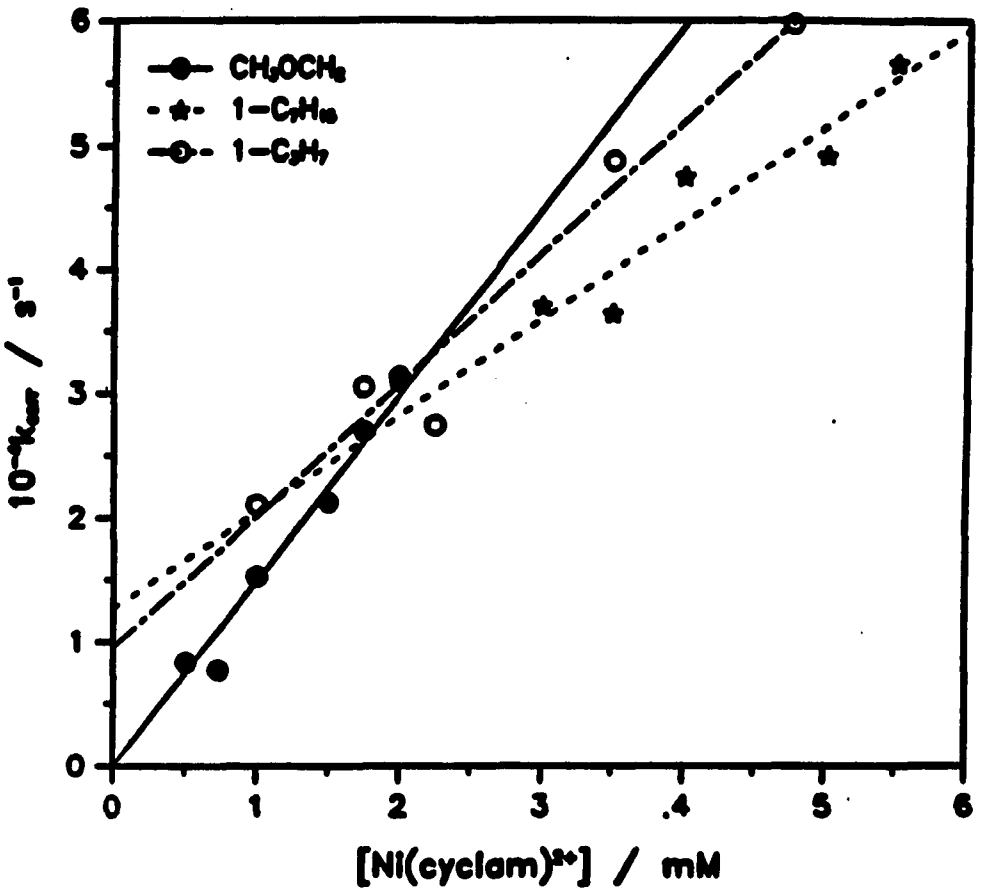

Figure II-1. The plot of the corrected rate constants versus $[Ni(cyclam)^{2+}]$ for the colligation of β-$Ni(cyclam)^{2+}$ with alkyl radicals. Kinetic data were obtained in 0.1 M $HClO_4$ at 25°C. Data are shown for the radicals CH_3OCH_2, 1-C_3H_7, and 1-C_7H_{15}

Table II-1. Colligation and homolysis rate constants[a] for the reaction $R^{\bullet}$ + β-Ni(cyclam)$^{2+}$ $RNi(cyclam)H_2O^{2+}$

alkyl radical	$k_{col}/10^7$ L mol^{-1} s^{-1}	$k_{hom}/10^3$ s^{-1}
CH_3	73. ± 2[b]	0.08 ± 0.02[c]
C_2H_5	1.3 ± 0.1[d]	6.8 ± 0.2[e]
1-C_3H_7	1.0 ± 0.1	5.3 ± 0.3
1-C_4H_9	1.0 ± 0.1	10.0 ± 0.3
1-C_5H_{11}	0.86 ± 0.09	5.8 ± 0.3
1-C_6H_{13}	0.90 ± 0.10	7.0 ± 0.3
1-C_7H_{15}	0.78 ± 0.13	8.5 ± 0.4
1-C_8H_{17}	0.81 ± 0.11	12. ± 1
iso-C_4H_9	<0.02[f]	.—
$C_6H_5CH_2$	<0.02[f]	.—
2-C_3H_7	<0.02[f]	.—
c-C_5H_9	<0.02[f]	.—
CH_3OCH_2	1.5 ± 0.1	2.5 ± 0.1
$ClCH_2$	1.9 ± 0.5[g]	27. ± 4
$BrCH_2$	4.8 ± 0.4[g]	39. ± 6

[a]Using the $ABTS^{\bullet-}$ method. [b]Using the $MV^{\bullet+}$ method, k_{col} = 72. ± 2 x 10^7 L mol^{-1} s^{-1}. [c]Using the oxygen method. [d]Using the $MV^{\bullet+}$ method, k_{col} = 1.2 ± 0.1 x 10^7 L mol^{-1} s^{-1}. [e]This value was measured using the $MV^{\bullet+}$ method; the $ABTS^{\bullet-}$ method gave more scattered data and k_{col} = 1.0 ± 0.4 x 10^4 s^{-1}. [f]These are upper limits based on the highest concentration of β-Ni(cyclam)$^{2+}$ used. [g]Obtained from analysis of the homolysis reaction, eq 11.

Kinetics of the Homolysis of $RNi(cyclam)H_2O^{2+}$

The kinetics of the second reaction phase in each laser flash are consistent with homolysis of $RNi(cyclam)H_2O^{2+}$ in the presence of the radical scavenger $ABTS^{\bullet-}$. This subsequent decrease in absorbance at 650 nm was enhanced by increasing the concentration of β-$Ni(cyclam)^{2+}$ so that the majority of alkyl radicals generated in the laser flash colligated with β-$Ni(cyclam)^{2+}$ to give $RNi(cyclam)H_2O^{2+}$. When appropriate, $RCo(cyclam)H_2O^{2+}$ radical precursors were used in place of the corresponding alkylcobaloxime to avoid the thermal reaction with $ABTS^{\bullet-}$. Then pseudo-first-order rate constants were observed to increase with $[ABTS^{\bullet-}]$ and decrease with increasing $[Ni(cyclam)^{2+}]$, consistent with eqs -8 and 3 and the rate law (eq 11).

$$RNi(cyclam)H_2O^{2+} \underset{k_{col}}{\overset{k_{hom}}{\rightleftharpoons}} R^{\bullet} + Ni(cyclam)^{2+} + H_2O \qquad (-8)$$

$$R^{\bullet} + ABTS^{\bullet-} \xrightarrow{k_A} \text{Products} \qquad (3)$$

$$k_{\psi} = \frac{k_{hom}k_A[ABTS^{\bullet-}]_{ave}}{k_A[ABTS^{\bullet-}]_{ave} + k_{col}[Ni(cyclam)^{2+}]} \qquad (11)$$

The values of k_{ψ} are listed in **Tables A-10 to A-22** for each alkyl nickel complex studied, except for $CH_3Ni(cyclam)H_2O^{2+}$. Typical

plots of $1/k_\psi$ vs. $[Ni(cyclam)^{2+}]/[ABTS^{\bullet-}]$ for three radicals, methoxymethyl, 1-propyl, and 1-octyl, are shown in **Figure II-2**. Estimates of the homolysis rate constant were obtained from the inverse of the intercept and from the value of k_{col}/k_A(slope). Nonlinear least-squares analyses were employed to give the homolysis rate constants, k_{hom}, which are listed in **Table II-1**.

The complexes $XCH_2Ni(cyclam)H_2O^{2+}$ (X = Cl, Br) decomposed so rapidly that the first stage of the reaction (colligation) could not be monitored cleanly. Therefore, both k_{col} and k_{hom} were obtained from eq 11.

The homolysis of $CH_3Ni(cyclam)H_2O^{2+}$ was studied using oxygen, as both $ABTS^{\bullet-}$ and $MV^{\bullet+}$ showed enhanced pseudo-first-order rate constants which did not correspond to clean unimolecular homolysis. The kinetics of the formation of $CH_3O_2Ni(cyclam)H_2O^{2+}$ were monitored at 360 nm (ε_{360} = 1 x 10^4 L mol^{-1} cm^{-1})[10] under conditions in which the majority of the methyl radicals generated in the flash colligated with β-$Ni(cyclam)^{2+}$ to give $CH_3Ni(cyclam)H_2O^{2+}$. These reactions required the use of $CH_3Co(cyclam)H_2O^{2+}$ as the radical source because of the strong absorption bands of $CH_3Co(dmgH)_2H_2O$ below 400 nm.

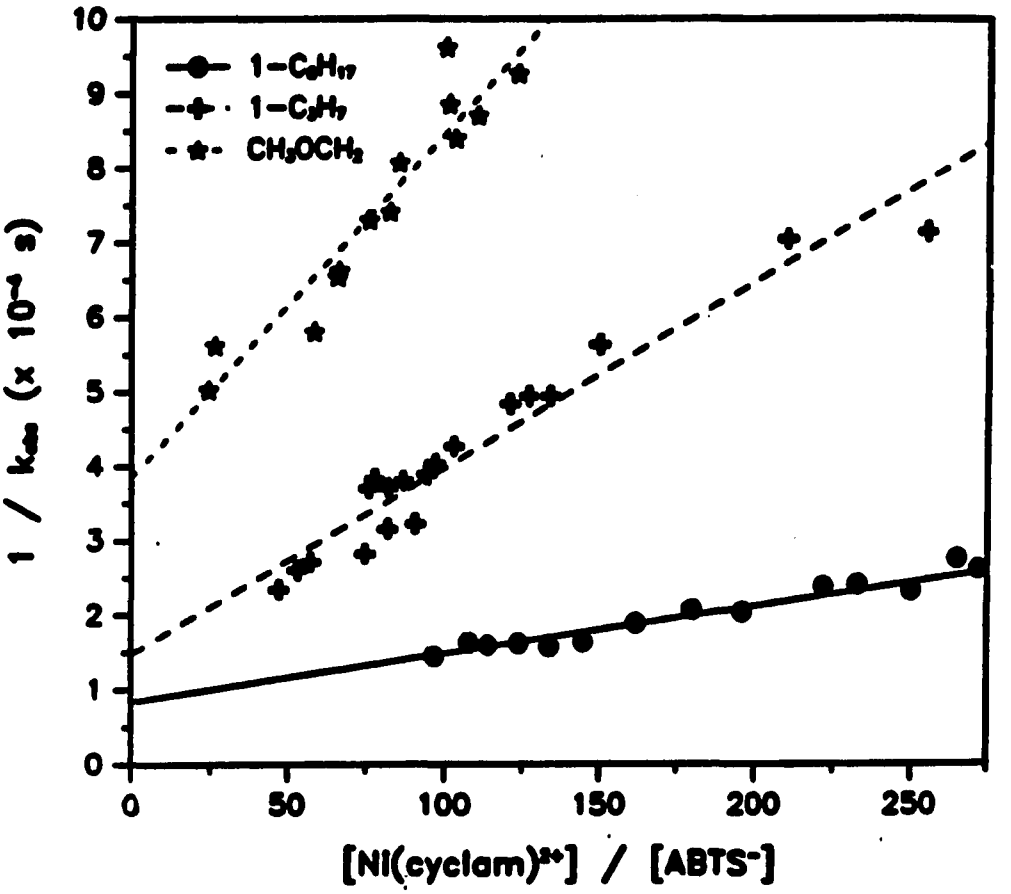

Figure II-2. The plot of $1/k_{\psi}$ versus $[Ni(cyclam)^{2+}]/[ABTS^{\bullet-}]$ for the homolysis of $RNi(cyclam)H_2O^{2+}$ in the presence of $ABTS^{\bullet-}$. Kinetic data were obtained in 0.1 M $HClO_4$ at 25°C using $RCo(dmgH)_2H_2O$ as radical precursor. Data are shown for the complexes of methoxymethyl, propyl, and octyl

Pseudo-first-order rate constants, obtained by varying the oxygen and β-Ni(cyclam)$^{2+}$ concentrations (**Table A-23**), were analyzed using eq 11 which yielded k_{hom} = 80 ± 20 s^{-1} for the homolysis of $CH_3Ni(cyclam)H_2O^{2+}$.

The homolysis reaction of $C_2H_5Ni(cyclam)H_2O^{2+}$ was also studied using $MV^{\bullet+}$ as radical scavenger and resulted in a value for k_{hom} which was similar to that obtained with $ABTS^{\bullet-}$. Using ethylcobaloxime, plots of the inverse of k_ψ versus the ratio of $[Ni(cyclam)^{2+}]/[MV^{\bullet+}]$ deviated from linearity; becoming more pronounced as the ratio of $[Ni(cyclam)^{2+}]/[MV^{\bullet+}]$ was increased. This phenomenon disappeared when ethylcobaloxime was replaced by ethylcobalt(cyclam), as shown in **Figure A-2** for the homolysis of $C_2H_5Ni(cyclam)H_2O^{2+}$. A deaerated solution of dimethylgyloxime was shown to react rapidly with $MV^{\bullet+}$. Thus, the enhanced rate in the cobaloxime containing reactions is presumably due to a reaction of $MV^{\bullet+}$ with free dimethylglyoxime.

Activation Parameters

The temperature dependence of the kinetics of homolysis of $C_2H_5Ni(cyclam)H_2O^{2+}$ was studied. The rate constants obtained at various temperatures are listed in **Table A-24**. The plot of ln(k/T) against 1/T is linear as shown in **Figure II-3**. Values of

$\Delta H^{\ddagger}$ = 74 kJ mol^{-1} and $\Delta S^{\ddagger}$ = 79 J mol^{-1} K^{-1} were calculated using the Eyring equation.

Decomposition of $CH_3Ni(cyclam)^{2+}$ in the Presence of $MV^{\bullet+}$ and $ABTS^{\bullet-}$

Analysis of the kinetic data from the homolysis of $CH_3Ni(cyclam)H_2O^{2+}$ in the presence of $MV^{\bullet+}$ gave a plot of $1/k_{\psi}$ vs. $[Ni(cyclam)^{2+}]/[MV^{\bullet+}]$ which was linear having an intercept value in the region expected for k_{hom}.[10] Yet, the slope from this plot was three times smaller than expected, yielding an estimate for k_{MV} which is larger than the known values. This suggests that a direct reaction of $MV^{\bullet+}$ with $CH_3Ni(cyclam)H_2O^{2+}$ may be contributing.

In the presence of $ABTS^{\bullet-}$, $CH_3Ni(cyclam)H_2O^{2+}$ decomposes with pseudo-first-order rate constants larger than k_{hom}, indicating that a direct reaction could be the primary decomposition pathway with these reagents.

Product Analysis

Laser flash photolysis of deaerated solutions containing 0.010 M β-$Ni(cyclam)^{2+}$ and 5 x 10^{-4} M $RCo(dmgH)_2H_2O$ (R = CH_3, C_2H_5) in both 1.0 M $HClO_4$ and 5 x 10^{-4} M $HClO_4$ gave hydrocarbon

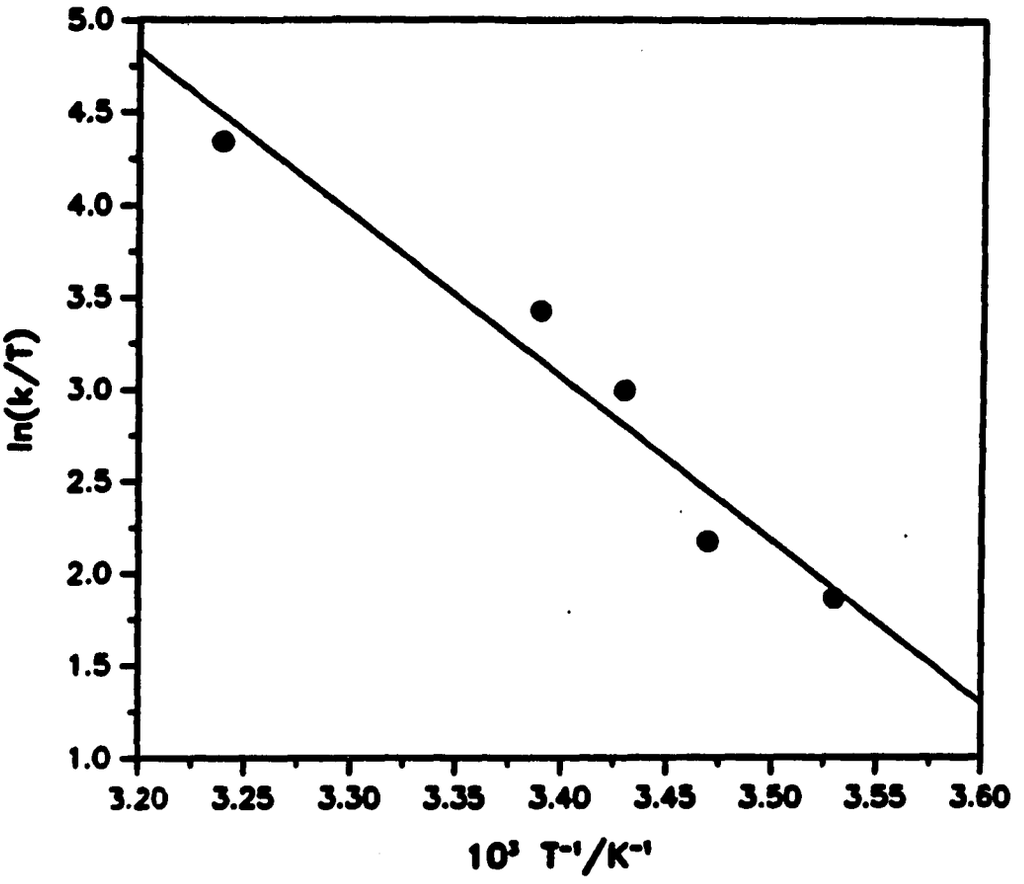

Figure II-3. The plot of Eyring equation for the homolysis of $C_2H_5Ni(cyclam)H_2O^{2+}$

products in self-reaction product ratios. In the case where R = CH_3, ethane was the only hydrocarbon detected either in the presence or absence of β-Ni(cyclam)$^{2+}$. Similarly, in the photolysis of ethylcobaloxime the relative amounts of ethane, ethylene and butane were unchanged either in the presence or absence of β-Ni(cyclam)$^{2+}$. The ratio of ethyl radical disproportionation to combination was measured in these studies to be $k_d/k_c = 0.45 \pm 0.03$.[22]

No UV-visible spectroscopic evidence was found for the formation of RNi(cyclam)H_2O^{2+} in the region 350-400 nm. In the absence of chromophore, all absorbance increases in this spectral region were shown to be caused by traces of oxygen.[10]

DISCUSSION

Alkyl radicals have been shown to react with β-Ni(cyclam)$^{2+}$ to generate a new series of organonickel macrocyclic complexes, RNi(cyclam)H_2O^{2+}. The decomposition of RNi(cyclam)H_2O^{2+}, where R = CH_3 and C_2H_5, gave the expected hydrocarbons in radical self-reaction product ratios.[22] This observation even at pH 0 indicates that acidolysis of RNi(cyclam)H_2O^{2+} is not an important decomposition pathway. Because no UV-visible spectroscopic evidence was found for the formation of RNi(cyclam)H_2O^{2+} in the region 350-400 nm, the kinetics of formation and decomposition of these transient organometallics were monitored through the use of kinetic probe reagents. These observations resulted in our obtaining colligation and homolysis rate constants.

Kinetics of the Colligation of β-Ni(cyclam)$^{2+}$ with Alkyl Radicals

The colligation rate constants, k_{col}, obtained for the series of alkyl radicals studied are summarized in **Table II-1**. Similar corrected rate constants, k_{corr}, were obtained regardless of which kinetic probe reagent, $ABTS^{\bullet-}$ or $MV^{\bullet+}$, was used. The colligation rate constants follow a reactivity order CH_3 > Primary (C_2H_5, 1-C_3H_7, 1-C_6H_{17}) > $CH_3CH(CH_3)CH_2$, $C_6H_5CH_2$,

Secondary (2-C_3H_7, cyclo-C_5H_9); also the substituted methyl radicals were found to be more reactive than ethyl according to the order $BrCH_2$ > $ClCH_2$ > CH_3OCH_2. Note that the increasing chain length of primary radicals has little effect on k_{col}, as values are in the range (0.78-1.20) x 10^7 L mol^{-1} s^{-1}. The reactions of iso-butyl, 2-propyl, and cyclopentyl radicals gave rates in which k_ψ for the formation reaction was so slow that overlap with k_ψ for the homolysis reaction occurred to such an extent that data analysis was prevented; thus, only upper limits on the colligation rate constants could be made.

This trend in reactivity arises from a combination of steric and electronic factors.[23] The pronounced steric effects observed in these reactions with β-Ni(cyclam)$^{2+}$ might be anticipated for reactions in which a planar, π-radical is converted to tetrahedral carbon within the coordination sphere of a metal ion. The energy required to oxidize Ni(cyclam)$^{2+}$ could be responsible for lowering the thermodynamics of these reactions to the extent that steric factors control the reactivity trend (vide infra). Thus colligation rate constants are observed to decline with the increasing bulk of substituents on the radical carbon. The reactivity observed for the substituted methyl radicals shows that rate constants for colligation are enhanced by radicals

which are more capable of oxidizing Ni(II). Therefore, chloro- and bromomethyl radicals react more rapidly than ethyl radical.

Kinetics of the Homolysis of $RNi(cyclam)H_2O^{2+}$

The homolysis of $RNi(cyclam)H_2O^{2+}$ complexes have been studied primarily using the radical scavenger $ABTS^{\bullet-}$. In one instance, for the homolysis of $C_2H_5Ni(cyclam)H_2O^{2+}$, $MV^{\bullet+}$ was used. The homolysis rate constants, k_{hom}, shown in **Table II-1**, follow the reactivity order CH_3 < CH_3OCH_2 < Primary (C_2H_5, 1-C_3H_7, 1-C_8H_{17}) < $CH_3CH(CH_3)CH_2$, $C_6H_5CH_2$, Secondary (2-C_3H_7, cyclo-C_5H_9) < Halomethyl ($ClCH_2$, $BrCH_2$). As in the colligation studies, the homolysis rate constants remained relatively unchanged as the chain length of the primary alkyl groups of $RNi(cyclam)H_2O^{2+}$ was varied, with rate constants in the range (0.53-1.20) x 10^4 s^{-1}. This trend in reactivity is consistent with that observed for unimolecular homolysis in other organometallic complexes.[24]

The least stable complexes are $XCH_2Ni(cyclam)H_2O^{2+}$ (X = Cl, Br), which decomposed so rapidly that both k_{col} and k_{hom} could be obtained only from the homolysis stage of the reaction. The instability of these organonickel complexes may be caused by resonance of the halomethyl group allowing electron donation back into the metal center.

The most stable complex is $CH_3Ni(cyclam)H_2O^{2+}$, which can survive for about one minute in the absence of scavenger. In the presence of either $ABTS^{\bullet-}$ or $MV^{\bullet+}$, $CH_3Ni(cyclam)H_2O^{2+}$ was seen to decompose more rapidly than expected for unimolecular homolysis. Therefore, oxygen was used as the radical scavenger, eq 12. The peroxyalkyl radical reacts with β-$Ni(cyclam)^{2+}$ in a fast reaction to yield $RO_2Ni(cyclam)H_2O^{2+}$, eq 13. Pseudo-first-order rate constants, eq 14, were obtained by

$$RNi(cyclam)H_2O^{2+} \underset{k_{col}}{\overset{k_{hom}}{}} R^{\bullet} + Ni(cyclam)^{2+} + H_2O \qquad (-8)$$

$$R^{\bullet} + O_2 \xrightarrow{k_{Ox}} RO_2^{\bullet} \qquad (12)$$

$$RO_2^{\bullet} + Ni(cyclam)^{2+} \xrightarrow{fast} RO_2Ni(cyclam)H_2O^{2+} \qquad (13)$$

$$k_{\psi} = \frac{k_{hom}k_{Ox}[O_2]}{k_{Ox}[O_2] + k_{col}[Ni(cyclam)^{2+}]} \qquad (14)$$

following the appearance of $RO_2Ni(cyclam)H_2O^{2+}$ at 360 nm. A nonlinear least-squares analysis gave the rate constants for homolysis, k_{hom}, and for the reaction with oxygen, k_{Ox}. The homolysis rate constant was found to be $k_{hom} = 80 \pm 20\ s^{-1}$, which is within experimental error of the pulse radiolysis value.[10] The rate constant for the reaction of $CH_3^{\bullet}$ with oxygen, k_{Ox} =

$(4.1 \pm 1.5) \times 10^9$ L mol^{-1} s^{-1}, is within experimental error of the literature values,[10,25] confirming the correctness of the reaction scheme adopted.

Plots of the inverse of the pseudo-first-order rate constants for the homolysis of $C_2H_5Ni(cyclam)H_2O^{2+}$ in the presence of $MV^{\bullet+}$ became curved at increasing ratios of $[Ni(cyclam)^{2+}]/[MV^{\bullet+}]$. This observation has been attributed to a competing reaction between $MV^{\bullet+}$ and free dimethylglyoxime ($HONC(CH_3)C(CH_3)NOH$ or $dmgH_2$), eq 15, which becomes important only at high β-$Ni(cyclam)^{2+}$ concentrations where the first term in the rate law (eq 16) has been minimized.

$$HONC(CH_3)C(CH_3)NOH + MV^{\bullet+} \longrightarrow MV^{+2} + [HONC(CH_3)C(CH_3)NOH]^- \quad (15)$$

$$-d[MV^{\bullet+}]/dt = \frac{k_{hom}k_{MV}[MV^{\bullet+}]}{k_{MV}[MV^{\bullet+}] + k_{col}[Ni(cyclam)^{2+}]} + k_{15}[dmgH_2] \quad (16)$$

Replacement of $C_2H_5Co(dmgH)_2H_2O$ with the $C_2H_5Co(cyclam)H_2O^{2+}$ precursor resulted in pseudo-first-order rate constants consistent with unimolecular homolysis of $C_2H_5Ni(cyclam)H_2O^{2+}$ in the presence of $MV^{\bullet+}$, **Figure A-2**. Photolysis of $C_2H_5Co(cyclam)H_2O^{2+}$ generates the stable $(H_2O)_2Co(cyclam)^{2+}$ complex, which does not react with $MV^{\bullet+}$.

Which Form of β-Ni(cyclam)$^{2+}$ is Reactive?

Experimental conditions were such that β-Ni(cyclam)$^{2+}$ was present in a rapidly-equilibrating mixture of four-coordinate (71%) and six-coordinate (29%) species.[26] This kinetic analysis is incapable of determining if the four-coordinate or both four- and six-coordinate species are reactive. With this in mind, attempts to react the six-coordinate complex cis-$(H_2O)_2$Ni(cyclam)$^{2+}$ with alkyl radicals proved unsuccessful.[27] Since the water molecules in the cis-complex are expected to be relatively inert to substitution[28] (as required to insure the cis configuration), R$^{\bullet}$ cannot compete effectively for a coordination site; therefore, no reaction takes place. On the other hand, six-coordinate β-Ni(cyclam)$(H_2O)_2^{2+}$ possesses labile water molecules which may be replaced by an alkyl radical, leaving open the question of its contribution in these colligation reactions.

A more telling result is the entropy of activation, $\Delta S^{\ddagger}$ = 79 J mol^{-1} s^{-1}, measured for the homolysis of C_2H_5Ni(cyclam)H_2O^{2+}. **Table II-2** shows $\Delta H^{\ddagger}$ and $\Delta S^{\ddagger}$ for this reaction along with the activation parameters for representative organocobalt and organochromium complexes.[24] These entropy values consist of an intrinsic term generated by the bond breaking and bond making contributions within the transition state, and a term

corresponding to solvation effects specific to the products being formed in the transition state. Homolysis of the organocobalt and organochromium complexes results in no change in coordination number of the metal ion; therefore, $\Delta S^{\ddagger}$ values for these complexes are smaller. The large $\Delta S^{\ddagger}$ value for $C_2H_5Ni(cyclam)H_2O^{2+}$ is consistent with a loss in coordination number upon homolysis, indicating that the planar form of β-$Ni(cyclam)^{2+}$ is the reactive form.

If the four-coordinate β-$Ni(cyclam)^{2+}$ is the only reactive form, "true" values of k_{col} are the rate constants in **Table II-1** divided by 0.71.

Comparison of Colligation Rate Constants for Complexes of Ni(II), Co(II), and Cr(II)

These studies have determined that steric effects play an important role in the colligation reactions of alkyl radicals with β-$Ni(cyclam)^{2+}$. Meanwhile, analogous reactions for Co(II) and Cr(II) complexes show only slight variation in colligation rate constants with the nature of the radical. **Table II-3** shows colligation rate constants for $RNi(cyclam)H_2O^{2+}$,[23] $(H_2O)_5CrR^{2+}$,[29] $RCo(cyclam)H_2O_{2+}$,[30] and RB_{12}.[29] Analysis of this list clarifies that metal carbon bonds are much weaker for $RNi(cyclam)H_2O^{2+}$ than for Co-R and Cr-R complexes. The enthalpy

Table II-2. Activation parameters[a] of unimolecular homolysis for organonickel, organocobalt, and organochromium complexes, RML^{n+}

RML^{n+}	$\Delta H^{\ddagger}$/kJ mol^{-1}	$\Delta S^{\ddagger}$/J mol^{-1} K^{-1}
$C_2H_5Ni(cyclam)H_2O^{2+}$ [b]	74 ± 6	79 ± 16
$C_2H_5CoL^1H_2O^{2+}$ [c]	107 ± 3	50 ± 8
$1\text{-}C_3H_7CoL^1H_2O^{2+}$ [c]	111 ± 3	63 ± 12
$C_2H_5CoL^2H_2O^{2+}$ [c]	105 ± 4	42 ± 12
$1\text{-}C_3H_7CoL^2H_2O^{2+}$ [c]	111 ± 4	59 ± 12
$2\text{-}C_3H_7CrL^3H_2O^{2+}$ [d]	110 ± 3	62 ± 6
$C_6H_5CH_2CrL^3H_2O^{2+}$ [d]	103 ± 2	28 ± 5

[a]At 25°C aqueous solution; [b]This study; [c]Ref. 24a; L^1 = $Me_6[14]aneN_4$; L^2 = $Me_6[14]4,11\text{-}dieneN_4$; [d]Ref. 24b; L^3 = $[15]aneN_4$.

of activation, $\Delta H^{\ddagger}$ = 74 kJ mol^{-1} (**Table II-2**), is significantly smaller than that found in Co-R and Cr-R complexes. Subtraction of 8-10 kJ mol^{-1} from $\Delta H^{\ddagger}$ for the enthalpic contribution of the colligation reaction gives an estimate of 65 kJ mol^{-1} for the bond dissociation enthalpy of $C_2H_5Ni(cyclam)H_2O^{2+}$. In fact the strongest metal carbon bond, as expressed by $-RTln(k_{col}/k_{hom})$, for $RNi(cyclam)H_2O^{2+}$ ($R = CH_3$ with $K = 10^7$ L mol^{-1}) is weaker than the least stable $RCo(cyclam)H_2O^{2+}$ analogue ($R = C_6H_5CH_2$, $K = 10^{11}$ L mol^{-1}).[23]

The equilibrium constants, K, for the organocobalt and organochromium complexes change dramatically in the series ($CH_3 > 1^o > 2^o$), without a corresponding change in the values of k_{col}, despite the fact that values of k_{col} lie in the activation-controlled region. We interpret these findings to suggest that colligation rate constants for these species experience a kinetic "leveling effect", imposed by the competition between radical attack and solvent dissociation from the five- or six-coordinate complexes. Therefore, while the favorable thermodynamics of the reactions of $R^{\bullet}$ with Co(II) and Cr(II) minimize the contribution of steric crowding in the transition state, the "leveling effect" keeps the colligation rate constants from reaching the diffusion controlled limit.

Table II-3. Rate constants[a] for the colligation of alkyl radicals with metal complexes, RML^{n+}

	$k_{col}/10^7$ L mol^{-1} s^{-1}			
R•	β-Ni(cyclam)$^{2+}$ [b]	$Cr(H_2O)_6^{2+}$ [c]	$(H_2O)_2Co(cyclam)^{2+}$ [d]	B_{12r} [e]
CH_3	73.	22	1.6	44
C_2H_5	1.3	19	1.1	51
1-C_3H_7	1.0	22	—	61
2-C_3H_7	<0.02	—	—	25
c-C_5H_{11}	<0.02	8	—	—

[a]At 25°C in aqueous solution. [b]Ref 23. [c]Ref 28. [d]Ref 29. [e]Ref 29.

The six-coordinate β-isomer, trans-$(H_2O)_2Ni(cyclam)^{2+}$, would be expected to possess colligation rate constants exhibiting a similar "leveling effect". The absence of this effect for β-$Ni(cyclam)^{2+}$, as evidenced by the nearly diffusion controlled rate constant for the reaction with $CH_3^{\bullet}$, is a further indication that square-planar β-$Ni(cyclam)^{2+}$ is the reactive species. The less favorable thermodynamics for colligation reactions of β-$Ni(cyclam)^{2+}$ allow increased steric crowding in the transition state to dramatically effect the colligation rate constants.

Decomposition of $CH_3Ni(cyclam)H_2O^{2+}$ in the Presence of $MV^{\bullet+}$ and $ABTS^{\bullet-}$

The enhanced pseudo-first-order rate constants from the decomposition of $CH_3Ni(cyclam)H_2O^{2+}$ in the presence of $MV^{\bullet+}$ indicate that a direct reaction between $CH_3Ni(cyclam)H_2O^{2+}$ and $MV^{\bullet+}$ may be contributing to the overall rate. Because the contribution of the direct reaction was small under the conditions of the experiment, the plot of $1/k_{\psi}$ vs. $[Ni(cyclam)^{2+}]/[MV^{\bullet+}]$ remained linear. One possible reaction could involve alkyl transfer to the delocalized radical probe, eq 17.

$$RNiL(H_2O)^{2+} + MV^{\bullet+} + H^+ \longrightarrow NiL^{2+} + [MV(R)(H)]^{2+} + H_2O \quad (17)$$

Using the homolysis rate constant obtained from the oxygen reaction (k_{hom} = 80 s^{-1}) in a nonlinear least-squares analysis, eq 18, we obtain k_{17} = (1.7 ± 0.2) x 10^5 L mol^{-1} s^{-1}.

$$k_{\psi} = \frac{k_{hom}k_{MV}[MV^{\bullet+}]}{k_{MV}[MV^{\bullet+}] + k_{col}[Ni(cyclam)^{2+}]} + k_{17}[MV^{\bullet+}] \qquad (18)$$

In the presence of $ABTS^{\bullet-}$, $CH_3Ni(cyclam)H_2O^{2+}$ decomposes with pseudo-first-order rate constants larger than k_{hom}. This suggests unimolecular homolysis is no longer the dominant decomposition pathway. This result is not surprising since $ABTS^{\bullet-}$ also reacts directly with substituted primary and secondary alkylcobaloximes. Again, an alkyl transfer reaction to $ABTS^{\bullet-}$ may become important at the longer reaction times afforded by the stability of $CH_3Ni(cyclam)H_2O^{2+}$, eq 19.

$$ABTS^{\bullet-} + CH_3NiLH_2O^{2+} \longrightarrow [ABTS\text{-}CH_3]^{2-} + NiL^{2+} + H_3O^{+} \qquad (19)$$

Summary

The kinetics of colligation reactions of a series of alkyl radicals with β-$Ni(cyclam)^{2+}$ were studied using laser flash photolysis of alkylcobalt complexes. The kinetics were obtained

by employing the kinetic probe competition method (with $ABTS^{\bullet-}$ or $MV^{\bullet+}$).

The kinetics of the unimolecular homolysis of a series of $RNi(cyclam)H_2O^{2+}$ were studied using $ABTS^{\bullet-}$, $MV^{\bullet+}$ or oxygen as radical scavenging agents. Activation parameters were obtained for the unimolecular homolysis of $C_2H_5Ni(cyclam)H_2O^{2+}$.

The colligation and homolysis rate constants are strongly influenced by steric and electronic factors. Kinetic and thermodynamic data obtained from these reactions were compared with those for other σ-bonded organometallic complexes.

BIBLIOGRAPHY

1. (a) Espenson, J. H. "Advances in Inorganic and Bioinorganic Mechanisms"; Sykes, G., Ed.; Academic: London, 1982; Vol. 1, p 1. (b) Johnson, M. D. "Reactions of Coordinated Ligands"; Braterman, P. S., Ed.; Plenum: New York, 1986; p 155.

2. (a) Jolly, P. W.; Wilke, G. "The Organic Chemistry of Nickel"; Academic: New York, 1974; Vol. 1. (b) Wilke, G. Angew. Chem., Int. Ed. Engl. 1988, 27, 185.

3. Walsh, C. T., Orme-Johnson, W. H. Biochemistry 1987, 26, 4901.

4. Kojima, N.; Fox, J. A.; Hausinger, R. P.; Daniels, L.; Orme-Johnson, W. H.; Walsh, C. T. Proc. Natl. Acad. Sci. U.S.A. 1983, 80, 378.

5. Albracht, S. P. J.; Ankel-Fuchs, D.; Van der Zwaan, J. W.; Fontija, R. D.; Thauer, R. K. Biochim. Biophys. Acta 1986, 832, 89.

6. (a) Bonner, W. A.; Grimm, R. A. "The Chemistry of Organic Sulfur Compounds"; Kharusch and Meyers, Eds.; Pergamon: New York, 1966; p 410. (b) Wackett, L.; Honek, J. F.; Begley, T. P.; Wallace, V.; Orme-Johnson, W. H.; Walsh, C. T. Biochemistry 1987, 26, 6012.

7. D'Aniello, M. J.; Barefield, E. K. J. Am. Chem. Soc. 1976, 98, 1610.

8. Ram, M. S.; Espenson, J. H.; Bakac, A. Inorg. Chem. 1986, 25, 4115.

9. Bakac, A.; Espenson, J. H. J. Am. Chem. Soc. 1986, 108, 719.

10. Sauer, A.; Cohen, H.; Meyerstein, D. Inorg. Chem. 1988, 27, 4578.

11. Bosnich, B.; Tobe, M. L.; Webb, G. A. Inorg. Chem. 1965, 4, 1109.

12. Bakac, A.; Espenson, J. H. Inorg. Chem. 1989, 28, 3901.

13. Kelley, D. K.; Espenson, J. H.; Bakac, A. Inorg. Chem. 1990, 29, 0000.

14. Yamazaki, N.; Hohokabi, Y. Bull. Chem. Soc. Japan 1971, 44, 63.

15. Bakac, A.; Espenson, J. H. Inorg. Chem. 1987, 26, 4353.

16. Maruthamuthu, P.; Venkatasubramanian, L.; Dharmalingam, P. Bull. Chem. Soc. Japan 1987, 60, 1113.

17. Watanabe, T.; Honda, K. J. Phys. Chem. 1982, 86, 2617.

18. Connolly, P. Ph.D. Dissertation, Iowa State University, Ames, Iowa, 1985.

19. Hoselton, M. A.; Lin, C.-T.; Schwartz, H. A.; Sutin, N. J. Am. Chem. Soc. 1978, 100, 2383. The energy of the laser pulse is 250 mJ.

20. The reaction of $^{\bullet}C_2H_5$ with $ABTS^{\bullet-}$ gives C_2H_4, amounting to (roughly) some 30% of the reaction, and presumably a species in which $^{\bullet}C_2H_5$ has added to a carbon on the aromatic ring:[13]

$$R^{\bullet} + ABTS^{\bullet-} \longrightarrow [ABTS\text{-}R]^{2-} + H^{+}$$

21. Barshop, B. A.; Wrenn, R. F.; Frieden, C. Anal. Biochem. 1983, 130, 130.

22. Bakac, A.; Espenson, J. H. J. Phys. Chem. 1986, 90, 325.

23. Kelley, D. K.; Espenson, J. H.; Bakac, A. Inorg. Chem. 1990, 29, 0000.

24. (a) Lee, S.; Espenson, J. H.; Bakac, A. Inorg. Chem. 1990, 29, 0000. (b) Shi, S.; Espenson, J. H.; Bakac, A. Inorg. Chem. 1990, 29, 0000.

25. Thomas, J. K. J. Phys. Chem. 1967, 71, 1919.

26. Anichini, A.; Fabbrizzi, L.; Paoletti, P.; Clay, R. M. Inorg. Chim. Acta Lett. 1977, 24, 21.

27. Marchaj, A. unpublished observations, Department of Chemistry, Iowa State University, Ames, Iowa, 1990.

28. (a) Rablen, D. P.; Dodgen, H. W.; Hunt, J. P. J. Am. Chem. Soc. 1972, 94, 1771. (b) Curzon, E. H.; Herron, N.; Moore, P. J. C. S. Dalton Trans 1980, 574. (c) Moore, P.; Sachinidis, J.; Willey, G. R. J. C. S. Dalton Trans 1984, 1323.

29. Espenson, J. H.; Connolly, P.; Meyerstein, D.; Cohen, H. Inorg. Chem. 1983, 22, 1009.

30. Bakac, A.; Espenson, J. H. Inorg. Chem. 1989, 28, 4319.

APPENDIX

Table A-1. Kinetic data of the reaction of methyl radical with β-Ni(cyclam)$^{2+}$

Conditions: $[CH_3Co(dmgH)_2H_2O]$ = 50 μM
λ = 600[a] and 650[b] nm
T = 25°C, in 0.10 M $HClO_4$

$[NiL^{2+}]$/μM	$[Probe]_i$/μM	$[Probe]_f$/μM	$10^{-4}k_\psi/s^{-1}$	$10^{-4}k_{corr}/s^{-1}$
40.	1.18[a]	1.10	4.90	3.34
39.	1.10[a]	1.02	4.89	3.42
60.	2.26[a]	2.18	7.26	4.41
59.	2.03[a]	1.95	6.55	3.99
49.	1.74[a]	1.64	5.46	3.21
30.	1.09[a]	0.99	3.62	2.14
29.	0.98[a]	0.88	3.86	2.50
65.	2.04[a]	1.94	7.57	4.91
45.	2.09[a]	1.99	5.77	3.16
44.	1.92[a]	1.82	5.33	2.86
43.	1.73[a]	1.65	5.19	2.98
55.	2.61[a]	2.51	7.59	4.31
54.	2.38[a]	2.28	7.52	4.51
53.	2.32[a]	2.22	6.63	3.71
35.	2.02[a]	1.92	5.27	2.69
34.	1.84[a]	1.74	4.78	2.46
33.	1.74[a]	1.66	4.82	2.62
52.	4.29[b]	4.01	9.01	3.74
50.	3.94[b]	3.64	8.19	3.19
48.	3.76[b]	3.56	8.57	3.88
70.	4.27[b]	4.01	10.8	5.50
66.	3.72[b]	3.51	9.07	4.47
64.	3.57[b]	3.36	8.82	4.36
34.	3.97[b]	3.64	7.68	2.70
30.	3.56[b]	3.26	7.33	2.84
28.	3.35[b]	3.05	6.22	1.93
60.	3.91[b]	3.66	8.91	4.04
58.	3.69[b]	3.46	8.88	4.30
56.	3.47[b]	3.23	8.43	4.01
54.	3.32[b]	3.12	8.68	4.48

[a]Using $MV^{\bullet+}$ as kinetic probe. [b]Using $ABTS^{\bullet-}$ as kinetic probe; L = cyclam.

Table A-2. Kinetic data of the reaction of ethyl radical with β-Ni(cyclam)$^{2+}$

Conditions: $[C_2H_5Co(dmgH)_2H_2O]$ = 50 μM
λ = 600[a] and 650[b] nm
T = 25°C, in 0.10 M $HClO_4$

$[NiL^{2+}]$/mM	$[Probe]_i$/μM	$[Probe]_f$/μM	$10^{-4}k_\psi/s^{-1}$	$10^{-4}k_{corr}/s^{-1}$
1.00	3.68[a]	3.45	6.92	2.15
1.00	3.19[a]	2.99	6.03	1.88
1.00	2.77[a]	2.61	5.95	2.36
1.00	2.43[a]	2.25	5.51	2.27
1.25	1.98[a]	1.87	5.84	3.23
1.25	1.68[a]	1.57	6.32	4.04
1.25	1.54[a]	1.44	4.57	2.47
1.25	1.29[a]	1.21	3.46	1.69
1.75	3.08[a]	2.93	7.46	3.46
1.75	2.76[a]	2.58	7.27	3.57
2.00	1.87[a]	1.75	6.95	4.35
2.00	1.61[a]	1.51	5.82	3.56
2.25	1.53[a]	1.45	5.61	3.49
2.25	1.14[a]	1.08	5.45	3.81
2.25	1.44[a]	1.36	6.39	4.36
3.00	1.58[a]	1.51	6.97	4.77
3.00	1.28[a]	1.21	6.85	4.95
1.00	3.12[b]	2.60	5.90	2.37
1.00	2.52[b]	2.10	5.45	2.54
2.00	2.98[b]	2.54	6.64	3.11
2.00	2.07[b]	2.27	6.61	3.37
2.00	2.43[b]	2.10	5.99	3.12
2.40	2.90[b]	2.58	7.12	3.86
2.40	2.61[b]	2.30	7.34	4.27
3.00	2.97[b]	2.63	8.20	4.73
3.00	2.63[b]	2.35	6.89	3.82
3.00	2.37[b]	2.11	6.93	4.09
3.00	2.14[b]	1.87	7.73	4.98
3.50	2.96[b]	2.67	8.73	5.34
3.50	2.66[b]	2.42	8.42	5.38

[a]Using $MV^{\bullet+}$ as kinetic probe. [b]Using $ABTS^{\bullet-}$ as kinetic probe; L = cyclam.

Table A-3. Kinetic data[a] of the reaction of 1-propyl radical with β-Ni(cyclam)$^{2+}$

Conditions: $[C_3H_7Co(dmgH)_2H_2O]$ = 60 μM
λ = 650 nm
T = 25°C, in 0.10 M $HClO_4$

$[NiL^{2+}]$/mM	$[ABTS^{\bullet-}]_i$/μM	$[ABTS^{\bullet-}]_f$/μM	$10^{-4}k_\psi/s^{-1}$	$10^{-4}k_{corr}/s^{-1}$
1.00	2.70	2.38	5.31	2.10
1.75	3.56	3.06	7.89	3.39
1.75	3.30	2.90	7.02	3.01
1.75	2.98	2.60	6.43	2.76
2.00	3.37	2.93	7.60	3.39
2.00	3.06	2.68	6.60	2.86
2.25	4.29	3.94	7.49	2.74
3.50	2.50	2.28	8.00	4.87
4.75	1.82	1.66	7.79	5.33
4.75	1.52	1.40	8.32	6.39

[a]Using $ABTS^{\bullet-}$ as kinetic probe; L = cyclam.

Table A-4. Kinetic data[a] of the reaction of 1-butyl radical with β-Ni(cyclam)$^{2+}$

Conditions: $[C_4H_9Co(dmgH)_2H_2O]$ = 60 μM

λ = 650 nm

T = 25°C, in 0.10 M $HClO_4$

$[NiL^{2+}]$/mM	$[ABTS^{\bullet-}]_i$/μM	$[ABTS^{\bullet-}]_f$/μM	$10^{-4}k_\psi/s^{-1}$	$10^{-4}k_{corr}/s^{-1}$
1.00	3.04	2.80	5.41	2.11
1.00	2.84	2.62	5.73	2.66
2.00	2.63	2.45	6.03	3.13
2.00	2.50	2.32	5.78	3.01
2.00	2.29	2.11	6.03	3.45
3.50	3.67	3.47	8.15	4.26
3.50	3.48	3.28	7.24	3.93
3.50	3.21	3.01	7.34	4.15
3.50	2.99	2.79	7.59	4.33
5.00	3.94	3.76	10.9	5.59
5.00	3.60	3.46	9.10	5.30
5.00	3.38	3.22	9.00	5.45
5.00	3.19	3.04	9.20	5.65
6.50	3.94	3.80	12.6	8.32
6.50	3.78	3.63	12.6	8.44
8.00	3.89	3.78	15.4	11.2
8.00	3.67	3.57	15.4	11.4
8.00	3.51	3.40	13.9	8.74
8.00	3.38	3.28	12.6	8.89
10.0	3.57	3.47	13.2	9.35
10.0	3.28	3.18	16.8	13.1

[a]Using $ABTS^{\bullet-}$ as kinetic probe; L = cyclam.

Table A-5. Kinetic data[a] of the reaction of 1-pentyl radical with β-Ni(cyclam)$^{2+}$

Conditions: $[C_5H_{11}Co(dmgH)_2H_2O]$ = 100 μM
λ = 650 nm
T = 25°C, in 0.10 M $HClO_4$

$[NiL^{2+}]$/mM	$[ABTS^{\bullet-}]_i$/μM	$[ABTS^{\bullet-}]_f$/μM	$10^{-4}k_\psi/s^{-1}$	$10^{-4}k_{corr}/s^{-1}$
2.80	3.15	2.66	7.64	3.51
3.50	2.50	2.15	6.51	3.26
3.50	2.18	1.85	6.50	3.46
3.50	1.81	1.55	6.77	4.07
3.50	1.44	1.23	6.47	4.13
4.20	2.66	2.35	8.09	4.64
4.20	2.04	1.79	7.41	4.56
5.00	2.92	2.64	8.81	5.22
5.00	2.66	2.40	7.77	4.51
5.80	2.53	2.34	9.35	6.25
5.80	1.90	1.74	9.54	6.92
6.50	2.90	2.64	11.1	7.32
6.50	2.43	2.20	9.43	6.23
6.50	2.17	1.98	10.8	7.78
6.50	1.77	1.61	8.52	6.06
8.00	2.16	1.99	9.61	6.80
8.00	1.75	1.63	10.0	7.60

[a]Using $ABTS^{\bullet-}$ as kinetic probe; L = cyclam.

Table A-6. Kinetic data[a] of the reaction of 1-hexyl radical with β-Ni(cyclam)$^{2+}$

Conditions: $[C_6H_{13}Co(dmgH)_2H_2O]$ = 100 μM
λ = 650 nm
T = 25°C, in 0.10 M $HClO_4$

$[NiL^{2+}]$/mM	$[ABTS^{\bullet-}]_i$/μM	$[ABTS^{\bullet-}]_f$/μM	$10^{-4}k_\psi/s^{-1}$	$10^{-4}k_{corr}/s^{-1}$
3.50	2.76	2.47	7.76	4.48
3.50	2.32	2.11	7.06	4.35
3.50	1.73	1.55	5.92	3.74
3.50	1.39	1.28	6.50	4.72
4.00	2.98	2.78	7.46	4.34
4.00	1.77	1.66	6.42	4.44
4.00	1.51	1.43	6.26	4.58
4.50	1.66	1.53	7.44	5.35
4.50	1.35	1.23	6.90	5.04
5.00	2.90	2.71	8.85	5.70
5.00	2.51	2.35	8.60	5.82
5.50	2.86	2.68	9.45	6.31
5.50	2.41	2.27	8.79	6.13
5.50	1.69	1.57	8.27	6.14
5.50	1.57	1.44	7.84	5.75
6.00	3.08	2.87	10.3	6.89
6.00	2.65	2.45	8.65	5.64
6.00	2.28	2.12	9.32	6.61
6.00	1.87	1.78	8.12	6.06
6.00	1.39	1.33	8.30	6.69
6.00	1.46	1.39	8.51	6.78

[a]Using $ABTS^{\bullet-}$ as kinetic probe; L = cyclam.

Table A-7. Kinetic data[a] of the reaction of 1-heptyl radical with β-Ni(cyclam)$^{2+}$

Conditions: $[C_7H_{15}Co(dmgH)_2H_2O]$ = 100 μM
λ = 650 nm
T = 25°C, in 0.10 M $HClO_4$

$[NiL^{2+}]$/mM	$[ABTS^{\bullet-}]_i$/μM	$[ABTS^{\bullet-}]_f$/μM	$10^{-4}k_\psi/s^{-1}$	$10^{-4}k_{corr}/s^{-1}$
3.00	2.94	2.70	7.53	4.07
3.00	2.73	2.50	6.69	3.49
3.00	2.12	1.95	6.09	3.55
3.50	3.12	2.90	6.96	3.44
3.50	2.58	2.40	6.48	3.52
4.00	2.79	2.57	8.52	5.14
4.00	2.51	2.31	7.78	4.72
4.00	2.28	2.12	7.07	4.36
5.00	2.86	2.71	7.80	4.59
5.00	2.55	2.41	7.35	4.46
5.00	1.92	1.80	8.07	5.69
5.50	2.57	2.43	9.09	6.08
5.50	2.31	2.16	8.08	5.30
5.50	2.07	1.94	8.09	5.56

[a]Using $ABTS^{\bullet-}$ as kinetic probe; L = cyclam.

Table A-8. Kinetic data[a] of the reaction of 1-octyl radical with β-Ni(cyclam)$^{2+}$

Conditions: $[C_8H_{17}Co(dmgH)_2H_2O]$ = 100 μM
λ = 650 nm
T = 25°C, in 0.10 M $HClO_4$

$[NiL^{2+}]$/mM	$[ABTS^{\bullet-}]_i$/μM	$[ABTS^{\bullet-}]_f$/μM	$10^{-4}k_\psi/s^{-1}$	$10^{-4}k_{corr}/s^{-1}$
3.00	3.78	3.51	8.18	3.62
3.00	3.33	3.08	7.10	3.07
3.00	2.79	2.63	7.15	3.84
3.00	2.39	2.24	7.15	4.15
3.50	3.02	2.78	7.25	3.51
3.50	2.63	2.44	7.18	3.90
3.50	1.87	1.76	6.42	4.12
4.00	3.57	3.41	9.31	5.08
4.00	3.36	3.16	7.13	3.15
4.50	2.99	2.72	8.36	4.50
4.50	2.15	1.99	7.50	4.70
4.50	1.91	1.76	6.75	4.23
5.00	3.20	3.05	8.13	4.34
5.00	2.93	2.81	8.22	4.75
5.00	2.41	2.28	8.02	5.04
5.00	2.29	2.14	8.22	5.28
5.50	3.05	2.88	9.36	5.61
5.50	2.47	2.35	8.48	5.45
5.50	2.32	2.15	8.08	5.06
5.50	2.04	1.91	8.78	6.08
5.50	1.78	1.67	8.92	6.51
6.00	3.29	3.12	10.0	6.09
6.00	3.02	2.86	8.63	4.97
6.00	2.84	2.69	9.50	5.86
6.00	2.27	2.17	9.58	6.75

[a]Using $ABTS^{\bullet-}$ as kinetic probe, P; L = cyclam.

Table A-9. Kinetic data[a] of the reaction of methoxymethyl radical with β-Ni(cyclam)$^{2+}$

Conditions: $[CH_3OCH_2Co(dmgH)_2H_2O]$ = 100 μM

λ = 650 nm

T = 25°C, in 0.10 M $HClO_4$

$[NiL^{2+}]$/mM	$[ABTS^{\bullet-}]_i$/μM	$[ABTS^{\bullet-}]_f$/μM	$10^{-4}k_\psi/s^{-1}$	$10^{-4}k_{corr}/s^{-1}$
0.51	2.79	2.05	4.29	0.896
0.51	1.99	1.71	3.71	0.867
0.51	1.64	1.40	3.58	1.20
1.00	3.07	2.75	6.37	1.80
1.00	2.57	2.31	5.37	1.52
1.00	2.21	1.99	5.02	1.70
1.50	3.17	2.93	6.74	2.06
1.50	2.79	2.57	6.28	2.13
1.75	3.34	3.16	7.68	2.81
1.75	2.82	2.64	7.35	3.18
2.00	4.54	4.38	9.14	2.64
2.00	4.30	4.10	9.45	3.24
2.00	3.96	3.74	9.11	3.34
2.00	3.59	3.41	9.03	3.81
2.00	1.87	1.77	6.75	3.95

[a]Using $ABTS^{\bullet-}$ as kinetic probe; L = cyclam.

Table A-10. Kinetic data of the homolysis of $C_2H_5Ni(cyclam)H_2O^{2+}$ in the presence of $MV^{\bullet+}$
Conditions: $[C_2H_5Co(cyclam)H_2O^{2+}]$ = 100 μM
λ = 600 nm, T = 25°C
in 0.10 M $HClO_4$

$10^3[Ni(cyclam)^{2+}]/M$	$10^5[MV^{\bullet+}]_{ave}/M$	$10^{-3}k_\psi/s^{-1}$
3.50	3.38	2.92
3.50	2.82	2.61
3.50	2.56	2.58
3.50	2.34	2.40
3.50	1.77	1.72
3.50	1.20	1.46
3.50	0.92	1.18
7.00	2.93	1.86
7.00	2.67	1.73
7.00	2.59	1.71
7.00	2.35	1.62
7.00	1.88	1.29
7.00	1.70	1.19
7.00	1.62	1.13
7.00	1.45	1.02
15.0	3.13	0.910
15.0	2.79	0.925
15.0	2.53	0.820
15.0	2.46	0.792
15.0	1.66	0.549
15.0	1.38	0.493
15.0	1.27	0.484
15.0	1.09	0.412
15.0	2.52	0.933
15.0	2.04	0.564
15.0	1.91	0.666

Table A-11. Kinetic data of the homolysis of $C_2H_5Ni(cyclam)H_2O^{2+}$ in the presence of $ABTS^{\bullet-}$
Conditions: $[C_2H_5Co(dmgH)_2H_2O^{2+}]$ = 100 μM
λ = 600 nm, T = 25°C
in 0.10 M $HClO_4$

$10^3[Ni(cyclam)^{2+}]/M$	$10^5[ABTS^{\bullet-}]_{ave}/M$	$10^{-3}k_\psi/s^{-1}$
5.00	2.64	3.37
5.00	2.41	3.15
5.00	2.21	3.00
5.00	3.95	3.72
5.00	3.76	3.64
5.00	3.36	3.75
5.00	3.20	3.61
6.50	2.84	2.88
6.50	2.58	2.83
6.50	2.34	2.46
6.50	2.12	2.48
6.50	3.96	3.81
6.50	3.67	3.54
6.50	3.42	3.42
6.50	3.16	3.27
8.00	2.76	2.27
8.00	2.41	2.17
9.00	2.73	2.08
9.00	2.49	2.03
9.00	2.29	1.98
9.00	2.10	1.88
10.0	3.55	2.47
10.0	3.41	2.46
10.0	3.14	2.26
10.0	2.93	2.09

Table A-12. Kinetic data of the homolysis of $1\text{-}C_3H_7Ni(cyclam)H_2O^{2+}$ in the presence of $ABTS^{\bullet-}$
Conditions: $[C_3H_7Co(dmgH)_2H_2O^{2+}] = 100\ \mu M$
$\lambda = 650$ nm, $T = 25^{\circ}C$
in 0.10 M $HClO_4$

$10^3[Ni(cyclam)^{2+}]/M$	$10^5[ABTS^{\bullet-}]_{ave}/M$	$10^{-3}k_{\psi}/s^{-1}$
1.25	1.65	2.70
1.25	1.61	2.62
1.25	1.25	2.48
1.75	3.72	4.28
1.75	3.30	3.85
1.75	3.06	3.68
1.75	2.14	3.17
1.75	1.93	3.11
2.00	1.95	2.35
2.00	1.57	2.03
2.00	1.65	2.07
2.00	1.49	2.03
2.00	1.33	1.78
3.50	1.67	1.42
3.50	1.37	1.40
3.50	4.27	2.70
3.50	4.03	2.63
3.50	3.71	2.58

Table A-13. Kinetic data of the homolysis of $1\text{-}C_4H_9Ni(cyclam)H_2O^{2+}$ in the presence of $ABTS^{\bullet-}$
Conditions: $[C_4H_9Co(dmgH)_2H_2O^{2+}] = 200\ \mu M$
$\lambda = 650$ nm, $T = 25^{\circ}C$
in 0.10 M $HClO_4$

$10^3[Ni(cyclam)^{2+}]/M$	$10^5[ABTS^{\bullet-}]_{ave}/M$	$10^{-3}k_{\psi}/s^{-1}$
5.00	4.63	5.24
5.00	4.16	4.61
5.00	3.46	3.84
5.00	3.02	3.45
5.00	2.41	3.43
5.00	2.11	2.83
5.00	1.28	1.90

Table A-14. Kinetic data of the homolysis of $1\text{-}C_5H_{11}Ni(cyclam)H_2O^{2+}$ in the presence of $ABTS^{\bullet-}$
Conditions: $[C_5H_{11}Co(dmgH)_2H_2O^{2+}]$ = 200 μM
λ = 650 nm, T = 25°C
in 0.10 M $HClO_4$

$10^3[Ni(cyclam)^{2+}]/M$	$10^5[ABTS^{\bullet-}]_{ave}/M$	$10^{-3}k_\psi/s^{-1}$
5.00	4.93	5.26
5.00	4.43	4.59
5.00	3.92	3.79
5.00	3.46	3.14
5.00	2.77	1.98
5.00	2.24	1.78
10.0	5.05	2.60
10.0	4.42	2.30
10.0	3.62	1.41
10.0	3.23	1.21
10.0	2.86	1.13
10.0	1.62	0.765
15.0	5.08	1.05
15.0	4.50	1.36
15.0	3.91	1.24
15.0	3.28	0.967

Table A-15. Kinetic data of the homolysis of $1\text{-}C_6H_{13}Ni(cyclam)H_2O^{2+}$ in the presence of $ABTS^{\bullet-}$
Conditions: $[C_6H_{13}Co(dmgH)_2H_2O^{2+}]$ = 100 μM
λ = 650 nm, T = 25°C
in 0.10 M $HClO_4$

$10^3[Ni(cyclam)^{2+}]/M$	$10^5[ABTS^{\bullet-}]_{ave}/M$	$10^{-3}k_\psi/s^{-1}$
5.00	4.75	3.54
5.00	4.26	3.55
5.00	3.71	3.02
5.00	3.26	2.63
5.00	2.88	2.46
5.00	2.50	2.09
5.00	2.08	1.87
5.00	1.78	1.70
10.0	3.66	1.75
10.0	3.21	1.15
10.0	2.30	1.14
10.0	1.93	0.978
10.0	1.72	0.882
10.0	1.41	0.779
10.0	1.12	0.627

Table A-16. Kinetic data of the homolysis of $1\text{-}C_7H_{15}Ni(cyclam)H_2O^{2+}$ in the presence of $ABTS^{\bullet-}$
Conditions: $[C_7H_{15}Co(dmgH)_2H_2O^{2+}]$ = 200 μM
λ = 650 nm, T = 25°C
in 0.10 M $HClO_4$

$10^3[Ni(cyclam)^{2+}]/M$	$10^5[ABTS^{\bullet-}]_{ave}/M$	$10^{-3}k_\psi/s^{-1}$
5.00	4.50	4.45
5.00	3.96	4.23
5.00	3.40	3.61
5.00	2.96	3.52
5.00	2.49	2.79
5.00	2.04	2.51
5.00	1.64	2.07
5.00	1.25	2.09
10.0	3.34	2.94
10.0	2.97	2.82
10.0	2.63	2.73
10.0	2.27	2.16
10.0	2.15	2.08
10.0	1.77	1.81
10.0	1.47	1.49
10.0	1.21	1.41

Table A-17. Kinetic data of the homolysis of $1\text{-}C_8H_{17}Ni(cyclam)H_2O^{2+}$ in the presence of $ABTS^{\bullet-}$
Conditions: $[C_8H_{17}Co(dmgH)_2H_2O^{2+}]$ = 100 μM
λ = 650 nm, T = 25°C
in 0.10 M $HClO_4$

$10^3[Ni(cyclam)^{2+}]/M$	$10^5[ABTS^{\bullet-}]_{ave}/M$	$10^{-3}k_\psi/s^{-1}$
3.00	3.10	0.692
3.00	2.79	0.617
3.00	2.63	0.630
3.00	2.41	0.623
3.00	2.23	0.639
3.00	2.07	0.614
3.00	1.85	0.532
3.00	1.67	0.486
3.00	1.53	0.493
3.00	1.35	0.422
3.00	1.29	0.416
3.00	1.13	0.363
5.00	2.00	0.431
5.00	1.84	0.383
5.00	1.35	0.328

Table A-18. Kinetic data of the homolysis of $CH_3OCH_2Ni(cyclam)H_2O^{2+}$ in the presence of $ABTS^{\bullet-}$
Conditions: $[CH_3OCH_2Co(dmgH)_2H_2O^{2+}]$ = 100 μM
λ = 650 nm, T = 25°C
in 0.10 M $HClO_4$

$10^3[Ni(cyclam)^{2+}]/M$	$10^5[ABTS^{\bullet-}]_{ave}/M$	$10^{-3}k_\psi/s^{-1}$
0.73	3.00	1.99
0.73	2.77	1.78
0.73	1.25	1.47
1.00	1.52	1.51
1.00	1.22	1.47
1.00	0.92	1.25
2.00	3.06	1.53
2.00	2.65	1.37
2.00	2.35	1.24
2.00	2.01	1.04

Table A-19. Kinetic data of the homolysis of $ClCH_2Ni(cyclam)H_2O^{2+}$ in the presence of $ABTS^{\bullet-}$
Conditions: $[ClCH_2Co(cyclam)H_2O^{2+}]$ = 100 μM
λ = 650 nm, T = 25°C
in 0.10 M $HClO_4$

$10^3[Ni(cyclam)^{2+}]/M$	$10^5[ABTS^{\bullet-}]_{ave}/M$	$10^{-3}k_\psi/s^{-1}$
6.00	6.32	1.10
6.00	5.96	1.03
6.00	5.72	0.970
6.00	5.35	0.967
6.00	5.04	0.893
6.00	4.53	0.875
6.00	3.93	0.645
6.00	3.40	0.553
6.00	2.72	0.467
6.00	2.23	0.348
6.00	1.95	0.288
6.00	1.40	0.253
2.50	2.16	0.782
2.50	1.83	0.651
2.50	4.09	1.28
2.50	3.73	1.19
2.50	3.49	1.06
2.50	3.13	0.953

Table A-20. Kinetic data of the homolysis of $ClCH_2Ni(cyclam)H_2O^{2+}$ in the presence of $ABTS^{\bullet-}$
Conditions: $[ClCH_2Co(dmgH)_2H_2O^{2+}]$ = 100 μM
λ = 650 nm, T = 25°C
in 0.10 M $HClO_4$

$10^3[Ni(cyclam)^{2+}]/M$	$10^5[ABTS^{\bullet-}]_{ave}/M$	$10^{-3}k_\psi/s^{-1}$
3.00	4.95	1.13
3.00	4.09	0.868
3.00	3.75	0.832
3.00	3.56	0.781
3.00	3.31	0.828
3.00	3.05	0.756
3.00	2.71	0.661
3.00	2.31	0.572
3.00	2.09	0.534
10.0	4.89	0.549
10.0	4.65	0.580
10.0	4.02	0.432
10.0	3.61	0.400
10.0	3.36	0.399
10.0	3.11	0.402
10.0	2.95	0.318
10.0	2.62	0.282
10.0	2.33	0.252
10.0	2.12	0.212
10.0	1.96	0.190

Table A-21. Kinetic data of the homolysis of $BrCH_2Ni(cyclam)H_2O^{2+}$ in the presence of $ABTS^{\bullet-}$
Conditions: $[BrCH_2Co(cyclam)H_2O^{2+}]$ = 100 μM
λ = 650 nm, T = 25°C
in 0.10 M $HClO_4$

$10^3[Ni(cyclam)^{2+}]/M$	$10^5[ABTS^{\bullet-}]_{ave}/M$	$10^{-3}k_\psi/s^{-1}$
3.00	5.55	1.31
3.00	5.08	1.03
3.00	4.26	0.959
3.00	3.60	0.838
3.00	2.60	0.774
3.00	1.72	0.627
5.00	4.63	1.03
5.00	4.06	0.980
5.00	3.13	0.662
5.00	2.16	0.580
8.00	4.75	0.626
8.00	4.17	0.542
8.00	3.60	0.439
8.00	2.87	0.363
8.00	2.08	0.249

Table A-22. Kinetic data of the homolysis of $BrCH_2Ni(cyclam)H_2O^{2+}$ in the presence of $ABTS^{\bullet-}$
Conditions: $[BrCH_2Co(dmgH)_2H_2O^{2+}]$ = 100 μM
λ = 650 nm, T = 25°C
in 0.10 M $HClO_4$

$10^3[Ni(cyclam)^{2+}]/M$	$10^5[ABTS^{\bullet-}]_{ave}/M$	$10^{-3}k_\psi/s^{-1}$
3.00	3.87	1.14
3.00	3.68	0.990
3.00	3.53	1.02
3.00	3.33	1.02
3.00	3.24	1.09
3.00	3.01	0.839
3.00	2.84	0.913
3.00	2.65	0.903
3.00	2.47	0.779
3.00	2.28	0.775
3.00	2.09	0.653
3.00	1.94	0.638
7.50	4.58	0.708
7.50	4.42	0.834
7.50	4.21	0.678
7.50	4.03	0.685
7.50	3.90	0.689
7.50	3.86	0.661
7.50	3.65	0.635
7.50	3.47	0.569
7.50	3.29	0.573
7.50	3.24	0.590
7.50	2.93	0.528
7.50	2.74	0.465
7.50	2.68	0.466
7.50	2.50	0.427

Table A-23. Kinetic data of the homolysis of $CH_3Ni(cyclam)H_2O^{2+}$ in the presence of oxygen
Conditions: $[CH_3Co(cyclam)H_2O^{2+}]$ = 100 μM
λ = 360 nm, T = 25°C
in 0.10 M $HClO_4$

$10^3[Ni(cyclam)^{2+}]/M$	$10^5[O_2]_{ave}/M$	k_ψ/s^{-1}
5.00	9.6	8.19
5.00	9.3	7.80
5.00	9.0	9.53
5.00	8.7	8.67
5.00	24.6	19.2
5.00	24.2	20.7
5.00	39.6	27.7
5.00	39.3	21.8
5.00	39.0	27.3
5.00	17.1	14.1
5.00	16.8	13.2
5.00	16.5	11.2
6.50	20.0	11.7
6.50	19.6	11.5
5.00	20.0	13.6
5.00	19.6	12.2
3.50	20.0	16.6
3.50	19.6	16.6
3.50	19.2	17.5
3.50	18.8	17.8
8.00	20.0	8.98
8.00	19.6	8.95
8.00	19.2	11.8
10.0	19.6	8.18

Table A-24. Homolysis rate constants[a] of $C_2H_5Ni(cyclam)H_2O^{2+}$ at different temperatures

Conditions: $[C_2H_5Co(cyclam)H_2O^{2+}]$ = 100 μM
λ = 650 nm, T = 25°C
in 0.10 M $HClO_4$

Temp./K	k_{hom}/s^{-1}
308.6	2.38×10^4
295.1	9.07×10^3
291.1	5.77×10^3
287.8	2.51×10^3
282.9	1.81×10^3

[a]The scavenger is $ABTS^{\bullet-}$.

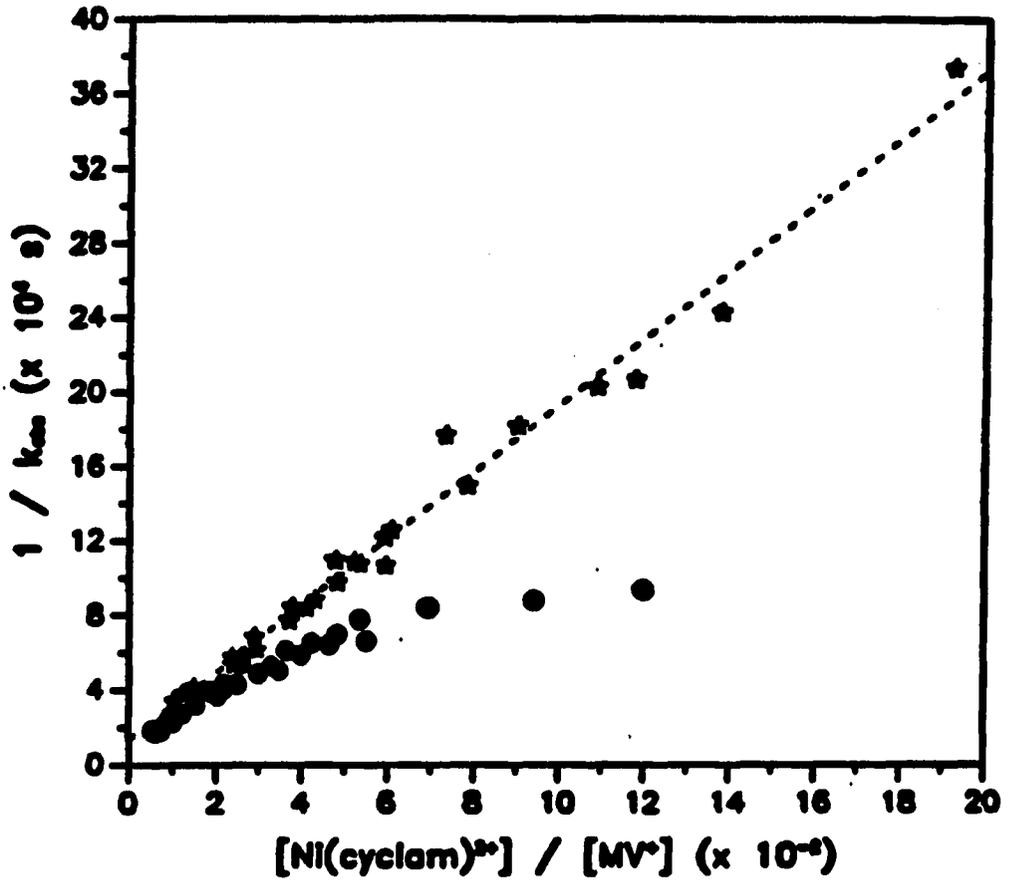

Figure A-1. The plot of $1/k_{obs}$ versus $[Ni(cyclam)^{2+}]/[MV^{+\bullet}]$ for the homolysis of $C_2H_5Ni(cyclam)H_2O^{2+}$ in the presence of $MV^{+\bullet}$. The data obtained using $C_2H_5Co(dmgH)_2H_2O$ (dots) and $C_2H_5Co(cyclam)H_2O^{2+}$ (stars) as radical precursors are shown

PART III. RATE CONSTANTS FOR THE REACTIONS OF ALKYL RADICALS WITH OXYGEN IN AQUEOUS SOLUTION

INTRODUCTION

The determination of accurate kinetics and mechanisms for the formation and subsequent reactions of peroxyalkyl radicals, $RO_2^{\bullet}$, is important for understanding the roles of these species as intermediates in combustion chemistry, radiation chemistry, atmospheric chemistry, and photochemistry.[1] Though reactions of alkyl radicals with oxygen, eq 1, have been extensively studied in the gas phase,[2] mechanistic uncertainity remains.

$$R^{\bullet} + O_2 \longrightarrow RO_2^{\bullet} \qquad k_{Ox} \tag{1}$$

At temperatures below 600 K the reaction is believed to follow the addition process, as shown in eq 1. At higher temperatures an equilibrium with the excited state, $^{*}RO_2^{\bullet}$, becomes more pronounced and olefin formation occurs, presumably via an excited adduct, eq 2.

$$RO_2^{\bullet} \longrightarrow {}^{*}RO_2^{\bullet} \longrightarrow {}^{*}R(-H)O_2^{\bullet}H \longrightarrow R(-H) + HO_2^{\bullet} \tag{2}$$

Fewer determinations have been made for the reactions of alkyl radicals with oxygen in the condensed phase.[3] This is due in part to the difficulties of generating radicals in solution and to the smaller extinction coefficients for the radical

transients in solution as compared to the gas phase.[4] Also, under some pulse radiolysis conditions eq 3, rather than

$$RO_2^{\bullet} + RH \longrightarrow ROOH + R^{\bullet} \qquad (3)$$

eq 1, is the rate determining step.[3] As a result many kinetic studies have yielded "oxygen rate constants" that are significantly lower than the true values.[5]

Using pulse radiolysis Sauer obtained an estimate for the rate constant for the reaction of methyl radical with oxygen by monitoring the intermediacy of a methylnickel transient, $CH_3Ni(cyclam)H_2O^{2+}$ (cyclam = 1,4,8,11-tetraazacyclotetradecane).[6] We have recently used laser flash photolysis to study the homolysis of a number of alkyl nickel complexes, $RNi(cyclam)H_2O^{2+}$ (R = CH_3, 1^{o}, substituted 1^{o}), in the presence of radical scavengers $ABTS^{\bullet-}$, $MV^{\bullet+}$, or oxygen, and have reported a scheme analogous to the pulse radiolysis study (eqs 4 and 5).[6,7]

$$RNi(cyclam)H_2O^{2+} \underset{k_{col}}{\overset{k_{hom}}{\rightleftharpoons}} R^{\bullet} + Ni(cyclam)^{2+} + H_2O \qquad (4)$$

$$R^{\bullet} + Scavenger \xrightarrow{k_S} Adduct \qquad (5)$$

While pulse radiolysis methods to generate alkyl radicals other than $CH_3^{\bullet}$ are limited and problematic,[8] laser flash photolysis of alkyl cobalt complexes, $RCo(dmgH)_2B$ (R = alkyl, substituted alkyl; dmgH = dimethylgyloxime; B = H_2O, pyridine) and $RCo(cyclam)H_2O^{2+}$, cleanly yields reagent concentrations of a series of alkyl radicals in a short time (< 1 μs).

The purpose of this research described here was to i) investigate the homolysis of a series of alkylnickel cyclam complexes in the presence of oxygen, ii) determine the kinetics of reactions of alkyl radicals with oxygen in aqueous acidic solution, and iii) compare the rate constants found in this study with previous solution and gas phase results.

EXPERIMENTAL

Reagents

The alkylcobaloxime(pyridine),[9] alkylcobalt(cyclam) perchlorate,[10] and nickel(II)(cyclam) perchlorate[11] complexes were prepared using literature procedures and characterized by UV-visible spectroscopy. Reagent stock solutions were prepared as needed, using distilled water which was purified by passage through a Milli-Q Millipore reagent water system, and stored in the dark. Stock solutions of $Ni(cyclam)^{2+}$ were prepared by dissolving the perchlorate salt in 0.01 M $HClO_4$ and the concentration was determined by UV-visible spectroscopic methods, ε_{448} = 45 L mol^{-1} cm^{-1}.[11] Molecular oxygen (99.5% pure, Air Products) was bubbled into a water filled vial until the solution was saturated (1.26×10^{-3} M) and aliquots from this solution were added to the reaction solutions. The perchloric acid (Fisher) and argon (99.99% pure, Air Products) were used as purchased.

Kinetics

Laser flash photolysis was employed to study the kinetics of these reactions. The flashlamp-pumped dye laser system has been

described by Connolly[12] and is based on another system in the literature.[13] The dye used was LD 490, which emits light in the spectral region where the alkylcobalt complexes have significant absorbances (490 nm). Alkyl cobaloximes were the primary radical precursors used in this study, but $RCo(cyclam)H_2O^{2+}$ complexes were employed whenever available. The latter complexes were preferred because, unlike organocobaloximes, they lack strong absorption bands below 400 nm that can complicate the analysis. In a typical experiment, a deaerated sample solution was prepared in a 1-cm quartz cell. Addition of the final reagent, saturated oxygen solution, filled the sample cell to capacity. The reaction solution was then flashed by a 0.6 μs laser pulse from a Phase-R DL-1100 pulsed dye laser, and the resulting signal was collected and stored on a Nicolet model 2090-3A digitizing oscilloscope. The reactions were monitored by following the changes in voltage (transmittance) over time at 360 nm. The oscilloscope was interfaced with an Apple II Plus microcomputer, which converted voltage vs. time data to absorbance vs. time data.

RESULTS

Formation and Homolysis of RNi(cyclam)H_2O^{2+} in the Presence of Oxygen

Laser flash photolysis of aqueous solutions containing 100-150 μM $RCo(dmgH)_2H_2O$ (or $RCo(cyclam)H_2O^{2+}$), 0.5-30 mM β-$Ni(cyclam)^{2+}$, 32-200 μM oxygen, and 0.10 M $HClO_4$ showed biphasic kinetics at 360 nm. The absorbance increase observed in the initial stage of the reaction was completed in < 5 μs. This initial reaction stage, containing contributions from the formation reactions of $RNi(cyclam)H_2O^{2+}$ and $RO_2Ni(cyclam)H_2O^{2+}$, was followed by a slower absorbance increase.

By increasing the ratio of $[Ni(cyclam)^{2+}]/[O_2]$ the magnitude of the initial reaction stage declined, while the absorbance change associated with the second stage of the reaction was enhanced. These observations indicated that in the initial stage of the reaction the majority of the alkyl radicals colligated with β-$Ni(cyclam)^{2+}$ to give $RNi(cyclam)H_2O^{2+}$. A minor amount of radicals reacted with oxygen to give $RO_2^{\bullet}$, which were rapidly captured by β-$Ni(cyclam)^{2+}$ to give the chromophore $RO_2Ni(cyclam)H_2O^{2+}$. Then the kinetics of the second stage of the reaction were consistent with homolysis of $RNi(cyclam)H_2O^{2+}$ in the presence of oxygen and β-$Ni(cyclam)^{2+}$ to give subsequent

formation of $RO_2Ni(cyclam)H_2O^{2+}$.

Kinetics of the Reactions of Alkyl Radicals with Oxygen

The kinetics of the homolysis of $RNi(cyclam)H_2O^{2+}$ were monitored by following the appearance of $RO_2Ni(cyclam)H_2O^{2+}$ at 360 nm (ε_{360} = 1 x 10^4 L mol^{-1} cm^{-1}) in the second stage of the reaction.[6] The reactions believed to be occurring are shown below:

$$RNi(cyclam)H_2O^{2+} \underset{k_{col}}{\overset{k_{hom}}{}} R^{\bullet} + Ni(cyclam)^{2+} + H_2O \qquad (4)$$

$$R^{\bullet} + O_2 \xrightarrow{k_{Ox}} RO_2^{\bullet} \qquad (1)$$

$$RO_2^{\bullet} + Ni(cyclam)^{2+} \xrightarrow{fast} RO_2Ni(cyclam)H_2O^{2+} \qquad (6)$$

Pseudo-first-order rate constants were obtained from experiments in which the concentrations of β-$Ni(cyclam)^{2+}$ and oxygen were varied, and corresponded to the rate law in eq 7.

$$\frac{-d[RNi(cyclam)H_2O^{2+}]}{dt} = \frac{k_{hom}k_{Ox}[O_2][RNi(cyclam)H_2O^{2+}]}{k_{Ox}[O_2] + k_{col}[Ni(cyclam)^{2+}]} \qquad (7)$$

These data for each radical studied are listed in **Tables A-1 to A-11**. Nonlinear least-squares analysis of the pseudo-first-order equation, eq 8, gave rate constants for the reactions

$$k_{\psi} = \frac{k_{hom}k_{Ox}[O_2]}{k_{Ox}[O_2] + k_{col}[Ni(cyclam)^{2+}]} \quad (8)$$

of alkyl radicals with oxygen, k_{Ox}, which are listed in **Table III-1**. In this analysis both k_{hom} and k_{col} are treated as known values.[7] A pictorial display of the data was afforded by plotting the inverse of the pseudo-first-order rate constants, $1/k_{\psi}$, versus the ratio of $[Ni(cyclam)^{2+}]/[O_2]$. **Figure III-1** illustrates the linear correlation obtained for three radicals, methoxymethyl, ethyl, and 1-hexyl. The oxygen rate constant, k_{Ox}, could be estimated from the value of $k_{col}/(slope)k_{hom}$.

Table III-1. Rate constants for the reaction alkyl radicals with oxygen[a]

alkyl radical	$k_{Ox}/10^9$ L mol^{-1} s^{-1}
CH_3	4.1 ± 1.5[b]
C_2H_5	2.1 ± 0.2
$1\text{-}C_3H_7$	3.5 ± 0.2
$1\text{-}C_4H_9$	1.8 ± 0.2
$1\text{-}C_5H_{11}$	3.8 ± 0.4
$1\text{-}C_6H_{13}$	3.9 ± 0.5
$1\text{-}C_7H_{15}$	1.6 ± 0.2
$1\text{-}C_8H_{17}$	2.4 ± 0.3
CH_3OCH_2	4.9 ± 0.4
$ClCH_2$	1.9 ± 0.4
$BrCH_2$	2.0 ± 0.5

[a]Obtained using eq 8 with known (fixed) values of k_{hom} and k_{col}; kinetics monitored at 360 nm. [b]Both k_{Ox} and k_{hom} calculated from eq 8; only k_{col} was fixed.

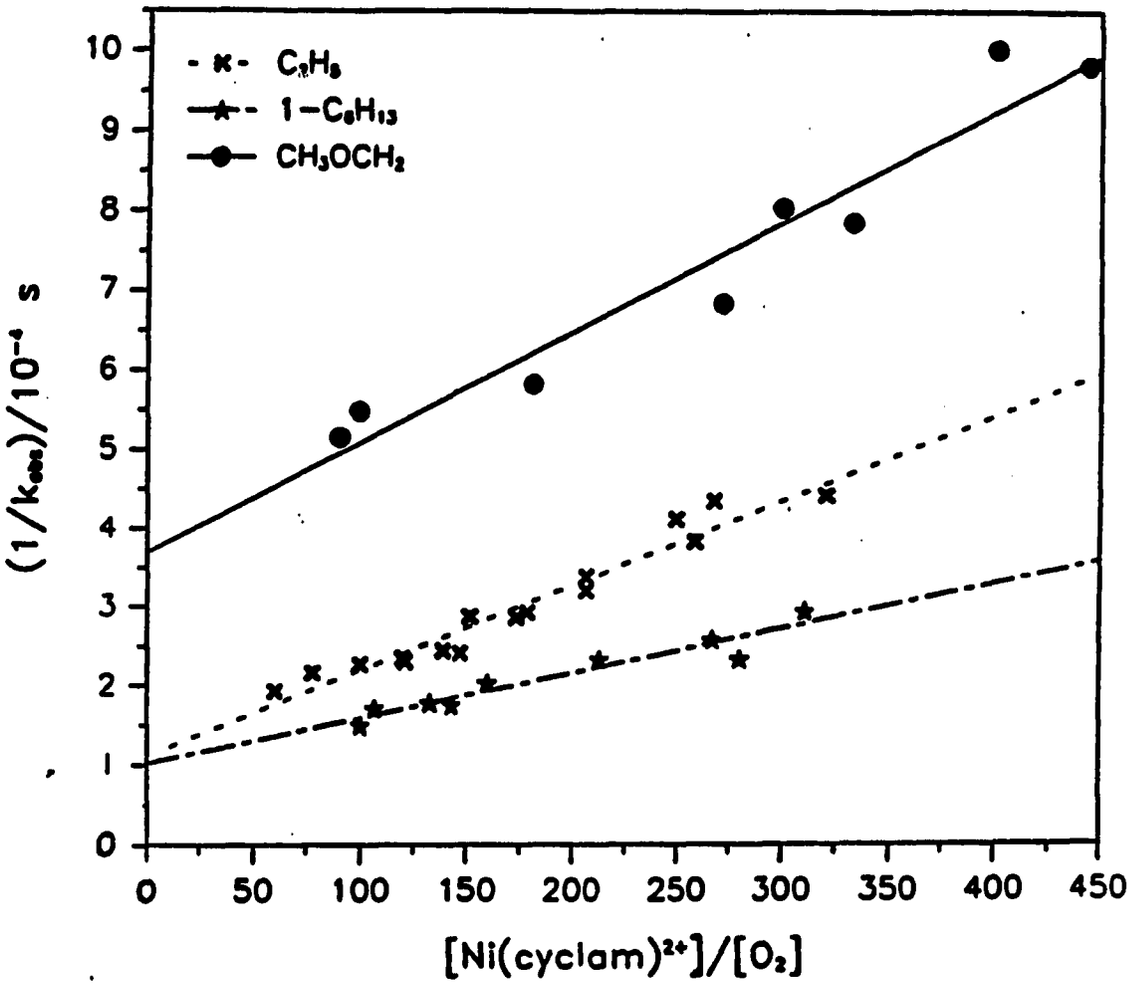

Figure III-1. The plot of $1/k_\psi$ versus [Ni(cyclam)$^{2+}$]/[O_2] for the homolysis of RNi(cyclam)H_2O^{2+} in the presence of oxygen. Kinetic data were obtained in 0.1 M $HClO_4$ at 25°C using radical precursors RCo(dmgH)$_2H_2O$ (for hexyl) and RCo(cyclam)H_2O^{2+} (for methoxymethyl and ethyl)

DISCUSSION

Formation and Homolysis of $RNi(cyclam)H_2O^{2+}$ in the Presence of Oxygen

Laser flash photolysis of solutions containing oxygen, β-$Ni(cyclam)^{2+}$, and $RCo(dmgH)_2H_2O$ (or $RCo(cyclam)H_2O^{2+}$) resulted in dramatic biphasic absorbance changes at 360 nm. The kinetics of the reaction phase immediately following the laser flash (eq 9) corresponded to the disappearance of $R^\bullet$ by two competing pathways: reacting with the excess reagents

$$RCo(dmgH)_2H_2O + h\nu + 2\ H^+ \longrightarrow R^\bullet + Co_{aq}^{2+} + 2\ dmgH_2 \qquad (9)$$

$$R^\bullet + Ni(cyclam)^{2+} + H_2O \longrightarrow RNi(cyclam)H_2O^{2+} \qquad k_{col} \qquad (-4)$$

$$R^\bullet + O_2 \longrightarrow RO_2^\bullet \qquad k_{Ox} \qquad (1)$$

$$RO_2^\bullet + Ni(cyclam)^{2+} + H_2O \longrightarrow RO_2Ni(cyclam)H_2O^{2+} \qquad (6)$$

β-$Ni(cyclam)^{2+}$ (eq -4) with known rate constant, k_{col}, and oxygen (eq 1) with rate constant k_{Ox}. The reagent concentrations were such that radical self-reactions did not contribute to the overall reaction. Though reactions 1 and -4 result in very small

absorbance changes, the rapid reactions of peroxyalkyl radicals with β-Ni(cyclam)$^{2+}$ yield $RO_2Ni(cyclam)H_2O^{2+}$ complexes, eq 6, resulting in an immediate absorbance increase at 360 nm.[6]

Using a sufficiently high ratio of [Ni(cyclam)$^{2+}$]/[O_2] a majority of the alkyl radicals produced in the laser flash colligated with β-Ni(cyclam)$^{2+}$ to form $RNi(cyclam)H_2O^{2+}$. This resulted in a larger absorbance increase for the homolysis stage of the reaction than for the initial stage. Therefore, determination of the pseudo-first-order rate constants for the homolysis reactions was an easily measurable process, even though the spectroscopic analysis was performed near the lower wavelength detection limit of our photomultiplier tube.

Kinetics of the Reactions of Alkyl Radicals with Oxygen

Rate constants for the reactions of a series of alkyl radicals with oxygen are listed in **Table III-1**. These values are large (k_{Ox} = 1.6-4.9 x 10^9 L mol^{-1} s^{-1}) and approach the diffusion controlled limit. Because these rate constants are so large, no trend in reactivity could be rationalized as the nature of the alkyl radical was varied.

With one exception, each of these k_{Ox}-values were obtained using eq 8 in which the rate constants for the colligation of $R^{\bullet}$ with β-Ni(cyclam)$^{2+}$, k_{col}, and homolysis of $RNi(cyclam)H_2O^{2+}$,

k_{hom}, were independently known from using the $ABTS^{\bullet-}$ method.[7] The rate constant for the homolysis of $CH_3Ni(cyclam)H_2O^{2+}$ was not obtained using the $ABTS^{\bullet-}$ method due to a direct reaction of $CH_3Ni(cyclam)H_2O^{2+}$ with $ABTS^{\bullet-}$. Therefore, two unknown rate constants, k_{hom} and k_{Ox}, were obtained from eq 8, giving 80 ± 20 s^{-1} and (4.1 ± 1.5) x 10^9 L mol^{-1} s^{-1}, respectively. The increased error on these values is a result of this treatment.

Comparison of Oxygen Rate Constants Determined in the Solution and Gas Phase

Rate constants for the reactions of alkyl radicals with oxygen both in solution and gas phase are listed in **Table III-2**. Thomas first reported in a pulse radiolysis study the rate constant for the reaction of $CH_3^{\bullet}$ with oxygen, k_{Ox} = (4.7 ± 0.7) x 10^9 L mol^{-1} s^{-1}, by monitoring the formation of $CH_3O_2^{\bullet}$ at 260 nm.[14] Our recent report for this reaction is in good agreement with this value and with that estimated by Sauer et al., k_{Ox} = 3.7 x 10^9 L mol^{-1} s^{-1}.[6] Likewise, the rate constant determined for the reaction of $C_2H_5^{\bullet}$ with oxygen, k_O = (2.1 ± 0.1) x 10^9 L mol^{-1} s^{-1}, agrees with Hickel's pulse radiolytically determined value, (2.9 ± 0.8) x 10^9 L mol^{-1} s^{-1}.[4]

Analysis of **Table III-2** shows that reactions of alkyl radicals with oxygen occur with higher rate constants in

Table III-2. Comparison of solution and gas phase rate constants (10^9 L mol^{-1} s^{-1}) for the reaction of alkyl radicals with oxygen

alkyl radical	solvent	k_{sol}	k_{Ox}
CH_3	H_2O	4.7 ± 0.7[a]	1.2[b]
		3.7[c]	
		4.1 ± 1.5[d]	
C_2H_5	H_2O	2.9 ± 0.8[e]	1.0[f]
		2.1 ± 0.1[g]	
$C_6H_5CH_2$	CH_3CN	3.4[h]	0.67[i]
	$2\text{-}C_3H_7OH$	2.5[h]	
	hexane	2.8[h]	
	hexadecane	1.0[h]	
$(CH_3)_3C$	cyclohexane	4.9[h]	1.4[j]

[a]Ref 14. [b]Ref 15. [c]Ref 6. [d]Ref 7b. [e]Ref 4. [f]Ref 2. [g]This study. [h]Ref 3. [i]Ref 16. [j]Ref 17.

water than in the gas phase.[15,16,17] While few rate constants have been reported for bimolecular reactions in both aqueous and gaseous environments, it has been shown that reactions of radical transients, i.e., H, OH, with gases having low affinity for the solvent, i.e., H_2, CO, O_2, occur with rate constants that are higher in the solution phase.[18] The reactions of alkyl radicals with oxygen would be expected to exhibit similar effects. These results are understood in terms of the large ratio of molar volume to free volume inherent in solutions. It has also been suggested that solvation of the solute particles by water or the caging in of the reactants by the solvent may account for the enhanced solution phase rate constants.[14]

Summary

The kinetics of the unimolecular homolysis of a series of $RNi(cyclam)H_2O^{2+}$ complexes were studied by monitoring the formation of the oxygen insertion product $RO_2Ni(cyclam)H_2O^{2+}$. The rate constants for the reactions of alkyl radicals with oxygen, k_O, were obtained from the analysis of the homolysis rate equation which contains the known rate constants for the colligation of $R^{\bullet}$ with β-$Ni(cyclam)^{2+}$, k_{col}, and for the homolysis of $RNi(cyclam)H_2O^{2+}$, k_{hom}. The higher rate constants for the reactions of alkyl radicals with oxygen in solution, as compared with those measured in the gas phase, were discussed.

BIBLIOGRAPHY

1. (a) Ingold, K. U. Acc. Chem. Res. 1969, 2, 1. (b) McKay, B. Prog. Energy Combust. Sci. 1977, 3, 105. (c) Howard, J. A. "Free Radicals"; Kochi, J. K., Ed.; Wiley: New York, 1973; Vol. II, Chapter 12. (d) Simic, M. G.; Karel, M. "Autoxidation in Food and Biological Systems"; Plenum: New York, 1980.

2. Wagner, A. F.; Slagle, I. R.; Sarzynski, D.; Gutman, D. J. Phys. Chem. 1990, 94, 1853 and refs cited therein.

3. Maillard, B.; Ingold, K. U.; Scaiano, J. C. J. Am. Chem. Soc. 1983, 105, 5095.

4. Hickel, B. J. Phys. Chem. 1975, 79, 1054.

5. Howard, J. A. Adv. Free Radical Chem. 1972, 4, 49.

6. Sauer, A.; Cohen, H.; Meyerstein, D. Inorg. Chem. 1988, 27, 4578.

7. (a) Kelley, D. G.; Bakac, A.; Espenson, J. H. Inog. Chem. 1990, 29, 0000. (b) Kelley, D. G.; Bakac, A.; Espenson, J. H. Inog. Chem. 1991, 30, 0000.

8. Bakac, A.; Espenson, J. H. Inorg. Chem. 1989, 28, 3901.

9. Yamazaki, N.; Hohokabi, Y. Bull. Chem. Soc. Japan 1971, 44, 63.

10. Bakac, A.; Espenson, J. H. Inorg. Chem. 1987, 26, 4353.

11. Bosnich, B.; Tobe, M. L.; Webb, G. A. Inorg. Chem. 1965, 4, 1109.

12. Connolly, P. Ph.D. Dissertation, Iowa State University, Ames, Iowa, 1985.

13. Hoselton, M. A.; Lin, C.-T.; Schwartz, H. A.; Sutin, N. J. Am. Chem. Soc. 1978, 100, 2383. The energy of the laser pulse is 250 mJ.

14. Thomas, J. K. J. Phys. Chem. 1967, 71, 1919.

15. Hochanadel, C. J.; Ghormley, J. A.; Boyle, J. W. J. Phys. Chem. 1977, 81, 3.

16. Nelson, H. H.; McDonald, J. R. J. Phys. Chem. 1982, 86, 1242.

17. Lenhardt, T. M.; McDade, C. E.; Bayes, K. D. J. Phys. Chem. 1980, 84, 304.

18. Schwartz, H. A.; Weston, R. E. "Chemical Kinetics"; Prentice-Hall, Inc.: Englewood Cliffs, New Jersey, 1972, p. 179.

APPENDIX

Table A-1. Kinetic data of the homolysis of $CH_3Ni(cyclam)H_2O^{2+}$ in the presence of oxygen
Conditions: $[CH_3Co(cyclam)H_2O^{2+}]$ = 100 μM
λ = 360 nm, T = 25°C
in 0.10 M $HClO_4$

$10^3[Ni(cyclam)^{2+}]/M$	$10^5[O_2]_{ave}/M$	k_ψ/s^{-1}
5.00	9.6	8.19
5.00	9.3	7.80
5.00	9.0	9.53
5.00	8.7	8.67
5.00	24.6	19.2
5.00	24.2	20.7
5.00	39.6	27.7
5.00	39.3	21.8
5.00	39.0	27.3
5.00	17.1	14.1
5.00	16.8	13.2
5.00	16.5	11.2
6.50	20.0	11.7
6.50	19.6	11.5
5.00	20.0	13.6
5.00	19.6	12.2
3.50	20.0	16.6
3.50	19.6	16.6
3.50	19.2	17.5
3.50	18.8	17.8
8.00	20.0	8.98
8.00	19.6	8.95
8.00	19.2	11.8
10.0	19.6	8.18

Table A-2. Kinetic data of the homolysis of $C_2H_5Ni(cyclam)H_2O^{2+}$ in the presence of oxygen
Conditions: $[C_2H_5Co(dmgH)_2H_2O^{2+}]$ = 150 μM
λ = 360 nm, T = 25°C
in 0.10 M $HClO_4$

$10^3[Ni(cyclam)^{2+}]/M$	$10^5[O_2]_{ave}/M$	k_ψ/s^{-1}
12.0	20.0	6.16
12.0	20.0	5.44
12.0	15.4	5.04
12.0	11.6	4.41
12.0	11.6	4.43
12.0	11.6	4.45
12.0	10.0	4.35
12.0	10.0	4.21
12.0	8.6	3.93
12.0	6.9	3.57
12.0	6.9	3.46
12.0	5.8	3.13
12.0	5.4	2.52
12.0	4.4	2.41
12.0	4.4	2.47
18.0	5.8	2.35
18.0	5.4	2.39
18.0	5.4	2.09
15.0	5.8	2.72
15.0	5.8	2.53
15.0	5.4	2.37
15.0	5.4	2.25
12.0	5.8	3.30
12.0	5.8	2.70
12.0	5.4	2.37
12.0	5.4	2.39
10.0	5.8	3.61
10.0	5.4	3.35
10.0	5.4	3.37
8.50	5.8	4.17
8.50	5.4	3.50
7.00	5.8	4.36

Table A-3. Kinetic data of the homolysis of $1\text{-}C_3H_7Ni(cyclam)H_2O^{2+}$ in the presence of oxygen
Conditions: $[C_3H_7Co(dmgH)_2H_2O^{2+}]$ = 100 μM
λ = 360 nm, T = 25°C
in 0.10 M $HClO_4$

$10^3[Ni(cyclam)^{2+}]/M$	$10^5[O_2]_{ave}/M$	k_ψ/s^{-1}
8.50	5.8	4.20
8.50	5.8	4.10
10.0	5.8	4.00
10.0	5.8	3.90
10.0	5.8	3.90
15.0	5.8	3.30
15.0	5.8	3.20
17.0	5.8	2.74
20.0	5.8	2.47
20.0	5.8	2.59
20.0	5.8	2.12
23.0	5.8	2.03
23.0	5.8	2.26
26.0	5.8	2.48
26.0	5.8	2.06
26.0	5.8	2.19
30.0	5.8	1.67
30.0	5.8	2.04

Table A-4. Kinetic data of the homolysis of $1\text{-}C_4H_9Ni(cyclam)H_2O^{2+}$ in the presence of oxygen
Conditions: $[C_4H_9Co(dmgH)_2H_2O^{2+}]$ = 150 μM
λ = 360 nm, T = 25°C
in 0.10 M $HClO_4$

$10^3[Ni(cyclam)^{2+}]/M$	$10^5[O_2]_{ave}/M$	k_ψ/s^{-1}
20.0	4.8	2.48
20.0	4.8	2.52
20.0	3.6	2.35
20.0	3.6	2.31
20.0	7.0	3.22
20.0	7.0	3.01
20.0	8.6	4.33
20.0	8.6	4.62
20.0	8.0	4.20
20.0	8.0	4.33
20.0	10.3	4.78
20.0	10.3	4.95
15.0	4.8	3.65
15.0	4.8	3.65
15.0	4.5	3.47
15.0	4.5	3.47
25.0	4.5	2.52
25.0	4.5	2.35
25.0	4.2	2.31
25.0	4.2	2.17

Table A-5. Kinetic data of the homolysis of $1\text{-}C_5H_{11}Ni(cyclam)H_2O^{2+}$ in the presence of oxygen
Conditions: $[C_5H_{11}Co(dmgH)_2H_2O^{2+}]$ = 150 μM
λ = 360 nm, T = 25°C
in 0.10 M $HClO_4$

$10^3[Ni(cyclam)^{2+}]/M$	$10^5[O_2]_{ave}/M$	k_ψ/s^{-1}
10.0	9.6	6.07
10.0	7.5	5.63
10.0	6.0	5.87
10.0	6.0	4.92
10.0	5.6	4.30
10.0	5.0	4.38
10.0	4.1	4.15
10.0	4.6	3.89
10.0	7.1	5.06
20.0	6.0	4.28
20.0	5.6	3.97
20.0	5.0	3.45
10.0	7.1	5.33
20.0	4.6	2.90
20.0	4.6	2.82

Table A-6. Kinetic data of the homolysis of $1\text{-}C_6H_{13}Ni(cyclam)H_2O^{2+}$ in the presence of oxygen
Conditions: $[C_6H_{13}Co(dmgH)_2H_2O^{2+}]$ = 100 μM
λ = 360 nm, T = 25°C
in 0.10 M $HClO_4$

$10^3[Ni(cyclam)^{2+}]/M$	$10^5[O_2]_{ave}/M$	k_ψ/s^{-1}
7.50	7.5	6.71
7.50	7.0	4.86
7.50	7.0	7.53
10.0	7.5	4.96
10.0	7.5	6.53
10.0	7.0	5.67
10.0	7.0	5.86
7.50	4.7	4.62
7.50	4.7	5.43
7.50	4.7	4.88
10.0	4.7	4.46
10.0	4.7	3.73
10.0	4.7	4.90
12.0	4.5	3.58
12.0	4.5	4.23
14.0	5.0	4.31
14.0	4.5	3.42

Table A-7. Kinetic data of the homolysis of $1\text{-}C_7H_{15}Ni(cyclam)H_2O^{2+}$ in the presence of oxygen
Conditions: $[C_7H_{15}Co(dmgH)_2H_2O^{2+}]$ = 150 μM
λ = 360 nm, T = 25°C
in 0.10 M $HClO_4$

$10^3[Ni(cyclam)^{2+}]/M$	$10^5[O_2]_{ave}/M$	k_ψ/s^{-1}
5.00	10.0	7.33
5.00	10.0	8.81
7.50	7.5	5.60
7.50	7.5	6.13
10.0	7.5	5.82
10.0	7.5	4.22
12.5	7.5	4.21
12.5	7.5	6.18
12.5	7.5	3.54
7.50	5.0	4.48
7.50	5.0	5.41
7.50	5.0	5.31
7.50	5.0	3.43
10.0	5.0	3.67
10.0	5.0	3.42
10.0	5.0	4.28
12.0	5.0	4.20
12.0	5.0	5.15
12.0	5.0	3.93
12.0	5.0	3.26
14.0	5.0	3.56
14.0	5.0	3.46

Table A-8. Kinetic data of the homolysis of $1\text{-}C_8H_{17}Ni(cyclam)H_2O^{2+}$ in the presence of oxygen
Conditions: $[C_8H_{17}Co(dmgH)_2H_2O^{2+}]$ = 100 μM
λ = 360 nm, T = 25°C
in 0.10 M $HClO_4$

$10^3[Ni(cyclam)^{2+}]/M$	$10^5[O_2]_{ave}/M$	k_ψ/s^{-1}
5.00	6.4	12.7
5.00	6.4	9.73
5.00	6.0	9.38
5.00	6.0	10.5
5.00	5.6	9.56
7.50	6.4	9.25
7.50	6.4	10.1
7.50	6.0	7.28
7.50	6.0	8.03
10.0	6.4	7.60
10.0	6.0	7.62
12.0	5.4	7.30
12.0	5.4	5.14
12.0	5.0	6.21
13.0	3.6	4.21
13.0	3.2	4.22

Table A-9. Kinetic data of the homolysis of $ClCH_2Ni(cyclam)H_2O^{2+}$ in the presence of oxygen
Conditions: $[ClCH_2Co(cyclam)H_2O^{2+}]$ = 200 μM
λ = 360 nm, T = 25°C
in 0.10 M $HClO_4$

$10^3[Ni(cyclam)^{2+}]/M$	$10^5[O_2]_{ave}/M$	k_ψ/s^{-1}
30.0	5.5	3.50
30.0	5.5	3.90
10.0	5.5	9.47
10.0	5.5	9.55
10.0	5.0	6.96
10.0	5.0	10.5
10.0	5.0	8.78
20.0	5.0	4.91
20.0	5.0	4.42
20.0	5.0	5.74
7.00	5.5	13.7
7.00	5.5	12.8
7.00	5.5	12.2
7.00	5.0	11.3
7.00	5.0	11.2
7.00	5.0	9.85
7.00	4.5	9.66
7.00	4.5	8.51
15.0	5.5	7.79
15.0	5.5	7.93
15.0	5.5	7.15
15.0	5.0	7.66
15.0	5.0	6.90
15.0	4.5	5.42
15.0	4.5	5.27
15.0	4.5	5.81
25.0	5.5	6.03
25.0	5.5	5.27
25.0	5.0	5.38
25.0	5.0	4.46
25.0	5.0	4.23
25.0	4.5	5.30
25.0	4.5	4.35

Table A-10. Kinetic data of the homolysis of $BrCH_2Ni(cyclam)H_2O^{2+}$ in the presence of oxygen
Conditions: $[BrCH_2Co(cyclam)H_2O^{2+}]$ = 250 μM
λ = 360 nm, T = 25°C
in 0.10 M $HClO_4$

$10^3[Ni(cyclam)^{2+}]/M$	$10^5[O_2]_{ave}/M$	k_ψ/s^{-1}
10.0	5.5	9.26
10.0	5.5	8.67
10.0	5.1	7.29
10.0	5.1	6.35
10.0	4.7	5.67
10.0	4.7	5.16
10.0	4.3	5.43
10.0	4.3	5.03
20.0	5.5	4.95
20.0	5.5	4.68
20.0	5.1	4.64
20.0	5.1	4.18
20.0	4.7	3.87
20.0	4.7	3.06
20.0	4.3	3.17
20.0	4.3	3.46
25.0	5.5	3.68
25.0	5.1	4.03
25.0	5.1	3.44
25.0	4.7	3.14
25.0	4.7	2.98
25.0	4.3	3.35
25.0	4.3	2.81
15.0	5.5	5.09
15.0	5.5	5.12
15.0	5.1	4.54
15.0	5.1	4.19
15.0	4.4	3.47
15.0	4.0	3.03
15.0	4.0	2.96
5.00	5.5	1.28
5.00	5.5	1.29
5.00	5.1	1.25
5.00	5.1	1.11
5.00	4.7	1.11
5.00	4.7	1.08
5.00	4.3	0.971
5.00	4.3	0.909

Table A-11. Kinetic data of the homolysis of $CH_3OCH_2Ni(cyclam)H_2O^{2+}$ in the presence of oxygen
Conditions: $[CH_3OCH_2Co(cyclam)H_2O^{2+}]$ = 200 μM
λ = 360 nm, T = 25°C
in 0.10 M $HClO_4$

$10^3[Ni(cyclam)^{2+}]/M$	$10^5[O_2]_{ave}/M$	k_ψ/s^{-1}
5.00	5.5	1.71
5.00	5.5	2.25
5.00	5.0	1.79
5.00	4.5	1.59
10.0	5.5	1.72
15.0	5.5	1.50
15.0	5.5	1.43
15.0	5.0	1.18
15.0	5.0	1.31
15.0	5.0	1.25
15.0	4.5	1.22
15.0	4.5	1.33
15.0	4.5	1.28
20.0	5.5	1.08
20.0	5.5	1.07
20.0	4.5	1.02

GENERAL SUMMARY

The kinetics of the reactions of $^{\bullet}C_2H_5$ with $Co(NH_3)_5X^{2+}$, $Ru(NH_3)_5X^{2+}$, and $Co(dmgH)_2(X)(Y)$ (X = Br, Cl, N_3, SCN; Y = H_2O, CH_3CN) complexes were studied using laser flash photolysis of ethylcobalt complexes. The kinetics were obtained by the kinetic probe method using $ABTS^{\bullet-}$ and $IrCl_6^{2-}$. Some relative rate constants were also determined by a competition method based on ethyl halide product ratios. The products of these reactions are largely (> 90%) the ethyl halide and ethyl thiocyanate, substantiating an inner-sphere mechanism. Minor but regular yields of C_2H_4 are also found (< 10%), suggesting a small contribution from the outer-sphere oxidation of $^{\bullet}C_2H_5$.

The kinetics of colligation reactions of a series of alkyl radicals with β-$Ni(cyclam)^{2+}$ were studied using laser flash photolysis of alkylcobalt complexes. The kinetics were obtained by employing the kinetic probe competition method (with $ABTS^{\bullet-}$ or $MV^{\bullet+}$).

The kinetics of the unimolecular homolysis of a series of $RNi(cyclam)H_2O^{2+}$ were studied using $ABTS^{\bullet-}$, $MV^{\bullet+}$ or oxygen as radical scavenging agents. Activation parameters were obtained for the unimolecular homolysis of $C_2H_5Ni(cyclam)H_2O^{2+}$.

The colligation and homolysis rate constants are strongly influenced by steric and electronic factors. Kinetic and thermodynamic data obtained from these reactions were compared with those for other σ-bonded organometallic complexes.

The kinetics of the unimolecular homolysis of a series of $RNi(cyclam)H_2O^{2+}$ complexes were studied by monitoring the formation of the oxygen insertion product $RO_2Ni(cyclam)H_2O^{2+}$. The rate constants for the reactions of alkyl radicals with oxygen, k_O, were obtained from the analysis of the homolysis rate equation which contains the known rate constants for the colligation of $R^{\bullet}$ with β-$Ni(cyclam)^{2+}$, k_{col}, and for the homolysis of $RNi(cyclam)H_2O^{2+}$, k_{hom}. The higher rate constants for the reactions of alkyl radicals with oxygen in solution, as compared with those measured in the gas phase, were discussed.

ACKNOWLEDGEMENTS

I would like to thank Professor Jim Espenson and Dr. Andreja Bakač for their guidance and friendship during my graduate career. I am also thankful to the members of my research group for their companionship, for listening to my ideas and sharing with me their own.

I would like to acknowledge God who loves me daily, my wife Lyn for her joy and love which give me direction, hope, and excitement, my parents and family for the love they instilled in me and put into the care packages and encouraging messages, and my friends for being there when I needed an ear, a beer, hoops, a hug, or a kick in the pants.

This work was performed at Ames Laboratory under contract no. W-7405-eng-82 with the U. S. Department of Energy. The United States government has assigned the DOE Report number IS-T 1492 to this thesis.